universität wien

MASTERARBEIT

Titel der Masterarbeit

"The microRNA-200 family and FDA approved drugs as inhibitors of tumour extravasation through the blood vessel endothelium"

verfasst von

Silvio Holzner, BSc

angestrebter akademischer Grad

Master of Science (MSc)

Wien, 2015

Studienkennzahl lt. Studienblatt:	A 066 834
Studienrichtung lt. Studienblatt:	Masterstudium Molekulare Biologie
Betreut von:	Ao. Univ. Prof. Dr. Georg Krupitza

Abbreviation

12(S)-HETE *12(S)-hydroxyeicosatetraenoic acid*
3` UTRs *3' untranslated regions*
5` UTRs *5' untranslated regions*
5-FU *5-fluorouracil*
5-FUH$_2$ *5-fluoro-dihydrouracil*
ADHD *Attention Deficit Hyperactivity Disorder*
ALOX *arachidonate lipoxygenase*
APC *Adenomatous Polyposis Coli*
APS *ammonium persulfate*
Bay-11 *Bay11-7082*
BECs *blood endothelial cells*
BHT *butylated hydroxytoulene*
CAFs *colon cancer associated fibroblasts*
CCID *circular chemorepellent-induced defects*
CCL227 *SW620*
CCL227-N *naive CCL227 (SW620)*
CCL227-R *resistant CCL227*
COX *cyclooxygenase*
CRC *colorectal cancer*
CYP *cytochrome P450*
DMSO *dimethylsulfoxid*
DPD *dihydropyrimidine dehydrogenase*
ECM *extracellular matrix*
EMT *epithelial-mesenchymal transition*
ERK1/2 *extracellular signal-regulated kinase 1/2*
EROD *ethoxyresorufin-O-deethylase*
FAP *Familial Adenomatous Polyposis*
FCS *Fetal Calf Serum*
FDA *Food and Drug Administration*
FdUMP *5-fluorodeoxyuridine monophosphate*
FdUTP *5-fluorodeoxyuridine triphosphate*
FUMP *5-fluorouridine monophosphate*
FUTP *5-fluorouridine triphosphate*
GFP *green fluorescence protein*
GSTA1 *glutathione S-transferase alpha 1*
HDAC *histone deacetylase*
HEK *Human Embryonic Kidney*
HNPCC *Hereditary non-polyposis Colorectal Cancer*
IARC *International Agency of Research on Cancer*
ICAM-1 *intracellular adhesion molecule 1*
IKK *IκB phosphorylation of IκB kinase*
LECs *lymphendothelial cells*
MC *methylcellulose*
MCF7 *Breast Cancer cell line*
MET *mesenchymal-epithelial transition*
miRNAs *microRNAs*
MLC2 *myosin light chain 2*
NF-κB *nuclear factor 'kappa-light-chain-enhancer*
OPRT *orotic acid phosphoribosyltransferase*
ORF *open reading frame*
pri-miRNAs *primary transcripts*
PVDF *polyvinylidenfluorid*
RISC *RNA-induced silencing complex*
RT-PCR *Real-Time PCR*
SDS *sodium dodecyl sulfate*
SFN *sulforaphane*
TBST *tris-buffered saline and tween*
TCF4 *T-cell factor 4*
TEMED *tetramethylethylenediamine*
TERT *telomerase reverse transcriptase*
TNFα *tumour necrosis factor alpha*
UGT1A1 *UDP glucuronosyltransferase 1 family, polypeptide A1*
Wnt *wingless pathway*
ZEB *zinc finger E-box binding homeobox*

Table of contents

1. Introduction

Colorectal cancer

Colorectal cancer (CRC) causes 655,000 deaths per year and consequently leads to a worldwide health problem (Cheng et al., 2011). Due to the global trend, CRC is one of the leading causes of cancer-related mortality. This is especially true in developing countries, Southern Europe and Eastern Europe (Ferlay et al., 2015). In accordance with the International Agency of Research on Cancer (IARC), colorectal cancer is the third most common cancer in men (746,000 cases, 10.0% of the total) and the second in women (614,000 cases, 9.2% of the total) worldwide (Ferlay et al., 2015; Mohan, Kavita, & Karuna, 2015). Due to an increased use of screening that allows the detection and removal of adenomatous polyps, colorectal cancer incidence rates have decreased (Edwards et al., 2014). Unfortunately, although colorectal cancer incidence rates have decreased, and improved chemotherapeutics are available, the survival rates for individuals with CRC have not seen an increase over the last 20 years (Cheng et al., 2011). CRC can be classified in two categories: sporadic and hereditary. Most common colorectal cancer cases are sporadic and originate from genetic- and environmental factors. The most important genetic factor is age. Of the patients diagnosed with CRC, 90% are over 50 years of age. Environmental factors include smoking, body weight, and excessive consumption of meat and alcohol (Botteri et al., 2008; Ferrari et al., 2007; Pischon et al., 2006). The hereditary form accounts for only about 5% of all colorectal cancers. The two main hereditary forms of CRC are hereditary non-polyposis colorectal cancer (HNPCC) and familial adenomatous polyposis (FAP). The HNPCC form is an autosomal-dominant disorder which results in defects in DNA mismatch repair. FAP is an autosomal-dominant disease and in ~80% of affected individuals a germline mutation in the adenomatous polyposis coli (*APC*) gen were subsequently found (Lawes & Boulos, 2002; Weitz et al., 2005). Other risk factors involved with the development of colorectal cancer are Crohn's Disease and Ulcerative Colitis (Weitz et al., 2005).

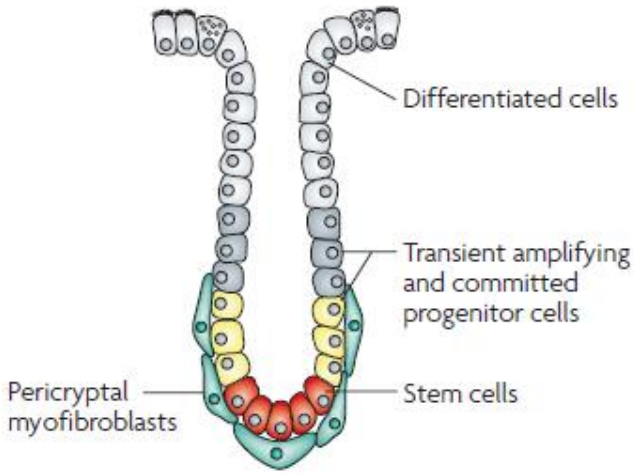

Figure 1: Schematic of the colonic crypt (Humphries & Wright, 2008).

The colon is composed of crypts, which are invaginated and folded to so-called rugae (Humphries & Wright, 2008). Within the colon, stem cells are located at the base of the crypts (Katz et al., 2002). The proliferation of the stem cells occurs in transit-amplifying compartment and the differentiation usually occurs distal to this compartment. Goblet cells secret mucus and pericryptal myofibroblasts are outside of the crypt (Fig.1) (Humphries & Wright, 2008; McDonald, Preston, Lovell, Wright, & Jankowski, 2006).

There are facts that indicate that cancer cells are derived from normal stem cells (Al-Hajj & Clarke, 2004; Shih et al., 2001). These facts are as follows: stem cells have an innate capacity for long-term proliferation, and neoplasia is mainly deregulated in self-renewal (Shih et al., 2001). However, studies indicated that 76% of adenomas were polyclonal (Preston et al., 2003). How can this be explained? Shih *et al.*, (2001) suggested a top-down morphogenesis of colorectal tumours. In this model, mutant cells at the surface epithelium spread laterally and down into crypts. The question arises: what are the implications of the top-down and bottom-up proposals? Several acquisitions of mutations (hits), which activate oncogenes (KRAS) or inactivate tumour suppressor genes (SMAD2, SMAD4, TP53), lead to colorectal cancer (Fig.2) (McDonald et al., 2006).

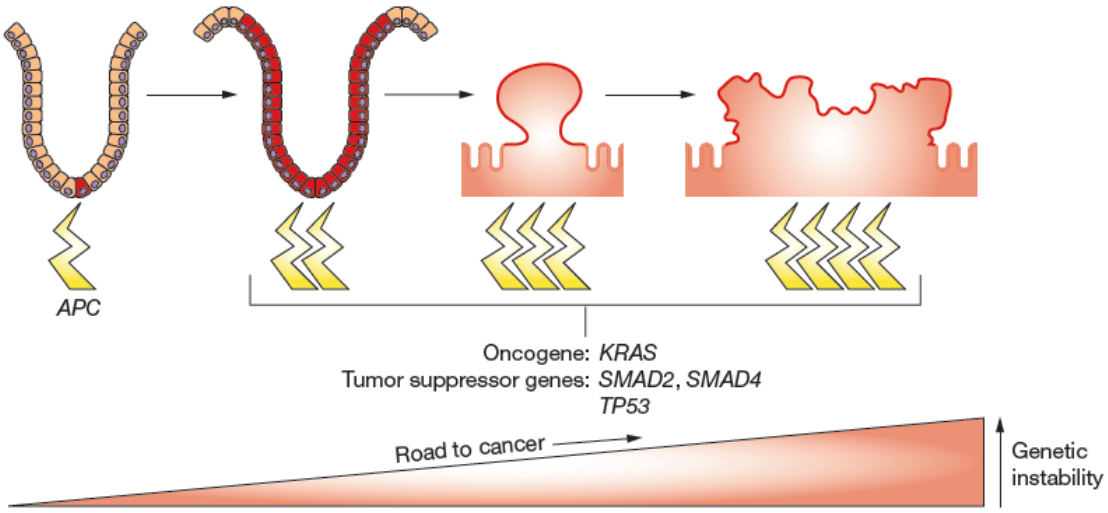

Figure 2: Development of colorectal cancer. The Vogelstein adenocarcinoma sequence presents an early mutation in the APC gene in a stem cell within a crypt resulting of a monocryptal adenoma formation. Following acquisition of mutations lead to develop of a solid tumour and an increased genetic instability (McDonald et al., 2006).

We can deduce that the APC gene is linked to act as a gatekeeper, because in 80% of colorectal cancer the APC gene is mutated. The tumour suppressor APC forms a destruction complex with Axin and two kinases (Ck1 and GSK). This destruction complex binds newly synthesized β-catenin and phosphorylates β-catenin for degradation, when Wnt (Wingless pathway) receptors are not engaged. If Wnt is present, the destruction complex is inhibited and β-catenin remains unphosphorylated. This results in an increased amount of β-catenin proteins, which activate the transcriptional activity of the T-cell factor 4 (TCF4). The resulting complex (β-catenin and TCF4) can then mediate transcription of target genes (Fig.3) (Kohn & Moon, 2005; McDonald et al., 2006; Radtke & Clevers, 2005).

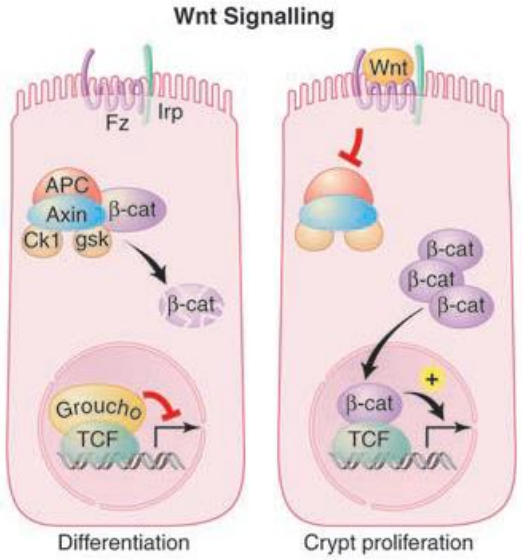

Figure 3: The Wnt signaling pathway. In the absence of secreted Wnt binding to frizzled, the destruction complex (APC, axin CK1, GSK) binds cytoplasmatic ß-catenin for degradation. If Wnt factor is binding to frizzled, the destruction complex remains unactivated and ß-catenin can bind to TCF4 to activate target genes. APC, adenomatous polyposis coli; CK1, cyclic kinase 1; GSK, glycogen synthase kinase; Fz, frizzled 7 transmembrane receptor; LRP, LDL-receptor-related protein; TCF, T-cell factor (Radtke & Clevers, 2005).

Taken together, the Wnt signalling pathway is identified to drive the crypt proliferation. The APC protein seems to be the key protein of most sporadic and hereditary colorectal cancers (Radtke & Clevers, 2005).

Metastasis

The primary cause of death in CRC progression is metastatic dissemination. Cancer cells from the primary tumour spread and colonize distant secondary tissues and organs (Deryugina & Quigley, 2006). Looking at the malignancy, CRC is among the 10 most common worldwide (Langheinrich et al., 2012).

Blood- and lymphatic vasculature intravasation

Cancer cells intravasate into existing or newly formed blood or lymphatic vessels to colonize in distant organs (Fig.4) (Pantel & Brakenhoff, 2004). It is known that colorectal cancer is especially likely to metastasize to the liver and the lungs. Colorectal cancer metastasis is a multistep event that is initiated by the poorly understood process of intravasation (Gout & Huot, 2008).

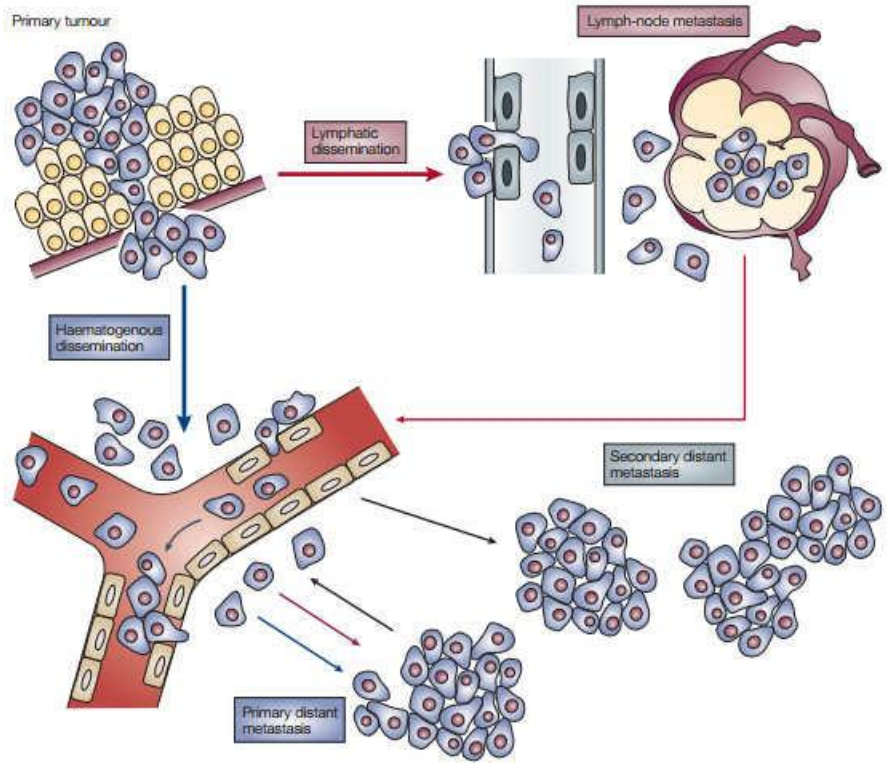

Figure 4: Scheme of metastatis. Invasive cancer cells disseminate through lymphatic (red arrows) or haematogenous (blue arrows) system. The lymphatic system includes lymph-node metastasis and can spread to colonize secondary distant organs. The haematogenous dissemination can occur from primary tumour, lymph-node metastasis or primary distant metastasis (Pantel & Brakenhoff, 2004).

Before dissemination the cancer cells have to proliferate, escape from the primary tumour, and invade into surrounding tissues. Then, the cancer cells must intravasate through a tight cell barrier to get into the blood or lymphatic vessels, where they circulate and reach secondary tissue and organs. After extravasation, cancer cells can disseminate and form metastatic foci (Deryugina & Quigley, 2006). The haematogenous intravasation includes interaction with leukocytes that can be annihilating, formation of aggregates with platelets to protect cancer cells from mechanical stress and leukocytes, and tumour-aggregation against intra capillary thrombosis formation (Fig.5) (Gout & Huot, 2008).

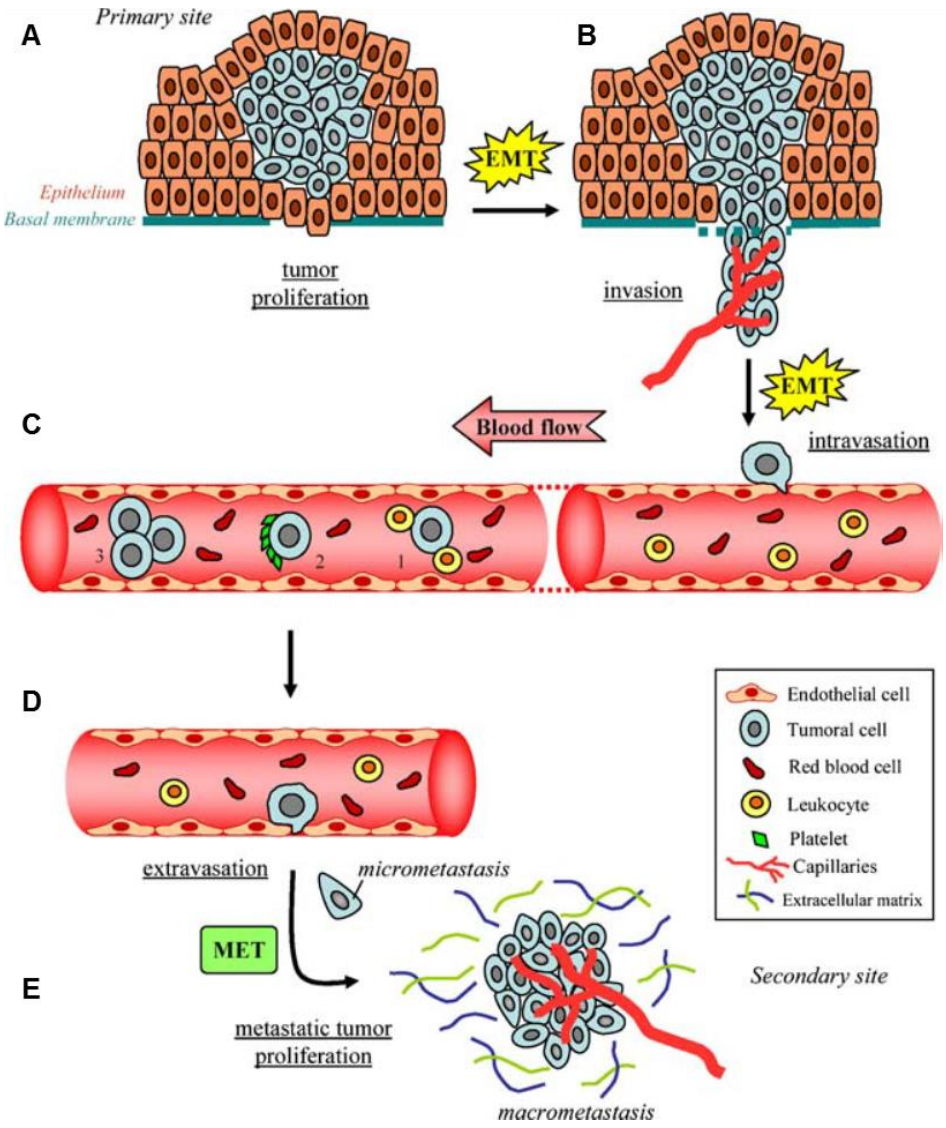

Figure 5: The haematogenous dissemination in detail: (A) Cancer initiation and proliferation, (B) invasion of surrounded tissue, (C) cancer EMT and intravasation into blood capillary. Survival in blood circulation through 1. Interaction with leukocytes, 2. Formation of aggregates with platelets to protect cancer cells from mechanical stress and leukocytes, and 3. Tumour-aggregation against intra capillary thrombosis formation, (D) extravasation, (E) cancer MET and metastasis in secondary distant organs (Gout & Huot, 2008).

The intravasation step is experimentally understudied, because modeling and methodological issues are problematic for most laboratories. Rather, the recapitulation of entry ports into vasculature remain complicated (Juncker-Jensen et al., 2013). Before cancer cells can escape from the primary tumour and intravasate, they have to undergo an epithelial-mesenchmal transition (EMT) process. Then metastatic cancer cells extravasate and revert through mesenchymal-epithelial transition (MET) to reactivate primary tumour-like characteristics (Lamouille, Subramanyam, Blelloch, & Derynck, 2013). In higher vertebrates, EMT is controlled during embryonic development;

particularly for gastrulation, delamination of the neural crest, and formation of the heart-valve and other organs (Gregory, Bert, et al., 2008). In adults, EMT is required for the process of wound healing. The EMT describes reversible events through which epithelial cells lose their cell-cell contacts, and is characterized by a mesenchymal phenotype (Gregory, Bracken, Bert, & Goodall, 2008; Lamouille et al., 2013; Tanaka & Ogishima, 2015). During EMT, mesenchymal markers are switched on and regulated by transcription factors such as zinc finger Snail, ZEB (ZEB1/ZEB2), and basic helix-loop-helix Twist (Lamouille et al., 2013; Wellner, Brabletz, & Keck, 2010). Also the reverse process (MET) is important in forming the kidney nephron epithelium during development (Gregory, Bert, et al., 2008). In the past years, it became increasingly evident that cancer initiation, progression, and metastasis are not only determined by cancer cells, but also by the tumour microenvironment. Cancer EMT may be facilitated and regulated by the surrounded stroma (Gout & Huot, 2008). Lymph endothelial (LECs) and blood endothelial cells (BECs) represent cellular components of tumour microenvironment. The analysis between LECs and BECs by gene expression profiling indicated that about 300 genes are differentially expressed (Langheinrich et al., 2012).

.

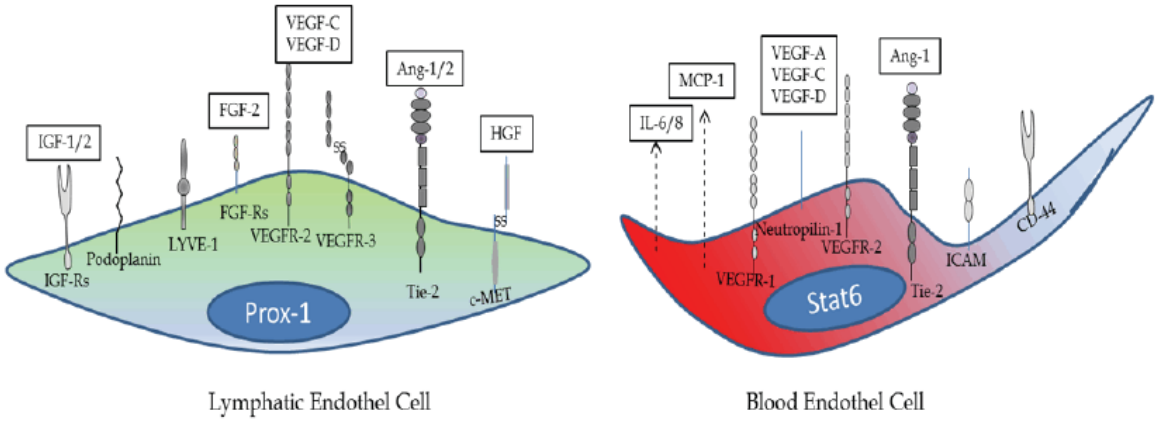

Figure 6: Schematic overview of gene expression profiles between lymphatic endothel cell and blood endothel cell. Abbreviations: signal transducer and activator of transcription 6 (Stat6), monocyte chemotactic protein-1 (MCP-1), interleukin 6/8 (IL-6/8), intracellular adhesion molecule (ICAM), angiopoietin-1 (Ang-1), vascular endothelial growth factor/receptor (VEGF/R), cluster of Differentiation 44 (CD-44), insulin like growth factor 1/2 (IGF-1/2), fibroblast growth factor 2 (FGF-2), hepatocyte growth factor (HGF), mesenchymal epithelial transition factor (c-MET), angiopoietin receptor 2 (Tie-2). Adapted from (Langheinrich et al., 2012).

If the seed and soil theory were accepted, metastasis would be a very inefficient process. The seed (primary cancer cells) will only infiltrate and grow in an appropriate soil (metastatic site). In contrast, Duda *et al.* (2014) demonstrated that the seed also brings its soil (stromal cells) to the secondary site. The provisional stroma (soil) creates the right growing conditions, until the metastatic cancer cells recruit new stroma. Altogether, EMT signaling pathways of cancer cells are the same as embryonic EMT signaling pathways; the surrounded stroma may act as an initiator of these signaling pathways (Gout & Huot, 2008). This Masters thesis will focus on the tumour-stroma interaction between colorectal adenocarcinoma cells and blood endothelial cells.

Treatment and Drug resistance

At present, the current strategies for colon cancer treatment are surgical resection followed by standard oncological principles. These strategies for treatment are dependent on the stage of the tumour. Patients are differentiated in three (I-III) stages, regarding cancer response. The advanced stages III and II undergo neoadjuvant therapy instead of resection (McKeown et al., 2014; Schwenk, 2002; Young-Fadok & Pemberton, 1998). The management of advanced colorectal cancer can be optimized using pharmacogenetics. For over 40 years, advanced colorectal cancer treatment was limited to the chemotherapeutic drug 5-fluorouracil (5-FU). The newly available drugs irinotecan and oxaliplatin, have changed the opportunities for advanced colorectal cancer treatment. Recent clinical studies found that patients who were treated with combination chemotherapy had an improved survival chance (Sanoff et al., 2008). Patients who have resistant metastatic colorectal cancer, anti-EGF or VEGF receptor therapy and three antibody therapies (bevacizumab, cetuximab, and panitumumab) are alternatively available (McKeown et al., 2014; McLeod et al., 2010).

5-Fluorouracil

The chemotherapeutic drug 5-FU is indispensable in the treatment of metastatic colorectal cancer (Fig.7). The success of 5-FU is due to the higher replication rate of cancer cells. In contrast, other chemotherapeutic drugs are not cancer cell specific and

affect normal cell growth as well as cancer cell growth (Farquharson et al., 2008). 5-FU has its metabolic activation in the S phase, with no activity in G0 or G1 phase. The treatment with 5-FU causes double-strand (and single-strand) DNA breaks, because of incorporation of FdUTP into DNA during S phase (De Angelis, Svendsrud, Kravik, & Stokke, 2006).

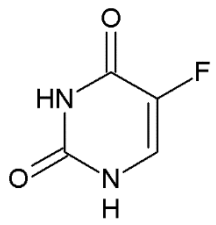

Figure 7: Chemical structure of 5-FU.

There are two main pathways to metabolize 5-FU, the catabolic and anabolic pathway. In the catabolic metabolism 5-FU is converted to 5-fluoro-dihydrouracil (5-FUH_2) (inactive form) by dihydropyrimidine dehydrogenase (DPD) primarily in the liver. The amount of the enzyme DPD is variegated in individuals and consequently, degrades 85% of the 5-FU into inactive metabolites. In the anabolic pathway, thymidine phosphorylase and orotic acid phosphoribosyltransferase (OPRT) metabolize 5-FU into three active metabolites: 5-fluorodeoxyuridine monophosphate (FdUMP), 5-fluorodeoxyuridine triphosphate (FdUTP), or 5-fluorouridine triphosphate (FUTP). These active metabolites are incorporated into DNA and RNA. 5-fluorouridine monophosphate (FUMP) is modified to FUTP (Fig.8) (Farquharson et al., 2008; Mader et al., 1997; Tamatani et al., 2012).

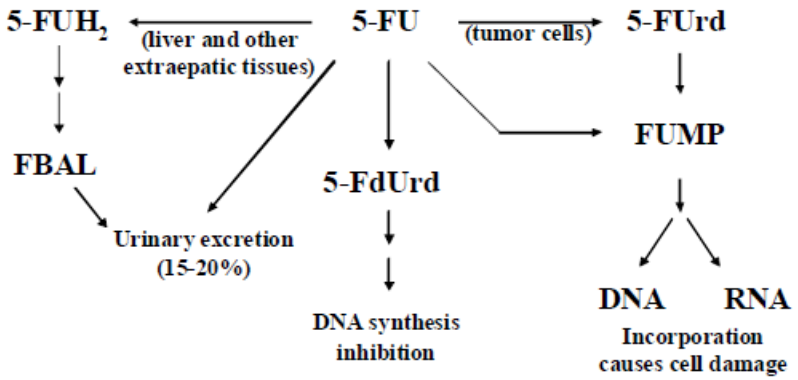

Figure 8: 5-FU metabolism pathways. Abbreviations: 5-FU, 5-fluorouracil; 5-FUH2, 5-fluoro-5, 6-dihydrouracil; 5-FUrd, 5-fluorouridine; 5-FdUrd, 5-fluoro-2'-deoxyuridine; FUMP, 5-fluorouridine-5'-monophosphate; FBAL, α-fluoro-β-alanine (Farquharson et al., 2008).

A consequence of prolonged treatment of this drug is an acquisition of resistance. Chemotherapeutic resistance is a very complex process including reduced activation or inhibition by metabolic enzymes, active cellular export of the drug and increased survival potential. Recent studies showed that the chemotherapeutic agent 5-FU used as a monotherapy, had a limited efficient in anti-tumour activity. These catabolic and anabolic enzymes influence the acquisition of 5-FU resistance: uracil phosphorylase, thymidine phosphorylase and orotic acid phosphoribosyltransferase (OPRT). In detail, reduced levels of OPRT and high levels of DPD were found in colorectal cancer cells resulting in inactivation of 5-FU (Mader et al., 1997; Miyazaki et al., 2006). Recently it was observed that the resistance of colon cancer cells to 5-FU increases the invasiveness into lymphatic vasculature (Senfter et al., 2015). In this project, we will focus on blood endothelial breaching.

Preliminary work

Our group used a *in vitro* colon cancer model with naïve CCL227 (CCL227-N) and their FU-resistant subclones (CCL227-R). Preliminary studies evidenced a supression in all miR-200 family members in the chemoresistant colon cancer subclones compared to still significant but already reduced miR-200 expression in the lymph node metastasis CCL227 (Fig.9) (Senfter et al., 2015). This miR-200 family is responsible for the repression of ZEB1 and SLUG. As a consequence of this miR-200 family loss, the transcription factors are derepressed resulting in E-cadherin inhibition (Fig.11A)

(Senfter et al., 2015). Therefore, three-dimensional spheroids from naïve CCL227 and from their resistant subclones were established, to mimic the *in vivo* architecture and physiology more closely compared to 2D monolayer cell model.

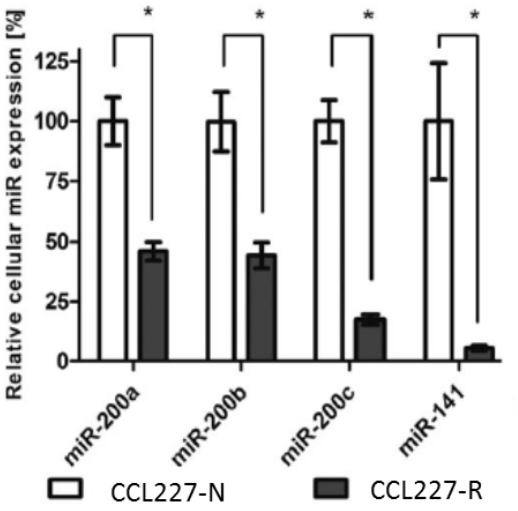

Figure 9: Cellular expression levels of miR-200 family in CCL227-R relative to CCL227-N (Senfter et al., 2015).

Multicellular spheroids

Spheroids are cell aggregates that are non-substrate adherent (Fennema, Rivron, Rouwkema, van Blitterswijk, & De Boer, 2013; Vinci et al., 2012). The formation of spheroids is restricted to a limited number of cell lines. The spheroid formation depends on cell to cell adhesion molecules E-cadherin and N-cadherin, and cell to extracellular matrix (ECM) integrin ß1 (Vinci et al., 2012). Vinci *et al.* (2012) also showed that CCL227 (SW620) cells form loose cell aggregates instead of tight spheroids (Fig.10A and B) (Ivascu & Kubbies, 2007; Vinci et al., 2012). The reduced E-cadherin levels in CCL227-N and CCL227-R lead to a bigger diameter than 500 µm of spheroids. Multicellular spheroids contain diffusion gradients, adhesion, and tight junction barriers, and heterogeneous tumour cell population of proliferating (Fig.10C; Fig.11B and C).

A

Cell line	Tumor type	Three-dimensional morphology
NCI-H23	Lung	C
MDA-MB-231[a]	Breast	C
MCF-7	Breast	C
DLD-1	Colon	T
HCT 116	Colon	T
RKO[a]	Colon	L
HT-29	Colon	T
SW620[a]	Colon	L
PC-3[a]	Prostate	L
A2780	Ovarian	L
IGROV-1[a]	Ovarian	L
SK-OV-3[a]	Ovarian	L
PANC-1[a]	Pancreatic	C
MIA PaCa-2	Pancreatic	L

B

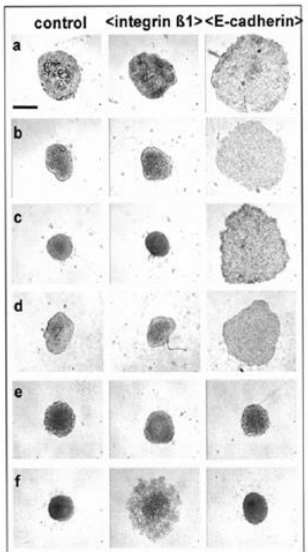

C

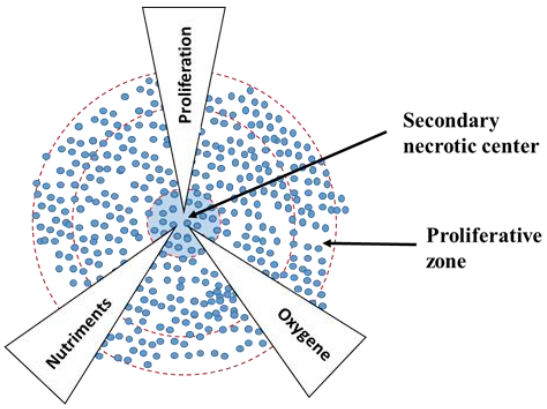

Figure 10: Spheroid morphology. (A) Several cancer cell-lines (SW620 = CCL227) and their three-dimensional morphology: C = compact aggregate, L = loose aggregate, T = tight spheroid. (B) Spheroid formation is inhibited by integrin ß1 and E-cadherin antibodies. (C) Different substrate dissemination and characteristics within a spheroid (Ivascu & Kubbies, 2007; Vinci et al., 2012).

Colon cancer spheroids are placed on lymphendothelial cell (LEC) monolayers to examine the process of intravasation by measuring tumour cell-induced 'circular chemorepellent-induced defects' (CCID). This three-dimensional cell co-culture assay was utilised to compare induced CCIDs by CCL227-N spheroids to those induced by CCL227-R spheroids.

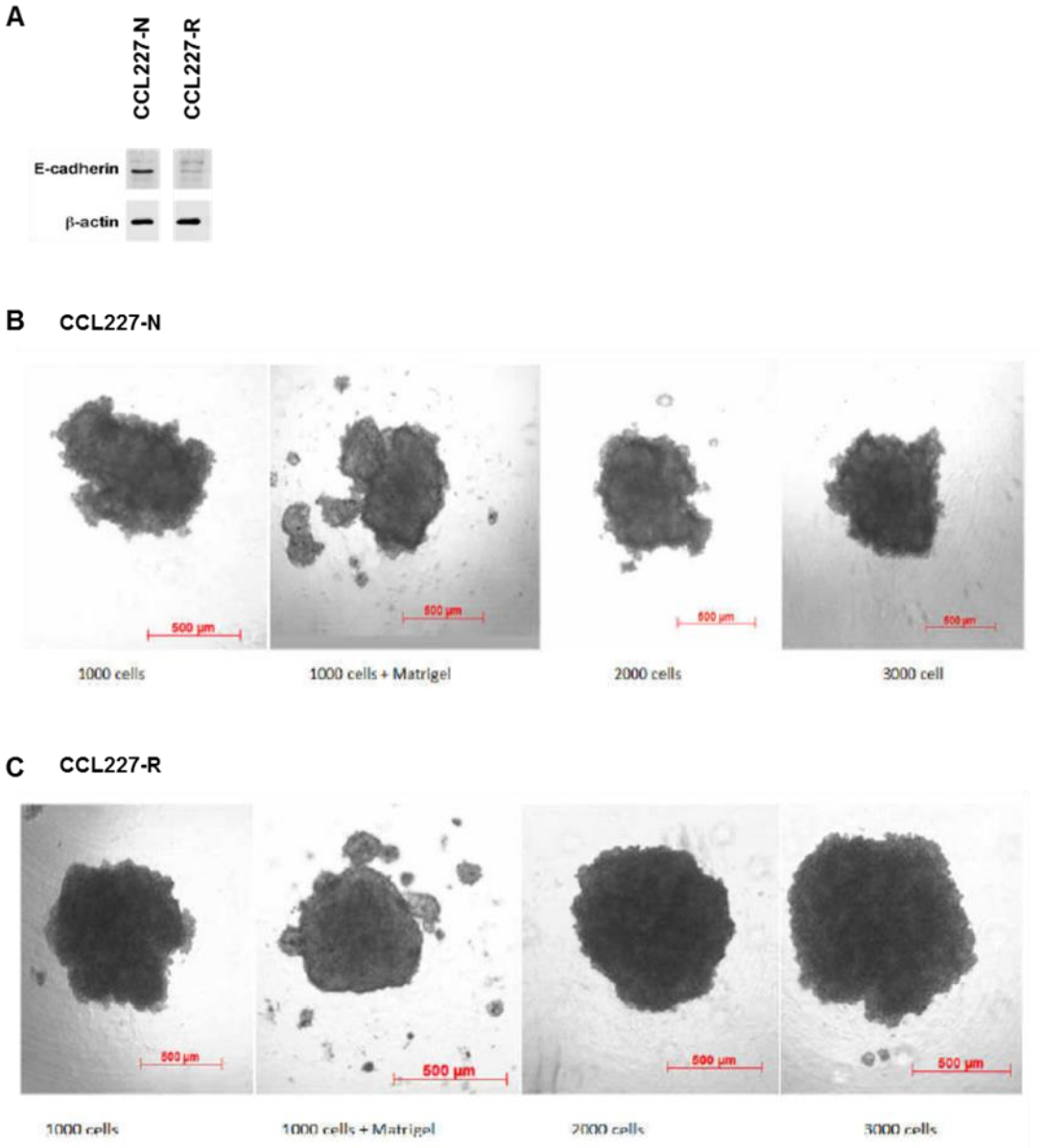

Figure 11: Spheroid formation. (A) Protein expression of E-cadherin in CCL227-N and CCL227-R. (B, C) Different parameters were tested to create stable and compact spheroids for CCID assay (Senfter et al., 2015).

Our group indicated with a trans-well experiment that microRNAs are horizontally transferred into LEC. Therefore, we demonstrated that the loss of exosomal-transferred microRNA in resistant colon cells contributes to intravasation into the lymphatic vasculature (Fig.12A and B). As consequence of reduced miR-200s levels in released exosomes, ZEB transcription factors are de-repressed and enhance activity for CCID formation in LECs (Senfter et al., 2015).

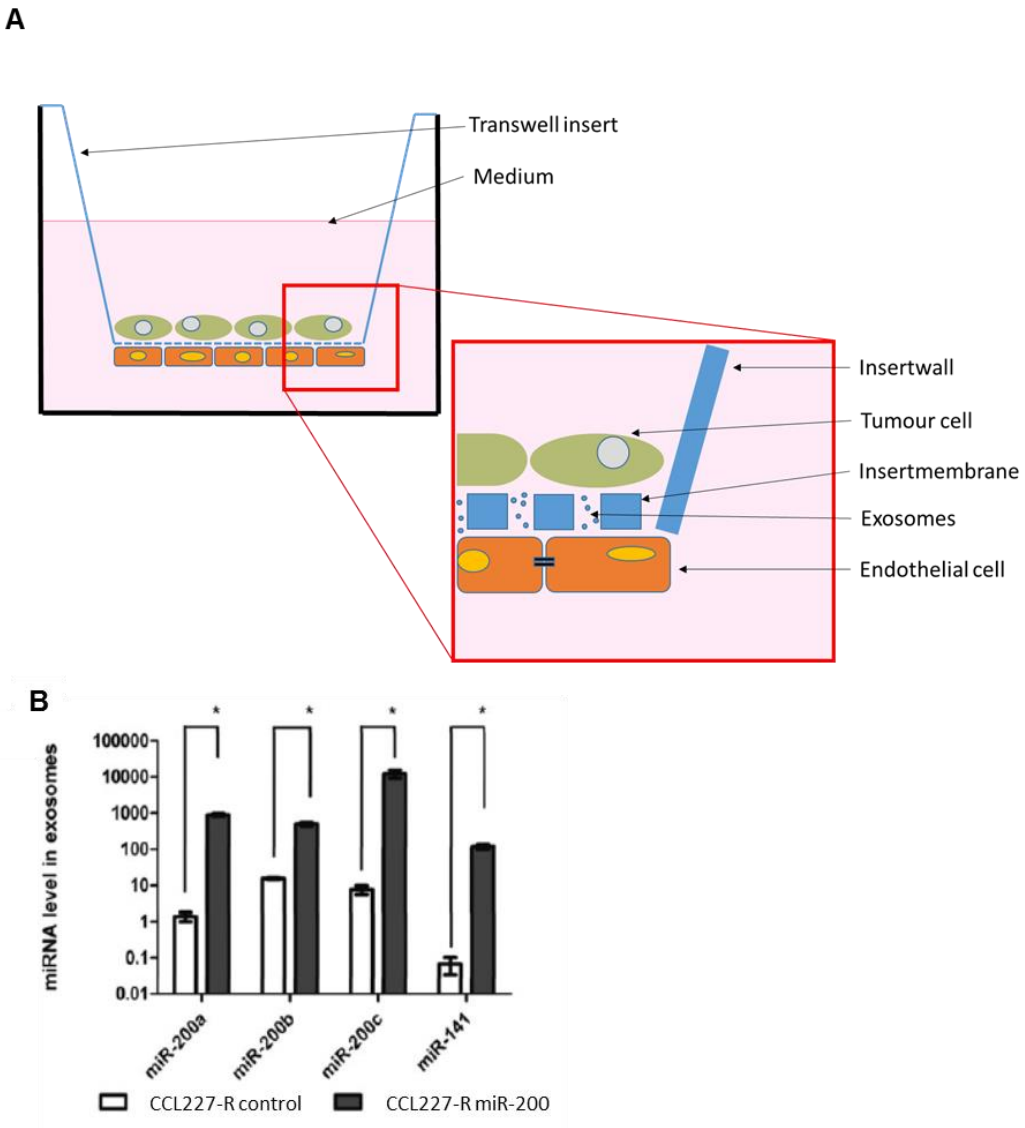

Figure 12: Horizontal microRNA transfer into LEC. (A, B) Co-culture of CCL227-R cells and confluent LECs in a trans-well experiment indicated exosomal-microRNA transfer through a pore size of 3.0 µm (Senfter et al., 2015).

Mechanisms of colon cancer intravasation

Intravasation is a multistep process, and in case of colon cancer, its mechanisms are not well understood. The mechanisms associated with intravasation lead to an increased survival potential of metastatic cells during intravasation, whereas non-metastatic cells undergo destruction when they interact with blood vessels (Gout & Huot, 2008). Understanding the mechanisms of tumour cell intravasation is important in the development of anti-metastatic therapy interventions.

1. Epithelial to mesenchymal transition and microRNA 200 family

Epithelial to mesenchymal transition (EMT)

The process of EMT is essential in tumour invasion and metastasis. This multistep process describes epithelial cells that lose their cell-cell contacts and acquire mesenchymal characteristics. A marker expression switch controlled by transcriptional repressors: zinc finger protein SNAI1, ZEB (ZEB1/ZEB2), and Twist-related protein 1 (TWIST1) characterize EMT. E-cadherin is down-regulated when ZEB transcription factors bind to the E-boxes in the gene promoter (Lamouille et al., 2013; Paterson et al., 2013). Based on this fact, Vonach *et al.* (2011) demonstrated an endothelial to mesenchymal transition-like process of LECs. The protein VE-cadherin, which is a marker of cell-cell cohesion of endothelial cells, was also negatively regulated by ZEBs. This endothelial to mesenchymal transition enables cancers cells to spread into lymphatic or blood vasculature (Vonach et al., 2011). EMT triggers the retraction of endothelial cells through which tumour cells can invade (Lamouille et al., 2013). In this project, we will focus on colon cancer cells that induce endothelial to mesenchymal transition of BECs.

MicroRNA 200-family

MicroRNAs (miRNAs) are single-stranded, small non-coding RNAs (18–22 nt in length) that regulate the expression of target genes by cleavage specific messenger RNA or inhibiting translation. First primary transcripts (pri-miRNAs) are transcribed in the nucleus by polymerase II and processed by the enzyme Drosha. The resulting hairpin intermediates (pre-miRNAs) are then transported

into the cytoplasm by exportin-5. Now the pre-miRNAs are processed into double-stranded miRNAs and separated by the enzyme Dicer. Afterwards, the miRNAs build a complex, so called RNA-induced silencing complex (RISC), and can either bind to open reading frames (ORF) or to 3` untranslated regions (3` UTRs) of mRNAs by base pairing. The perfect base pairing leads to a cleavage of mRNAs, whereas imperfect base pairing leads to translational repression. In contrast, base pairing at the 5` untranslated regions (5` UTRs) of mRNAs causes translational activation. Other pathways are to bind directly protein-coding genes in the nucleus or mRNA binding proteins in the cytoplasm (Fig.13) (Aslam, Patel, Singh, Jameson, & Pringle, 2012).

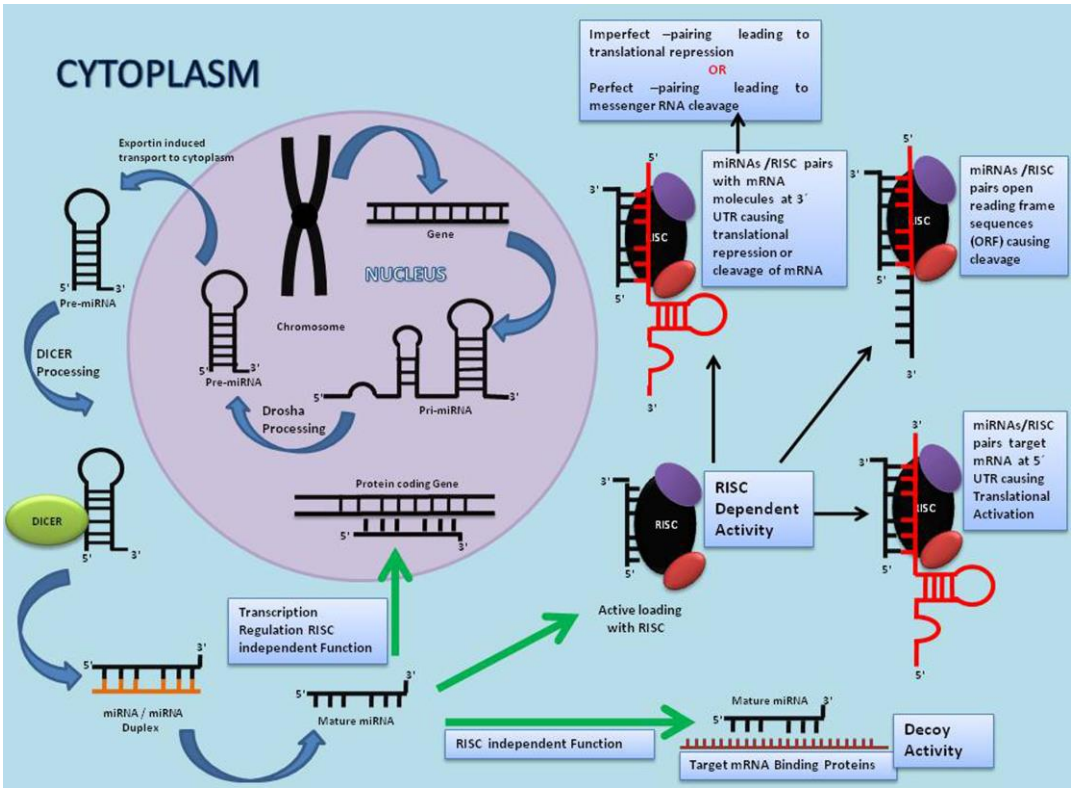

Figure 13: MicroRNA synthesis and following pathways responsible for miRNA functions (Aslam et al., 2012).

Therefore, a deregulation in microRNA expression that targets tumour oncogenes or suppressors contributes to cancer metastasis specifically in CRC (de Krijger, Mekenkamp, Punt, & Nagtegaal, 2011). In all stages of colorectal cancer, microRNAs are involved. It is already known that microRNAs recently act as regulators of EMT. Particularly, the microRNA-200 family members (miR-200a, miR-200b, miR-200c, miR-141 and miR-429) play a crucial role in

the EMT process. Paterson *et al.* (2013) found that cells in the invasive front of colorectal tumours have lost miR-200 family members resulting in a higher motility and lost cell-cell contacts to intravasate more likely into the blood or lymphatic system (Fig.14).

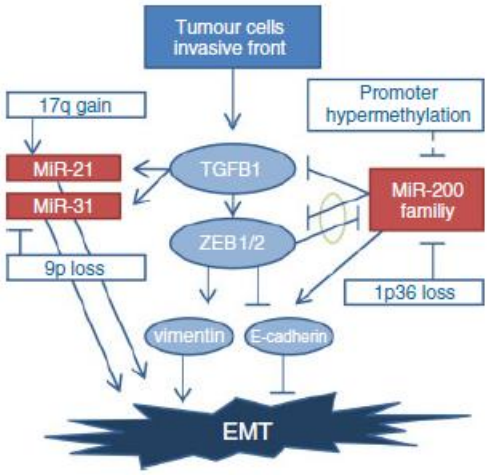

Figure 14: Schematic description of the EMT regulation in CRC. Particularly miR-200 family, miR-21 and miR-31 are involved in inducing EMT (de Krijger et al., 2011).

MicroRNAs charged in exosomes

Exosomes are ~40 to 100 nm vesicles and secreted by different mammalian cell types. Exosomes contain proteins, transcription factors and RNA molecules including miRNAs. Cancer progression can be facilitated based on the fact that these microRNAs which are charged in exosomes are able to influence gene expression in distant cell types. Hence, exosomes can be seen as vehicles of miRNA transfer from malignant cells (Camacho, Guerrero, & Marchetti, 2013; Kahlert, 2014; Van den Boorn, Daßler, Coch, Schlee, & Hartmann, 2013). Yang *et al.* (2011) reported an enhanced invasiveness of breast cancer cells provoked by miRNA in exosomes.

Collectively, recent studies indicated that a general loss of miR-200 family drives invasion and metastasis (Senfter et al., 2015).

2. Endothelial mobility and inhibition of FDA approved drugs

Motility markers denote the retraction of endothelial cells and therefore the protein expression of myosin light chain 2 (MLC2), extracellular signal-regulated kinases 1/2 (ERK1/2) and intracellular adhesion molecule 1 (ICAM-1) by western blot analysis allows an evaluation of their migratory status (Kerjaschki et al., 2011; Viola et al., 2013; Vonach et al., 2011). MLC2 and ERK mediate endothelial cell mobility, whereas ICAM-1 is responsible for adhesion, a process required for cell-cell contact. These proteins are particularly regulated by the 'endothelial retraction factor' 12(S)-hydroxyeicosatetraenoic acid (12(S)-HETE), the transcription factor NF-κB which promotes endothelial cell migration and CYP1A1, a member of the cytochrome P450 family (CYP) (Kretschy et al., 2013; Viola et al., 2013; Vonach et al., 2011).

12(S)-HETE

In humans, the enzymes lipoxygenase (ALOX), cyclooxygenase (COX), and cytochrome P-450-dependent monooxygenase (epoxygenase) use arachidonic acid as their substrate and the resulting metabolites are essential in cell signalling. ALOX12 and ALOX15 generate 12(S)-HETE, which is involved in various cancers. Interestingly, MCF7 spheroid formation altered the gene expression resulting in 12(S)-HETE overexpression. 12(S)-HETE induces CCIDs in lymphatic endothelial cell monolayers (Fig.15) (Kerjaschki et al., 2011; Vonach et al., 2011).

NF-κB

The activation of NF-κB is associated to inflammation and in tumour cell proliferation, survival, angiogenesis, and invasion. NF-κB pathway is also reported to control the adhesion of MCF-7 breast cancer spheroids to LECs and CCID formation (Fig.15) (Viola et al., 2013). In addition, NF-κB mechanism is involved in the acquisition of drug resistance (Baldwin, 2001).

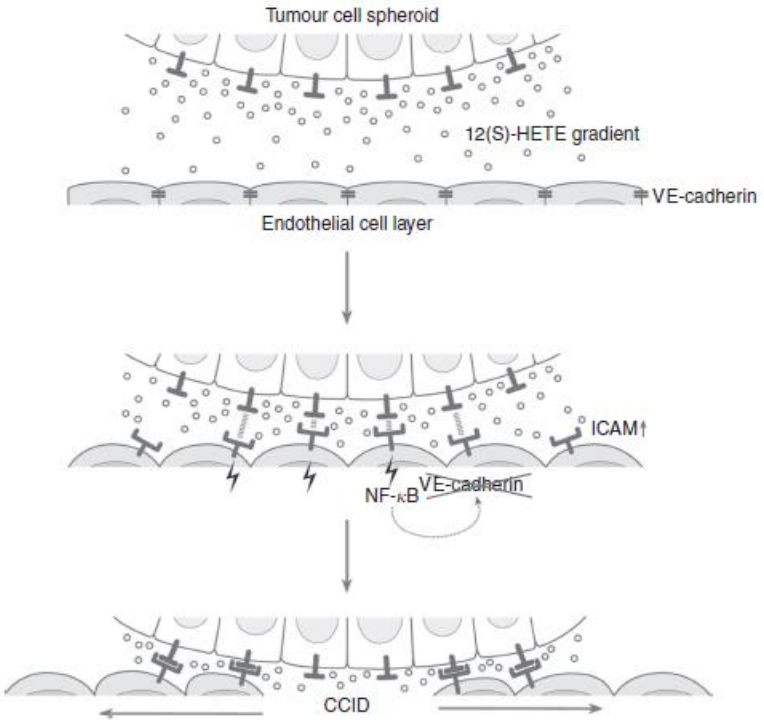

Figure 15: Interaction between tumour cell spheroid and endothelial cells. 12(S)-HETE is secreted by tumour cell spheroid and causes NF-κB activation associated with ICAM-1 expression. Tumour spheroid attaches to endothelial cells and additionally NF-κB inhibits the adhesion protein VE-cadherin. Finally, a migration of endothelial cells occurs and CCID is formed (Kerjaschki et al., 2011; Viola et al., 2013; Vonach et al., 2011).

Cytochrome P450 family (CYP)

It is know that human CYP1A1 family member metabolizes arachidonic acid as their main substrate for the synthesis of their metabolites and is involved in metastases (Teichmann et al., 2014; Viola et al., 2013).

Food and Drug Administration (FDA) drugs

Recently it was shown that some pharmaceuticals have potential in anti-metastatic interventions they have not been developed for (Kerjaschki et al., 2011; Teichmann et al., 2014; Viola et al., 2013; Vonach et al., 2011). Selected drugs were screened regarding to their CCID inhibitory activities and most of them are FDA-approved (exceptions: baicalein, Bay11-7082, proadifen).

Baicalein

A natural flavonoid that is extracted from the roots of *Scutellaria baicalensis* or *Scutellaria radix*. Compared to other flavonoids, baicalein shows more effectively anticancer activity and induced cytotoxicity. Baicalein is a strong inhibitor in CCID formation by inhibiting ALOX12/15 (Chao, Su, & Liu, 2007; Kerjaschki et al., 2011; Ma et al., 2005).

Bay11-7082

This compound is an inhibitor of the activation of the transcription factor NF-κB. In the cytosol, inhibitors of κB (IκB) inactivate NF-κB. After inflammation or cellular stresses, NF-κB is activated by IκB phosphorylation of IκB kinase (IKK) and degradation. Bay11-7082 facilitates the inactive complex of NF-κB and IκB by inhibiting the activity of IKK (Krishnan, Bencze, Cohen, & Tonks, 2013; Rauert-Wunderlich et al., 2013; Strickson et al., 2013). It was demonstrated that the attachment of MCF-7 spheroids to LEC monolayers is required for CCID formation. Bay11-7082 causes a loss of cell adhesion of MCF-7 spheroids to LECs (Viola et al., 2013).

Proadifen

Proadifen is described to inhibit glibenclamide-sensitive K^+ channels, platelet thromboxane synthesis and neuronal nitric oxide synthase. Additionally proadifen is a cytochrome P-450 (CYP) inhibitor and that is crucial for drug metabolism (Kretschy et al., 2013).

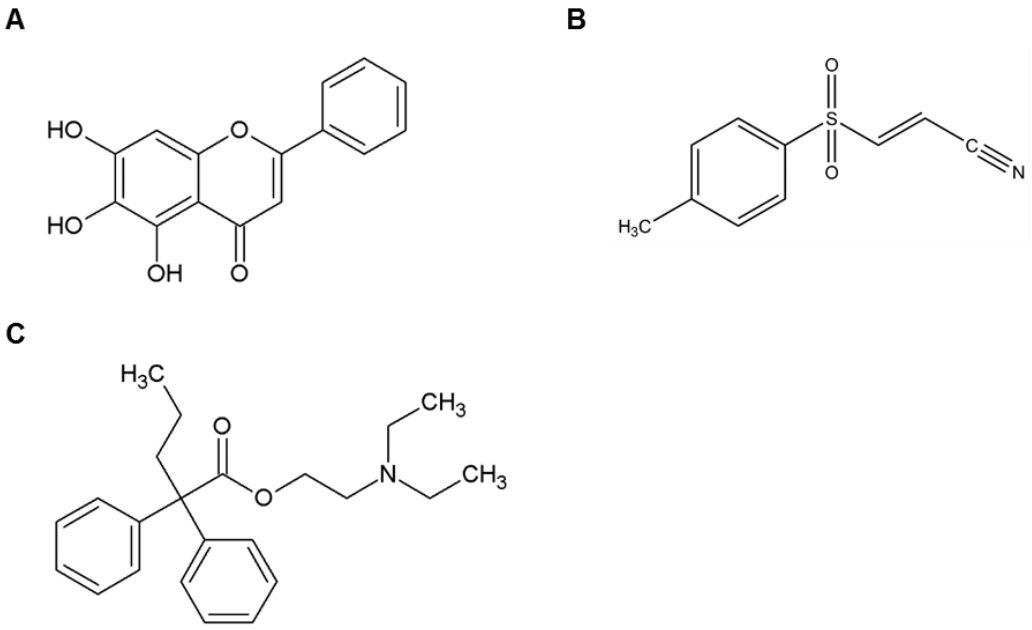

Figure 16: Chemical structure of (A) baicalein, (B) bay-11 and (C) proadifen.

Nifedipin

Nifedipin blocks the binding sites of calcium channel receptors and this causes an influx inhibition of exogenic calcium. This leads to a relaxation in the smooth muscle cells and therefore, a common treatment in coronary heart diseases and hypertonia (Kretschy et al., 2013).

Isoxsuprine

Isoxsuprine leads to relaxation of uterine and vascular smooth muscle by acting as a beta-adrenergic agonist. In humans, isoxsuprine is used as a vasodilator and for the treatment of premature labour. Isoxsuprine is also applied in veterinary medicine to treat hoof-related problems and to increase circulation within the hoof in horses (Kretschy et al., 2013).

Acetohexamide

Acetohexamide is a medication used to treat diabetes mellitus type 2. It stimulates active beta cells in the pancreas to release insulin. The pancreas has to produce insulin and therefore it is not possible to treat diabetes mellitus type 1 (Kretschy et al., 2013).

Carbamazepine

Carbamazepine acts as a calcium antagonist and therefore inhibits voltage-gated sodium channels and K^+ channels. The compound is commonly used to treat epilepsy, phantom limb syndrome, bipolar disorders, schizophrenia, post-traumatic stress disorders or neuropathic pain. Carbamazepine also act as an antiepileptic, mood-stabilizing drug (Teichmann et al., 2014).

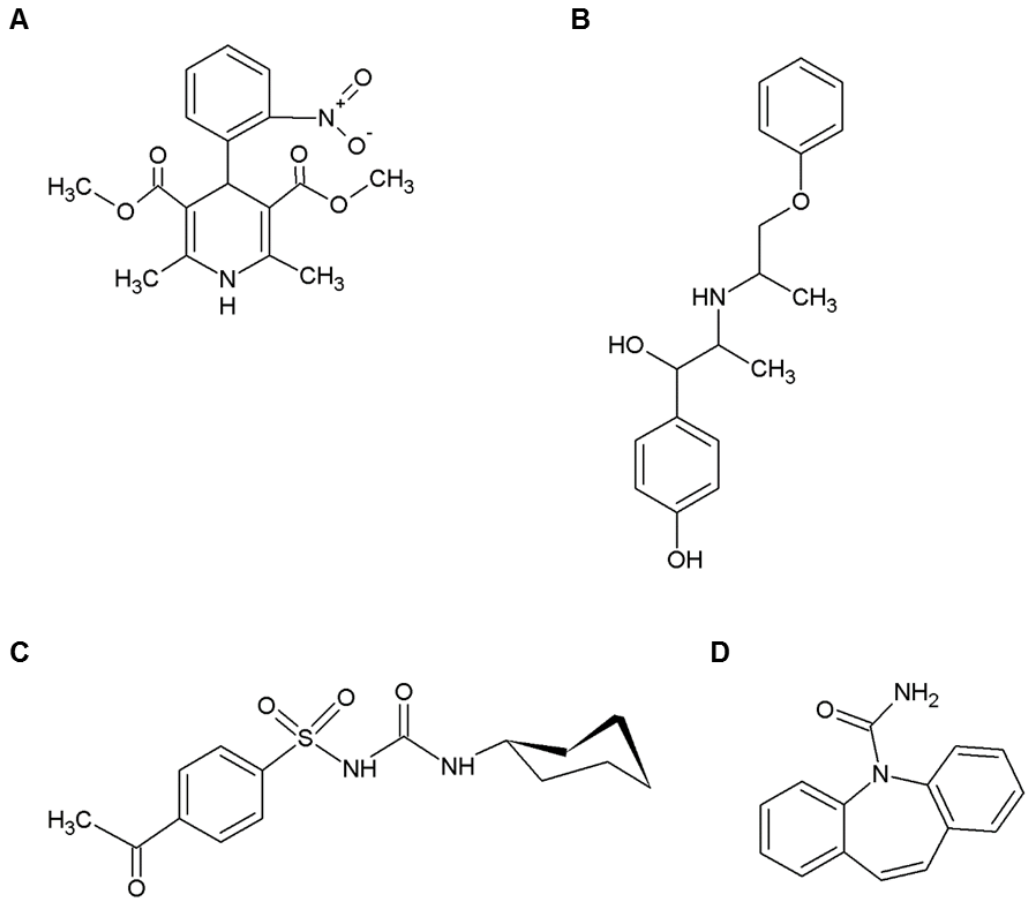

Figure 17: Chemical structure of (A) nifedipin, (B) isoxsuprine, (C) acetohexamide and (D) carbamazepine.

Fenofibrate

Fenofibrate reduces cholesterol levels in patients and is used for the treatment of hypercholesterolemia and hypertriglyceridemia. The effect is based on the activation of the nuclear receptors PPARα (Garcia-Ramírez, Hernández, Palomer, Vázquez-Carrera, & Simó, 2015).

Vinpocetine

In Eastern Europe vinpocetine is used to treat cerebrovascular disorders and age-related memory impairment. The drug is usually developed to enhance the cerebral blood-flow and protect neurons. Vinpocetine has also anti-inflammatory effects and is a promising medication for treatment of Parkinson's disease and Alzheimer's disease (Liu et al., 2014).

Ketotifen

In fact, ketotifen is actually a mast cell stabilizer and used as anti-allergic drug. However, as a Ca^{2+} channel blocker, ketotifen can induce apoptosis in leukemia cells, mast cells, and breast cancer cells. Ketotifen also showed *in vitro* effects in MDR1-mediated multidrug resistance of human breast cancer cells (Kim, Park, Kim, & Lee, 2014).

Guanfacine

Guanfacine, a selective α_{2A} receptor agonist used to treat of hypertension and attention deficit hyperactivity disorder (ADHD). These receptors are located in the locus coeruleus and the prefrontal cortex. Additionally guanfacine activates the central nervous system α_{2A} norepinephrine autoreceptors and this results in a decreased systolic and diastolic blood pressure (Freeman et al., 2015; Ruggiero et al., 2014).

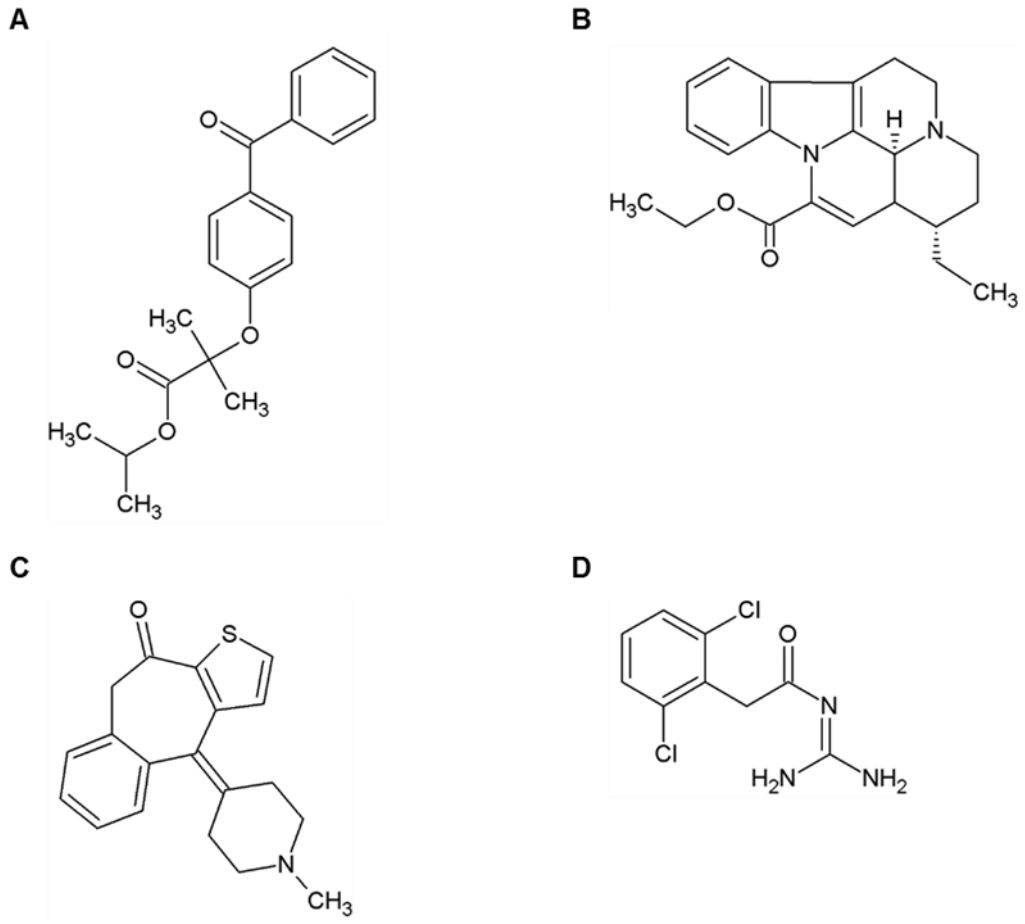

Figure 18: Chemical structure of (A) fenofibrate, (B) vinpocetine, (C) ketotifen and (D) guanfacine.

Aims of the Study

The tumour stroma is the main part (80%) of the tumour mass in some carcinomas. This complex structure is composed of BECs and LECs, together with specialized fibroblasts, termed cancer-associated fibroblasts (CAFs), pericytes, and inflammatory cells embedded in an extracellular matrix (ECM) (Dolznig et al., 2011; Rupp et al., 2014). It was already shown that increasing resistance to 5-FU enforces intravasation into LECs. These drug resistant colon cancer cells have lost the expression of the miR-200 family. This cancer-derived microRNA family is known to regulate lymphendothelial EMT markers (Senfter et al., 2015). In this project, we will focus on the interactions between drug resistant malignant colon cells and BECs. Do LECs have a higher sensitivity to CCL227 spheroid induced CCID formation than BECs and what are the mechanisms of colon cancer intravasation/extravasation? Do miR-200 family members repress EMT transcription factors in BECs and inhibit CCID formation?

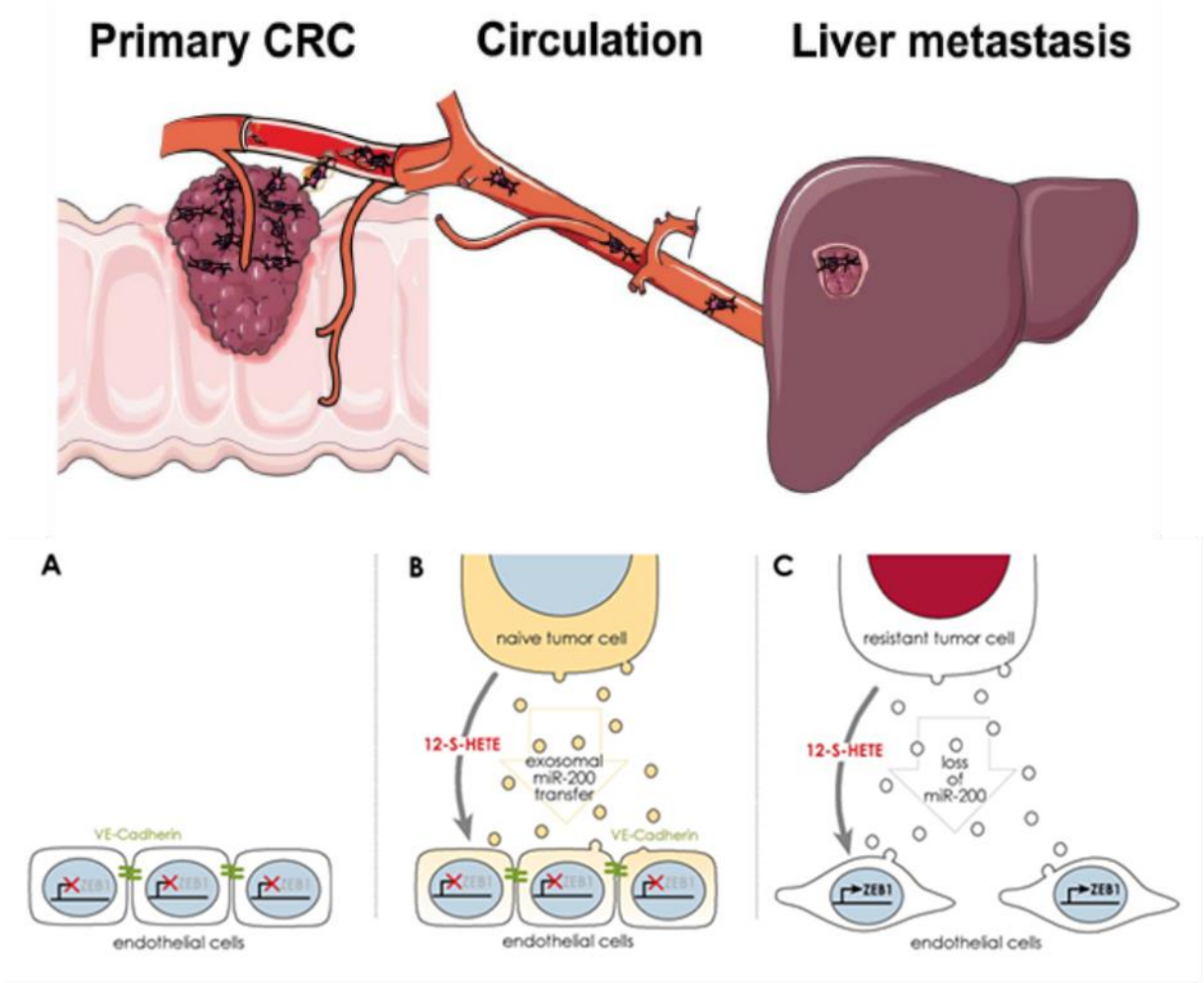

Figure 19: Our model system. CRC breaching through blood vessels and metastasis in the liver. Representation of (A) blood endothelial cell connection through VE-cadherin (green), (B) naïve colon cancer cells secretion of CCID inducing 12(S)-HETE (red) and exosomal miR-200 family, which may facilitates VE-cadherin and supresses ZEB transcription factors, to blood endothelial cells (BECs) and (C) drug resistant colon cancer cells, which have lost miR-200 family and therefore induce CCIDs by 12(S)-HETE induced ZEB transcription factors (Hur et al., 2012).

We aimed to re-express silenced microRNAs intending to inhibit the increased intravasativ properties of drug resistant colon cancer cells. Recently it was demonstrated that LEC migration is driven by tumour cell derived 12-S-HETE. Therefore, we analysed different pathways (12(S)-HETE, NF-κB, CYP) which may regulate CCID formation. The goal of this approach was to identify molecules and pathways, which are involved in this process to find possible targets for therapeutic interventions. Therefore, we screened some selected FDA-approved drugs to discover activities they have not been developed for.

2. Materials and Methods

Reagents and Antibodies

5-Fluorouracil (5-FU)

60 mM 5-FU stock 20 ml
156.096 mg 5-FU
dilute in 20 ml 0.9% NaCl
filtered

Methylcellulose (MC)

MC 15 mg/ml stock 500 mL
8.06 g methylcellulose (Sigma)
dissolve autoclaved MC in 60°C 250 ml basel medium
add 250 ml cold basel medium, stirro/n at 4°C (using magnetic stirrer)
aliquote final stock solution and clear by centrifugation (5000g, 2h, RT)

Agaroses gel electrophoresis Reagents

10x TBE buffer
108 g Tris Base (Merck)
55 g Boric acid (Merck)
40 ml 0.5 M EDTA pH 8.0 (Sigma Aldrich)
Fill up with water to 1L

Western blotting Reagents

2x SDS-lysis buffer 10 ml
1 ml 0.5 M Tris-HCl pH 6.8
3 ml 20% SDS
2 ml Glycerin (Merck)
37 µl 0.5 mM EDTA (Sigma Aldrich)
1Tablet PhosSTOP phosphatase Inhibitor cocktail (Roche)
1 Tablet complete mini EDTA-free protease inhibitor cocktail (Roche)
Fill up to 10ml with ddH2O and store at -20°C

4% stacking gel (for 2 Gels)
0.65 ml Acrylamid 30% (Bio-Rad)
1.25 ml ddH2O
3.1 ml 0.5 M TRIS-HCl pH=6.8
50 µl 10% SDS
8 µl 40 % APS (Fluka)
5 µl Temed (Bio-Rad)

10% separating gel (for 2 Gels)
3.0 ml Acrylamid 30% (Bio-Rad)
3.0 ml ddH2O
3.8 ml 1M TRIS-HCl pH=9.1
100 µl 10% SDS
20 µl 40% APS (Fluka)
5 µl Temed (Bio-Rad)

Electrophoresis buffer 1L
28.8 g Glycerin
6 g Tris-Base
2 g SDS-dry chemical Bio-Rad

Transfer buffer pH 8.3 1L
2.9 g Glycerin
5.8 g Tris-Base
3.7 ml 10% SDS
200 ml Methanol (Merck)

10x Tris buffered saline (TBS) pH 7.4
136.9 mM NaCl (Merck)
5.4 mM KCl (Merck)
49.5 mM Tris-Base
Fill up with water to 900 ml and adjust pH value to 7.4 with HCl

5x Sample buffer 10 ml
275 mg DTT (Merck) dissolve in 5 ml ddH2O
5 ml Glycerin + tip Bromphenolblue (Merck)

1x TBST 1L
100 ml 10x TBS pH 7.4
1 ml Tween 20 (Merck)
900 ml water

5x Tris-Glycin buffer pH 8.3
125 mM Tris Base (Merck)
1250 mM Glycin (Merck)
10% SDS (Pharmacia)

Blocking solution
5 g non-fat milk powder 47
in 50 ml 1x TBST

Primary antibodies

Rabbit anti-zinc finger E-box-binding homeobox 1 (ZEB1), goat anti-SLUG were from Santa Cruz Biotechnology (Santa Cruz, CA, USA). Rabbit anti-ZEB2 was from Millipore (Merck, Darmstadt, Germany), mouse anti-VE-cadherin was from Beckman coulter (Fullerton, CA, USA), rabbit anti-TWIST was from Abcam and rabbit anti-SNAI was from Cell Signaling (Danvers, MA, USA).
Monoclonal mouse anti-phospho-p44/42 MAPK (Erk1/2) (Thr202/Tyr204) (E10), monoclonal rabbit antip44/42 MAPK (Erk1/2) (137F5), polyclonal rabbit anti-phosphomyosin light chain 2 (MLC2) (Ser19), polyclonal rabbit anti-MLC2 and polyclonal rabbit anti-myosin-binding subunit of myosin phosphatase (MYPT1) were from Cell Signaling (Danvers, MA, USA). Monoclonal mouse anti-b-actin (clone AC-15) was from Sigma-Aldrich, polyclonal rabbit anti-phospho-MYPT1 (Thr696) was from Upstate (Lake Placid, NY, USA). Mouse monoclonal anti-CD54 (ICAM-1) antibody was from Immunotech (Marseille, France)

Secondary antibodies

Peroxidase-conjugated polyclonal swine anti-rabbit IgG (1:5000), peroxidase-conjugated polyclonal rabbit anti-mouse IgG (1:10000), peroxidase-conjugated polyclonal rabbit anti-goat IgG (1:10000) were from DakoCytomation (Glostrup, Denmark).

Methods

Cell culture

The colon cancer cell line CCL227 (lymph node metastasis) was purchased from the American Type Culture Collection (Rockville, MD, USA). From this cell line drug resistant subclones CCL227 against 125 µM 5-FU (CCL227-R) were originated by continuous addition of 5-FU over a period of time. All cells were grown in RPMI 1640 medium (Gibco) supplemented with 10% heat inactivated fetal calf serum (FCS, Gibco), 25 mg/ml Gentamycin (Gibco) and maintained in humidified atmosphere containing 5% CO2 at 37°C. The subclones CCL227-R were cultured with additionally added of 5-FU. Telomerase-immortalised human blood endothelial cells (BECs) and cancer-associated fibroblasts (CAFs) were grown in EGM2 MV (EBM2-based medium CC3156 & supplement CC4147; Lonza, Walkersville, USA) and G-418. BECs were generated from human dermal microvascular endothelial cells (C-12260) obtained from Promocell (Heidelberg, Germany). Human dermal microvascular endothelial cells were separated with polyclonal rabbit anti-human podoplanin antibody and sheep anti-rabbit dynabeads (M-280; Dynal 11203, Invitrogen, Lofer, Austria). Afterwards telomerase-immortalised human blood endothelial cells (BECs) were stained with anti-CD31 (Dynal 11128) and incubated at 4°C for 30 min (Schoppmann et al., 2004). Colon cancer associated fibroblasts (CAFs) were isolated from fresh samples of colon adenocarcinomas received at the Institute of Pathology at the Medical University of Vienna, in accordance with the institutional ethical guidelines (Dolznig et al., 2011).

Spheroid formation

$2x10^4$ cells / ml (2000 cells / spheroid) of the cell lines CCL227 or CCL227-R were transferred to RPMI medium containing 20% methylcellulose solution (final concentration 0.3%). 150 µL of this cell suspension was converted to each well of a 96 well plate (Greiner Bio-one, Cellstar 650185, Kremsmünster, Austria) and centrifuged 15 min at 1200 rpm to allow spheroid formation within 6 days at 37°C and 5% CO_2. To generate more stable and compact spheroids 1.7% matrigel was added.

Circular chemorepellent- induced defects assay (CCID)

In this assay, the sizes of the cell free areas were measured that are formed directly underneath the tumour spheroids in the endothelial monolayer. Blood endothelial cells (BECs) were seeded into 24-well plates 3 days before and grown until 90% confluence. These BECs were incubated with a 1:5000 dilution of cyto-tracker green (Molecular Probes, Invitrogen) for 1h in EGM2V medium. Spheroids were washed and transferred to the cyto-tracker-stained BEC monolayer. After 3 h of co-cultivation, the gap sizes underneath the tumour spheroids were photographed using a fluorescence microscope Axiovert (Carl Zeiss, Germany) to visualize the cyto-tracker-stained BEC cells. The sizes of the cell free areas were calculated with the program Axiovison Rel. 4.8 (Carl Zeiss, Germany). The CCID size of 10 or more spheroids was measured.

Spheroid treatment with inhibitors

Colon cancer spheroids were collected and washed twice with fresh medium to remove the methylcellulose. Then the spheroids were pre-treated with different inhibitors for 30 min in 1 ml EGM2V medium. All inhibitors were fresh prepared in DMSO and diluted to the indicated final concentrations. The DMSO concentration of 0.1% was kept constant. Afterwards, this 1 ml medium with spheroids were transferred to confluent cyto-tracker-stained BEC monolayers and incubated for 3 h at cell culture conditions. The sizes of the cell free areas were calculated with the program Axiovison Rel. 4.8 (Carl Zeiss, Germany).

Western blotting

Lysate preparation

Blood endothelial cells (BECs) were seeded in T25 flasks and grown until 80% confluence. BECs were either transfected with the miR-200 family precursors (5 nM of miR-200a, b, c, 141, and 429) for 24 h or treated with FDA-drugs for 0.5, 1, 2, 4 h. Afterwards the cells were washed twice with cold PBS, placed on ice and lysed with the 2x SDS-lysis buffer. For a total cell lysis samples were sonicated 5-10 times on ice. As controls served samples harvested on the beginning of the cell treatment. For further analysis samples were stored at -20°C. The protein concentration was measured with a photometer at 260 nm.

Sodium dodecyl sulfate polyacrylamide gel electrophoresis

Protein samples of equal amount were mixed with 5x Loading Dye and Lysis buffer to a final volume of 20 µL, denatured at 95°C for 5 min and loaded onto a 10% polyacrylamide gel. For establishing a 10% polyacrylamide gel the separating gel was prepared primarily (Tab.1). Ammonium persulfate (APS) and N,N,N',N'-tetramethylethylenediamine (TEMED) were added as the last components to start and catalyze the acrylamide polymerization. The mixed solution was filled between a glass and ceramic plate separated by 0.75 mm chamber. In order to receive a straight gel surface isopropanol was added. After polymerization isopropanol was removed and the stacking gel solution (Tab.2) was added. Before polymerization a comb of 10x5 sample slots was adjusted on the top. The polyacrylamide gel together with the plates (comb removed after polymerization) were transferred to a Hoefer SE250/SE260 Mighty Small electrophoresis chamber filled with 1x Tris-glycin buffer pH 8.3. After a short centrifugation samples were loaded in the slots of the gel. The electrophoresis was performed 1 h first at 70 Volt to concentrate the samples and then increased to 110 Volt for separating.

Immunoblotting

Afterwards the separated proteins were transferred to a PVDF -membrane (GE Healthcare, Little Chalfont, UK). The membrane was activated with methanol for 15 sec and a "sandwich" was assembled in the following order: pre-wetted sponge, Whatman paper, protein gel (separated from glass and ceramic plates; stacking gel was removed), PVDF-membrane and Whatman paper, sponge. The "sandwich" was placed in a transfer chamber with cold transfer buffer and performed with 100 Volt for 1 h. After the transfer the equal sample loading was checked with Ponceau S (Sigma Aldrich) staining. The membrane was put into the Ponceau S solution for 5 min and washed until the protein bands were red labeled and visible only. The membrane were documented and washed in TBST pH 7.4. Free and non-specific binding sites were blocked by 5% fat reduced dry milk in TBS-0.1% Tween for 1 h. Afterwards the membrane was incubated over night at 4°C with the primary antibody. The next day the membrane was washed again and incubated with the secondary antibody (peroxidase-conjugated goat anti-rabbit IgG, 1:10000; anti-rabbit IgG, 1:5000 or anti-mouse IgG,

1:10000, Darko) for 1 h at RT. Subsequently washed 3x with TBST pH 7.4 each time 10 min, dried on filter papers and incubated in an ECL detection solution mixed 1:1 (Thermo Scientific, Portsmouth, IL, USA) for 1 min. To detect the chemiluminescence the membranes were exposed on to Amersham Hyperfilms (GE-Healthcare, Buckinghamshire, UK).

12(S)-HETE assay

Performed by S. Brenner, affiliation: Dr. Walter Jäger, Department of Clinical Pharmacy and Diagnostics

CCL227-R colon cancer cells were seeded in 3.5-cm dishes and grown in 2.5 ml complete RPMI medium without selection pressure. The next day, the medium was changed for serum-free medium, the cells were at least 80% confluent, and kept at 37°C for 24 h. Then arachidonic acid was added to the cells for 4 h, medium aspirated, shortly and strongly centrifuged to remove debris. To stabilize eicosanoids in samples butylated hydroxytoulene (BHT, 1:1000) was added to the supernatants and then stored at -80°C in a cryotube.

NF-κB luciferase assay

Performed by A. Atanas, affiliation: Dr. Verena Dirsch, Department of Pharmacognosy

HEK293-NF-κB-Luc cells ($10x10^6$) (Panomics, Fremont, CA, USA) were seeded in 20 ml full growth DMEM medium in a 15-cm dish. The following day, cells were transfected with an expression plasmid for green fluorescence protein (GFP) (pEGFP-N1; Clontech, Mountain View, CA, USA). A total of 30 ml Lipofectamin 2000 (Invitrogen) and 7.5 mg DNA were mixed in 2 ml transfection medium and incubated for 20 min at RT and then added to the cells. After incubation for 6 h in humidified atmosphere containing 5% CO2, $4x10^4$ cells per well were seeded in serum- and phenol red-free DMEM in a transparent 96-well plate. The next day, cells were treated with selected drugs and 2.5 mM parthenolide as a specific inhibitor of NF-κB (control). One hour after treatment, cells were stimulated with 2 ng/ml human recombinant TNFα for additional 4 h. Luminescence of the firefly luciferase and fluorescence of the GFP were quantified on a GeniusPro plate reader (Tecan, Grödig, Austria). The luciferase signal

derived from the NF-κB reporter was normalised by the GFP-derived fluorescence to account for differences in cell number.

Ethoxyresorufin-*O*-deethylase (EROD) assay selective for CYP1A1 activity

Performed by W. Chatuphonprasert, affiliation: Dr. Walter Jäger, Department of Clinical Pharmacy and Diagnostics

CCL227 colon cancer cells were grown in phenol red-free RPMI 1640 tissue culture medium (PAN Biotech, Aldenbach, Germany), supplemented with 10% FCS and 1% PS (Invitrogen, Karlsruhe, Germany) under standard conditions at 37°C in a humidified atmosphere containing 5% CO2. Before treatment, the cells were transferred to RPMI 1640 medium (Invitrogen, Karlsruhe, Germany) supplemented with 2.5% charcoal-stripped FCS (PAN Biotech, Aldenbach, Germany) and 1% P/S. After 18 h of incubation, ethoxyresorufin (final concentration 5.0 µM, Sigma-Aldrich, Munich, Germany) was added with or without drugs of the indicated concentrations and 0.4 ml aliquots of the medium were sampled after 30 and 210 min. Selected compounds were dissolved in DMSO and diluted with medium (final DMSO concentration <0.1%). Experiments were carried out in triplicate. Blanks contained DMSO in the medium of the compounds. Subsequently, the formation of resorufin was analysed by spectrofluorometry (PerkinElmer LS50B, Waltham, MA, USA) with an excitation wavelength of 530 nm and an emission wavelength of 585 nm.

RT-PCR

RNA-isolation using TRI REAGENT

Template cDNAs were prepared from isolated RNA of harvested blood endothelial cells or colon cancer spheroids. TRI REAGENT (Sigma) was used for total RNA isolation. 400 µL TRI REAGENT was added either to 6-well plates or to 10-20 spheroids and incubated 5 min at RT. Lysates were transferred into a 1.5 ml tube and mixed with 100 µl chloroform for 15 sec. After 15 min of incubation at RT, samples were centrifuged at 12000 g, 4°C for 15 min and 3 phases were generated. The first uncoloured aqueous phase (RNA) was transferred into a new tube and mixed with 200 µl chloroform, shacked for 5 min at RT and centrifuged again at 12000 g, 4°C for 15 min. The aqueous

phase was removed again and transferred into a new tube. 200 µl isopropanol was added, incubated for 10 min at RT and centrifuged at 12000 g, 4°C for 15 min. The supernatant was discarded and the pellet was resuspended with 400 µl 75% ethanol and centrifuged at 12000 g, 4°C for 15 min. The supernatant was removed, pellet was air dried and solved in 5-10 µl DEPC water.

Sodium acetate/ethanol precipitation of RNA

This method was used for desalination and concentration of RNA. To isolate RNA the pellet was dissolved in 50 µl DEPC and 150 µl 3 M Na-acetate solution (pH 5.5) was added. After overnight incubation at -20°C, tubes were centrifuged at 14000 g at 4°C for 30 min. Supernatant was removed, pellet washed with 200 µl 70% ethanol and air dried for 5-10 min. Afterwards the pellet was resuspended in 5 µl DEPC. The RNA level was photometric measured using nanodrop (Thermo Scientific).

c-DNA synthesis

From the isolated RNA an unspecific cDNA was synthesised with subsequent RT-qPCR. An amount of 10 ng RNA in 5 µl RNase-free water were used. Total RNA was reverse transcribed with TaqMan MicroRNA RT Kit (Applied Biosystems) for each miR member separately. The conditions for reverse transcriptase were 30 min at 16°C, 30 min at 42°C and 5 min at 85°C followed by holding on 4°C.

Table 1: Master Mix c-DNA synthesis

REAGENTS	CONC.	µL/SAMPLE
DNTPS-MIX	100 mM	0.15
MULTISCRIBE ENZYM	50 U/µl	1.00
RT-PUFFER	10X	1.5
RNASE INHIBITOR	20 U/µl	0.19
RNASE-FREE WATER	/	4.16
PRIMER	5X	3

TOTAL VOLUME	10 µl+5 µl RNA (2 ng/µl)

Real-Time PCR

An amount of 10 µl containing 5 µl TaqMan master mix, 3.17 µl RNAse free H_2O, 0.5 µl TaqMan primer and 1.33 µl c-DNA was prepared. Afterwards the Real-Time PCR was performed in a Rotor Gene Corbett 6000 Q PCR. For the reaction the conditions were 2 min at 50°C, 10 min at 95°C, cycling (50 repeats): step1 15 sec at 95°C, step 2 60 sec at 60°C. PCR products were analysed on quantative Rotor-Gene software. Relative transcript expression was calculated using the Pfaffel method (Holzapfel & Wickert, 2007). As a control the stable miRNA RNU 6B was used.

Table 2: Master Mix Real-Time PCR

REAGENTS	**CONC.**	**µL/SAMPLE**
REAKTION BUFFER	2x	5
RNASE-FREE WATER	/	3.17
TAQMAN MIR-200A,B,C,141		0.5
TAQMAN RNU 6B		0.5
TOTAL VOLUMEN		8.67 µl

miR transfection

On the day of transfection the BEC cells had a confluence of 80% or the colon cancer spheroids were 6 days of cultivation. All microRNAs precursors (200a, 200b, 200c, 141, 429) and negative scramble control were diluted (in 100 µl) to a final concentration of 5 nM in RPMI or EGM2V without serum and antibiotics. The transfection reagent was used from siPORT NeoFX (Ambion). 10 µl siPORT reagent was mixed with 90 µl of RPMI and blended 1:1 with the diluted microRNA solution. Thereafter the solution was incubated for 10 min at room temperature. The mixture was gently added to either the cells or the spheroids in 2.3 ml RPMI medium and after 24 h the medium was changed to complete RPMI medium.

Isolation of exosomes

Colon cancer cells were grown in a T75 flask until 80% of confluence. Afterwards the cells were washed with PBS and kept 24 h in RPMI without FCS and antibiotics. Then the medium was changed to RPMI with 10% exosomes free FCS for further 24 h to allow exosome production. Thereafter the supernatant was collected, centrifuged at 3000 g for 15 min and transferred to a new 15 ml tube. The exosomes in the supernatant were obtained by ExoQuick-TC (System Biosciences). The extraction occurred by 2 ml ExoQuick per 5 ml colon cancer supernatant and refrigerated overnight. The next day, the supernatant was centrifuged at 1500 g, 4°C for 30 min to receive a beige pellet. The supernatant was removed and the beige pellet centrifuged at 1500 g, 4°C for 10 min. To remove all the deposits of the ExoQuick, the pellet was centrifuged again at 1500 g, 4°C for 5 min. Afterwards the pellet was resuspended in 10-100 µl DEPC water.

Bio Rad protein assay

The exosomal protein concentration was measured with a photometric protein assay. The concentration was approximated to a protein standard according to the manufacturer's protocol (Bio Rad). In a 96-well plate 10 µl of the diluted sample (1:10-30) and the standards were mixed with 200 µl dye reagent (Bio Rad) and incubated for 5 min. For analysing of the plate, an Asys reader was used.

Statistical analysis

Dose-response curves were analysed using Excel 2013 software and Prism 6 software package (GraphPad, San Diego, CA, USA). The values were expressed as mean ± SEM and significance was appropriated by a non-parametric Student's t-test and one-way ANOVA. Statistical significance differences were set to $*P<0.05$.

3. Results

Tumour derived microRNA regulates receptiveness of the vasculature and inhibits extravasation

Establishment of three-dimensional spheroids

Recent studies showed that cell surface expression of E-cadherin, N-cadherin and integrin ß1 were crucial for spheroid generation (Ivascu & Kubbies, 2007). It was also discovered that in the sub clone CCL227-R the expression of E-cadherin was dramatically decreased compared to the naïve CCL227 cell line (Senfter et al., 2015). It is crucial for subsequent experiments to generate compact and stable spheroids, because of the shear forces in the process of transferring spheroids to the BEC monolayer in the CCID assay. Therefore, different parameters like cell number, FCS concentration and the addition of matrigel were tested aiming for compact spheroid production. The spheroid generation of CCL227-N and CCL227-R clones was well-established by Daniel Senfter (Senfter et al., 2015).

The formation of compact spheroids is restricted to a limited number of cell lines. Some cell lines did not generate stable spheroids until matrigel was added. It was reported that these tumour cell lines form loose three-dimensional aggregates (Vinci et al., 2012). Hence, matrigel was tested in different concentrations to get compact and stable CCL227 spheroids. The most stable spheroids were achieved with an addition of 2.5% (final concentration 25 µg/ml protein) matrigel. It was reported that spheroids consisting of 1000 cells were less stable compared to spheroids of 2000 cells. The reduction of FCS did not increase the stability. We found that using 2000 cells, 10% FCS and 0.3% methylcellulose which were cultivated for 6 days yielded the most stable spheroids (Fig.20A and B).

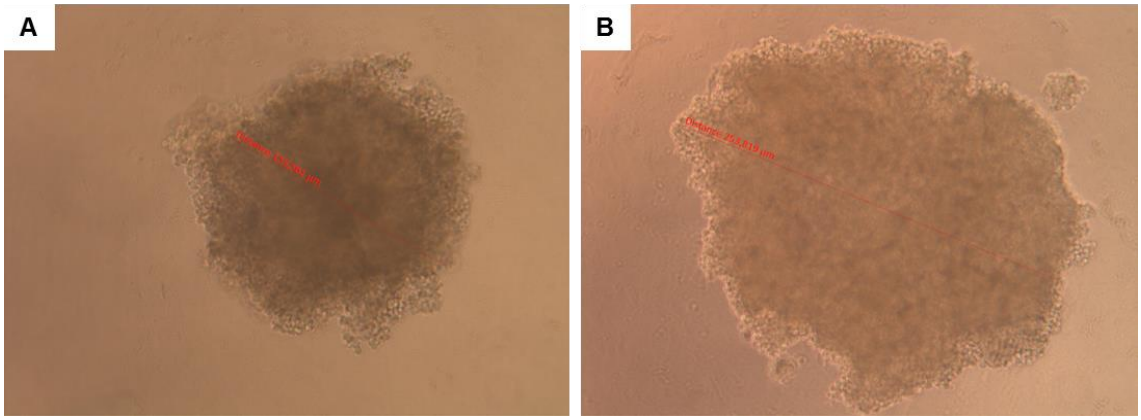

Figure 20: Spheroid morphology. (A) CCL227-N spheroid, (B) CCL227-R spheroid.

Comparison of tumour breaching malignancy

The formation of metastases is comprised of multiple sequential steps, in which malignant cells disseminate from the primary tumour to colonize distant organs (de Krijger et al., 2011). Time-lapse videos recently revealed formation of "circular chemorepellent induced defects" (CCID) within lymphendothelial cells directly underneath MCF-7 breast cancer spheroids (Kerjaschki et al., 2011). Whereas spheroids of nontumourigenic mammary gland epithelial cell line MCF-10A or human lung fibroblasts did not induce such entry gates (Kerjaschki et al., 2011). A similar centrifugal migration of lymph- and blood endothelial cells was seen with the CCL227 colon cancer spheroid model. Spheroids generated from naïve CCL227 (CCL227-N) cells were compared to those induced by 5-FU resistant CCL227 (CCL227-R) spheroids. CCL227 colon cancer spheroid breaching was observed through lymph-endothelial and blood-endothelial cells.

Time course experiments evidenced that CCL227-R spheroids enforce CCID formation in LEC monolayers compared to CCL227-N spheroids (Fig.21A-H). This effect could be reproduced on BEC monolayers (Fig.22A-H).

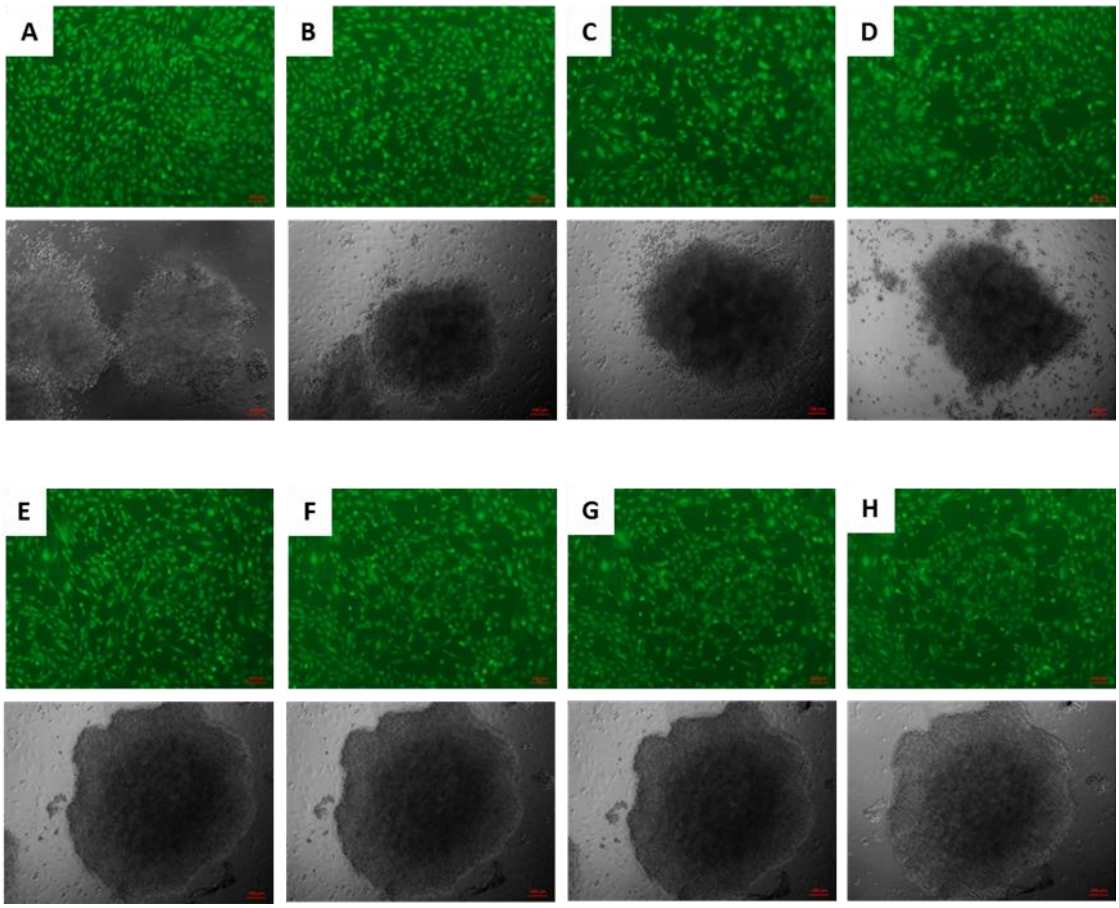

Figure 21: Time lap experiments show CCID formations by naïve and resistant colon cancer spheroids. CCL227-N (A-D) and CCL227-R (E-H) spheroids induce CCIDs in LEC monolayers (cyto-tracker green) after 0.5, 1, 1.5 and 2 h of co-cultivation. Scale bars: 200 μm.

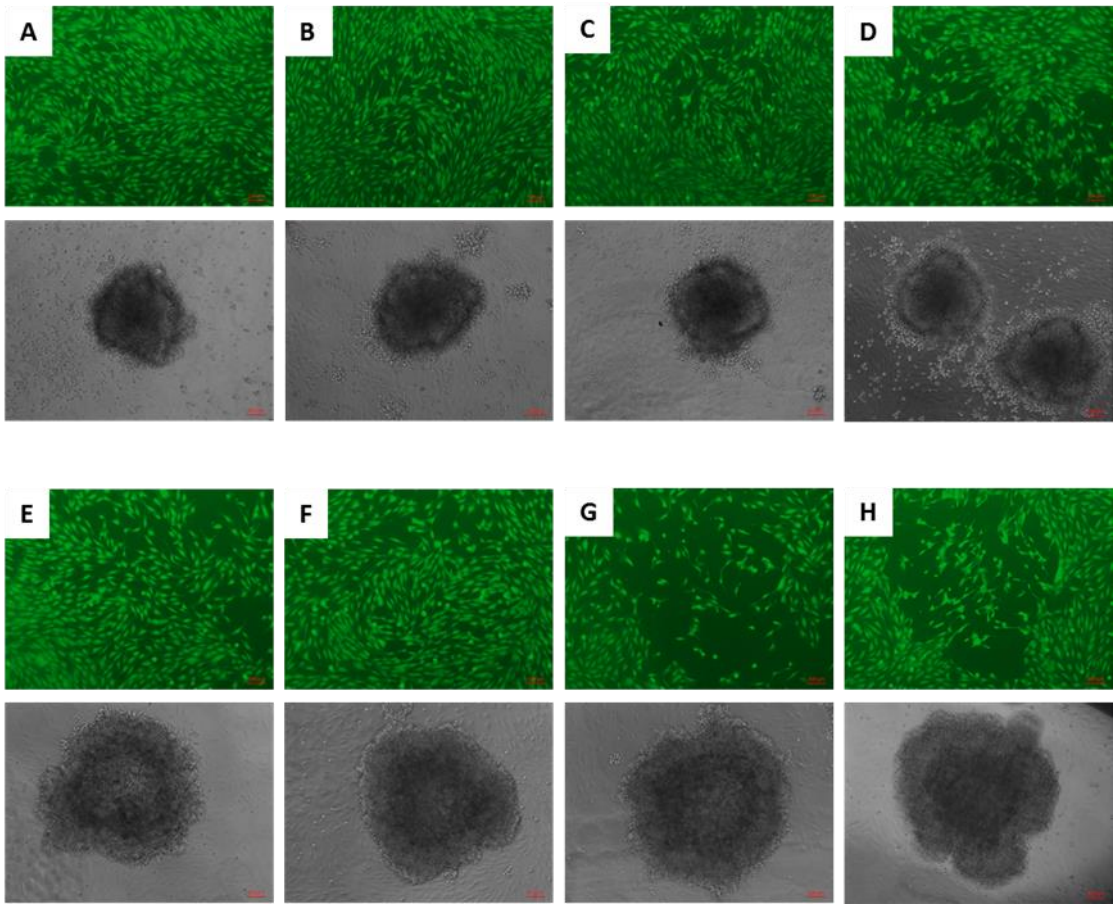

Figure 22: Time lap experiments show CCID formations by naïve and resistant colon cancer spheroids. CCL227-N (A-D) and CCL227-R (E-H) spheroids induce CCIDs in BEC monolayers (cyto-tracker green) after 0.5, 1, 1.5 and 2 h of co-cultivation. Scale bars: 200 μm.

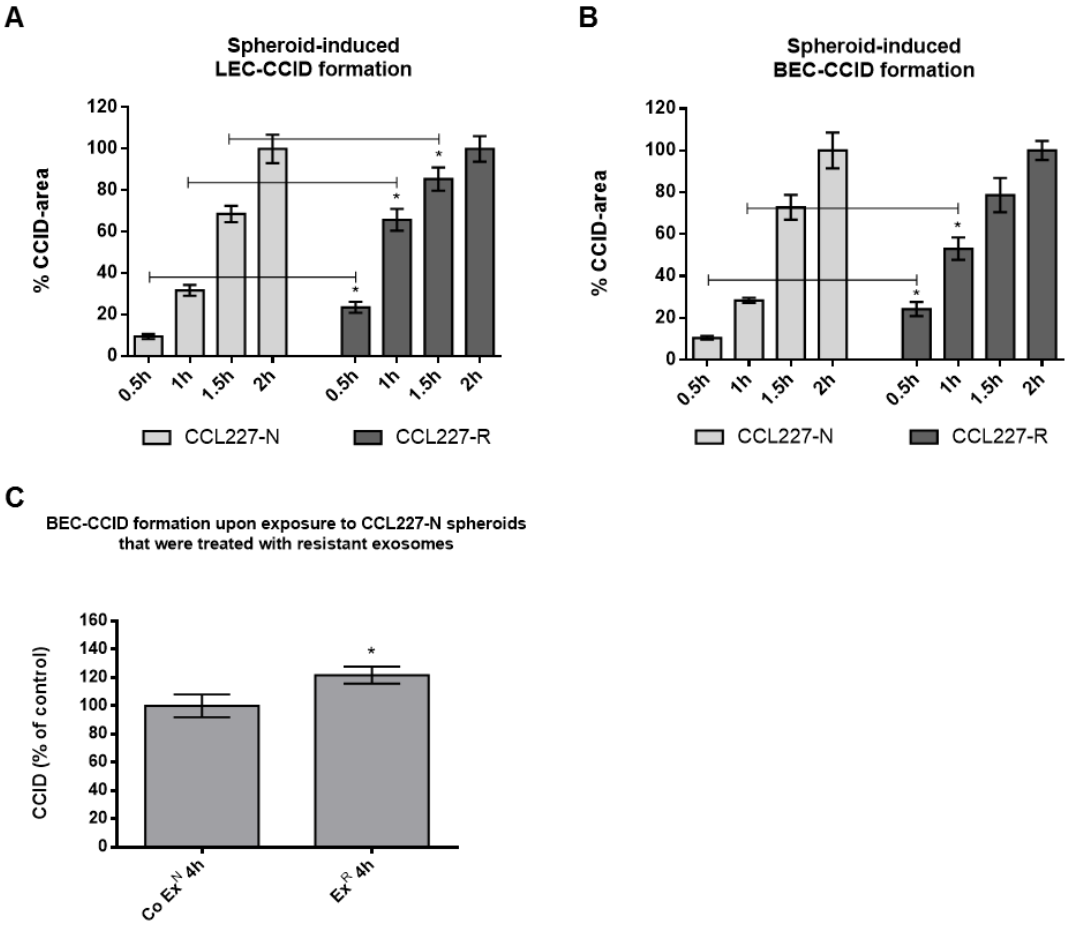

Figure 23: Distinct intravasative properties of naïve and resistant colon cancer phenotypes. Comparison of Spheroid induced (A) LEC-CCID and (B) BEC-CCID formation after 0.5, 1, 1.5 and 2 h. (C) CCL227-N spheroids were incubated with 100 µg exosomal protein derived from naïve (Ex^N) and resistant (Ex^R) CCL227 for 30 min and co-cultivated for 4 h. t-test; $P < 0.05$ and error bars indicate means ± S.E.M.

In detail, CCL227-R spheroids induced LEC-CCID formation significantly stronger within 1.5 h compared to CCL227-N spheroids (Fig.21A-H). CCL227-R increased CCID formation by 15% after 0.5 h, by 35% after 1 h and by 20% after 1.5 h (Fig.23A). The CCID formation in BEC monolayer indicated that CCL227-R spheroids induced BEC-CCID formation significantly stronger within 1 h compared to CCL227-N spheroids (Fig.22A-H). CCL227-R increased CCID formation by 15% after 0.5 h and by 25% after 1 h (Fig.23B). Recently it was shown that CCL227 cells, during the acquisition of drug resistance against 5-FU, have lost the expression of the miR-200 family members. These miR-200 family members are packed into exosomes and released from the cancer cells (Mader et al., 1997; Senfter et al., 2015). Hence, exosomes derived from CCL227-N cells are enriched with miR-200 family members,

whereas CCL227-R exosomes are almost free of miR-200 family members (Senfter et al., 2015). Therefore, we analysed the role of exosomes as potential modulators of CCID formation. An increase of BEC-CCID formation upon exposure to naïve spheroids that were treated with exosomes derived from CCL227-R was observed after 4 h (Fig.23C). Therefore, exosomes from cancer cells influenced the process of CCID formation. We assume that this effect was due to a dilution of miR-containing exosomes of naïve CCL227 cells by miR-depleted exosomes from CCL227-R cells.

Colon cancer derived exosomes reduce CCID formation

A trans-well experiment and subsequent qPCR confirmed an increase of CCL227 derived miRs level in LECs thereby verifying that miRs are horizontally transferred between distinct cell types using exosomes as vehicle (Senfter et al., 2015). By this experimental set-up, it was approved that microRNAs were deposited in cancer-derived exosomes and horizontally transferred into LECs (Senfter et al., 2015).

Notably, colon cancer cells are known to disseminate through both, lymph endothelial- and blood vasculature and here we demonstrate that the metastatic property of colon cancer cells is not only able to modulate the response of adjacent LECs but also of BECs. To confirm our assumption, CCL227-R spheroids were treated with miR-200 rich exosomes derived from naïve colon cancer cells. The BEC-CCID formation was decreased by 20% after 4 h upon treatment (Fig.24).

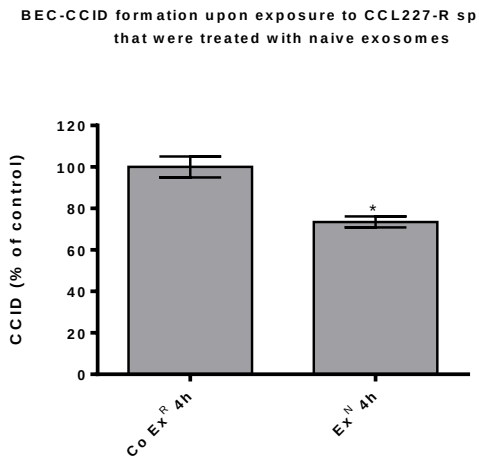

Figure 24: Reduced invasiveness upon treatment with exosomes. CCL227-R spheroids are pretreated 30 min with miR-200 rich exosomes derived from CCL227-N cells and co-cultivated for 4 h (t-test; $P < 0.05$); error bars indicate means ± S.E.M.

Selected miRs-200 repress ZEB transcription factor expression in BECs and inhibit CCID formation

Members of the microRNA-200 family comprising miR-200a, miR-200b miR-200c, miR-141 and miR-429 (Paterson et al., 2013) regulate EMT. To examine which of these members impose the strongest effect on ZEB family expression in BECs, 5 nM miRs precursors were separately transfected. The expression of ZEB1, ZEB2, SNAI, TWIST (SLUG was not expressed) and VE-cadherin were analysed by Western blotting (Fig.25A and B).

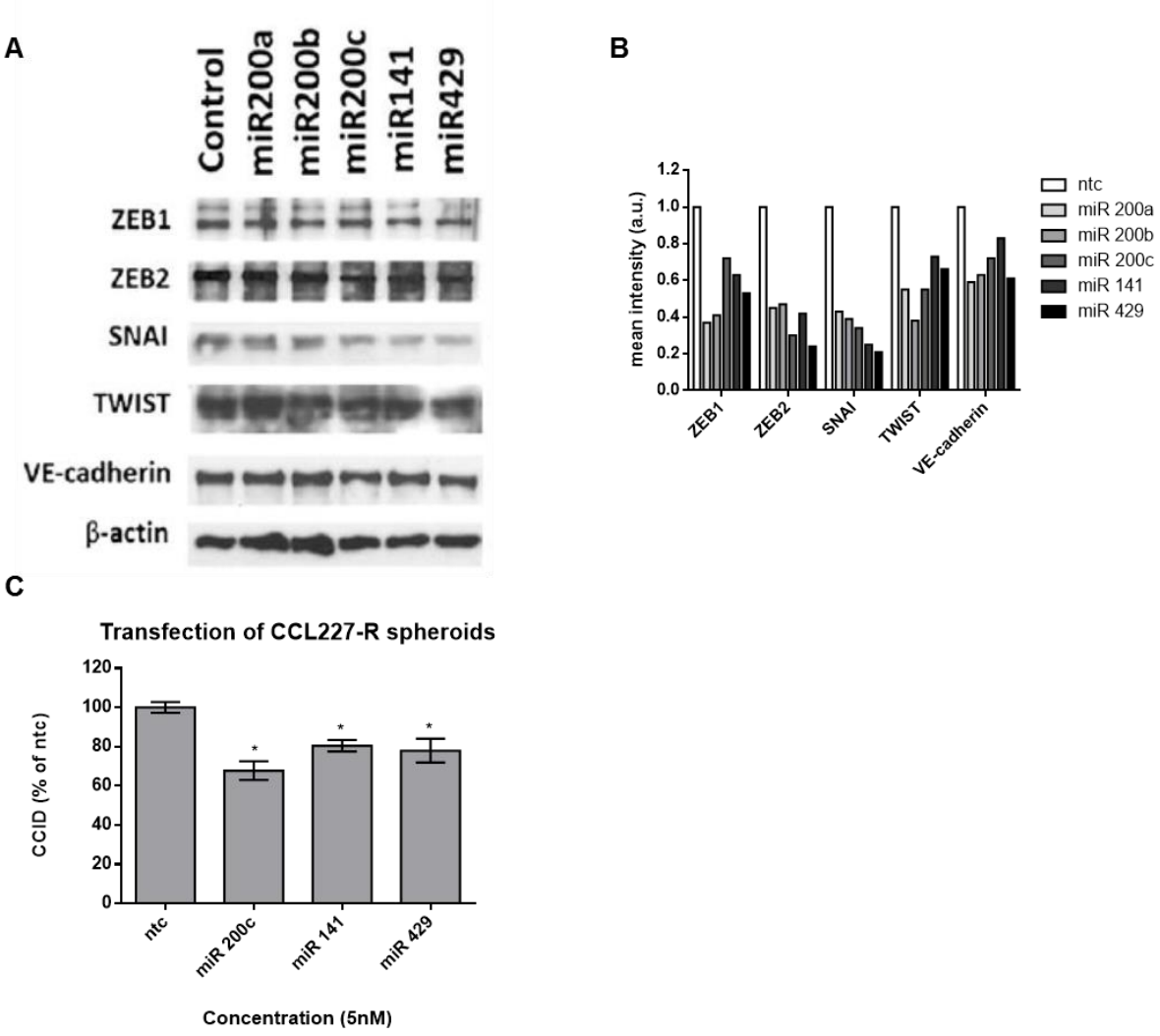

Figure 25: Effect of miR-200 family members on the expression of EMT markers and CCID formation. (A) Detection of the EMT-related transcription factors ZEB1, ZEB2, SNAI, TWIST and VE-cadherin in BECs after transfected with 5 nM miR-200 family precursors or non-targeting control by western blotting. (B) Densitometry analysis of the different transcription

factors normalized by ß-actin expression, represented by mean intensity (arbitrary units). (C) Resistant CCL227 spheroids were transfected with 5 nM miR-200c, miR-141 and miR-429 precursor separately and placed on the BEC monolayer to reverse the highly invasive phenotype. Asterisks indicate significance (one-way ANOVA; $P < 0.05$); error bars indicate mean ± S.E.M.

Western blot analysis indicated a repression of ZEB1, ZEB2, SNAI and TWIST upon transfection of all miRs-200 family members. However, also VE-cadherin was down regulated. Therefore, unlike reciprocal expression (regulation) of E-cadherin by ZEBs in epithelial cells, VE-cadherin in endothelial cells does not seem to be regulated by ZEBs. ZEB1 protein was markedly repressed by miR-200a and miR-200b. TWIST protein was effectively inhibited upon transfection with miR-200c and miR-141. The EMT-inducing transcription factor SNAI1 plays a key role in the mechanism of invasion and metastases through the TGF-β1/SMAD signalling pathway mediated by SNAI1/E-cadherin expression in CRC (Ji et al., 2015). Vitamin D receptor (VDR) repression is a specific effect SNAI1 in CRC progression that is not shared by other EMT inducers such as ZEB1, ZEB2 and TWIST (Larriba et al., 2009). Zheng *et al.* (2014) found that one miR (miR-132) inhibits cell invasion and EMT in CRC through targeting ZEB2. Hence, ZEB2 and SNAI1 seem to play a significant role in the metastatic progression of CRC. In BECs ZEB2 and SNAI1 were most effectively inhibited by miR-200c, miR-141 and miR-429 (Fig.25A and B). Therefore, we attempted to inhibit CCID formation with miR-200c, miR-141 and miR-429 separately, which had the strongest effects on the expression of SNAI1 and ZEB2 in BECs. Resistant colon cancer spheroids were transfected with selected miRs and placed on BEC monolayers. All three precursors (miR-200c, miR-141, miR-429) inhibited CCID-formation significantly (30%, 20%, 20%, respectively) (Fig.25C).

Meidhof *et al.* (2015) found that treatment with the class I HDAC-inhibitor mocetinostat (Fig.26A) treatment reduced the expression of ZEB1 on both mRNA and protein level and weakly upregulated miR-200 family members. Mocetinostat also led to a global increase of histone H3 and H4 acetylation and of the active histone marks (H3ac, H4ac, H3K9ac and H3K4me3) at ZEB1 target gene loci. Treatment of chemo-resistant pancreas carcinoma cells became weakly chemo-sensitive in presence of mocetinostat alone, but mocetinostat had a sensitizing effect for gemcitabine induced apoptosis. Another HDAC-inhibitor is sulforaphane (SFN), a natural secondary metabolite present mostly in the sprouts of cruciferous vegetables (Myzak, Dashwood, Orner, Ho, & Dashwood, 2006; Myzak, Tong, Dashwood, Dashwood, & Ho, 2007). SFN is also

identified to lead to a global increase in histone H3 and H4 acetylation in HT-29 colon cancer cells similar to mocetinostat in cancer cells (Dashwood & Ho, 2007). R,S-Sulforaphane is the synthetic form of the naturally occurring R-Sulforaphane. The R-isomer is the bioactive HDAC-inhibitor (Fig.26B). Therefore, CCL227-N or CCL227-R spheroids were pre-treated with mocetinostat or sulforaphane (R,S-Sulforaphane, a racemic mixture of R- and S-isomers; R-isomer is biologically active) for 20 min and then placed on BEC monolayers to analyze CCID formation. After 3h, mocetinostat and sulforaphane reduced the migration of BECs dose dependently that was induced by CCL227-N and CCL227-R spheroids. Mocetinostat inhibited CCL227-R-induced CCIDs more efficiently (30%, 35%, 40%) than CCIDs induced by CCL227-N spheroids (20%, 25%, 30%) (Fig.27A and B). In contrast, sulforaphane inhibited CCL227-R-induced CCID formation (0%, 10%, 15%, 20%) less efficiently than that induced by CCL227-N spheroids (20%, 20%, 25%, 25%) (Fig.27A and B).

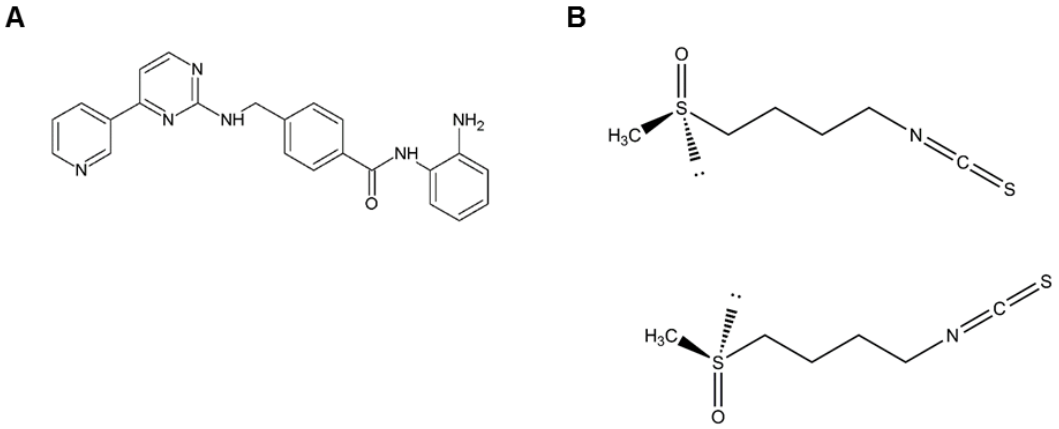

Figure 26: Chemical structures of (A) mocetinostat and (B) R,S-sulforaphane.

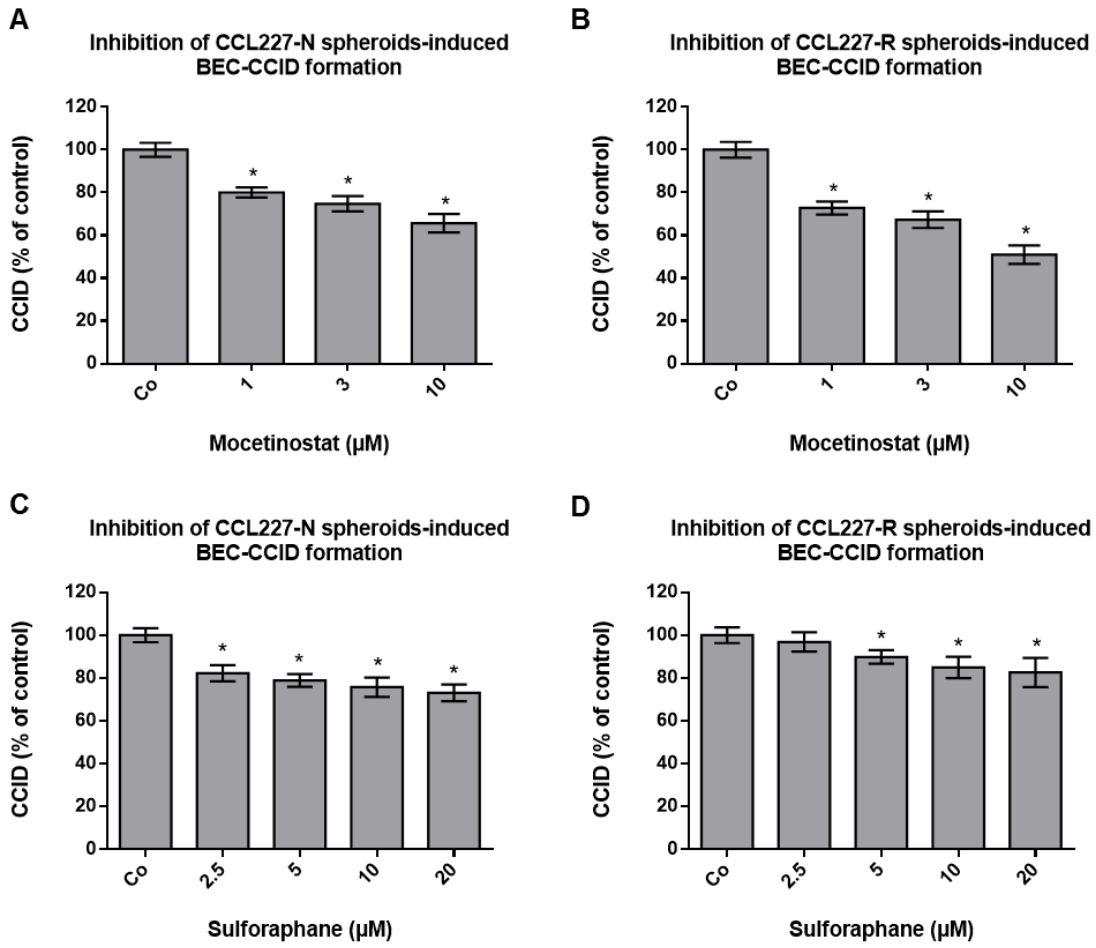

Figure 27: CCID formation inhibition by HDAC-inhibitors. (A-D) Inhibitory effect of mocetinostat and sulforaphane on CCID formation. CCL227-N or CCL227-R spheroids were placed on BEC monolayers and co-cultivated for 3 h either with medium alone and solvent (DMSO; Co) or with increasing concentrations of mocetinostat and sulforaphane. Areas of CCIDs underneath the spheroids were measured. Asterisks indicate significance (one-way ANOVA; $P < 0.05$); error bars indicate mean ± S.E.M.

Colon cancer entry into adjacent stroma

Tumour stroma is involved in the invasive properties of malignant tumours (Dolznig et al., 2011) and to better understand tumourigenesis not only cancer cells are in focus but also the tumour microenvironment. Since CRC spheroids cause the retraction of lymph- and blood endothelial barriers thereby mimicking tumour intra/extra-vasation, it was tested whether they also cause CCID formation in fibroblast monolayers, which would resemble tumour invasion.

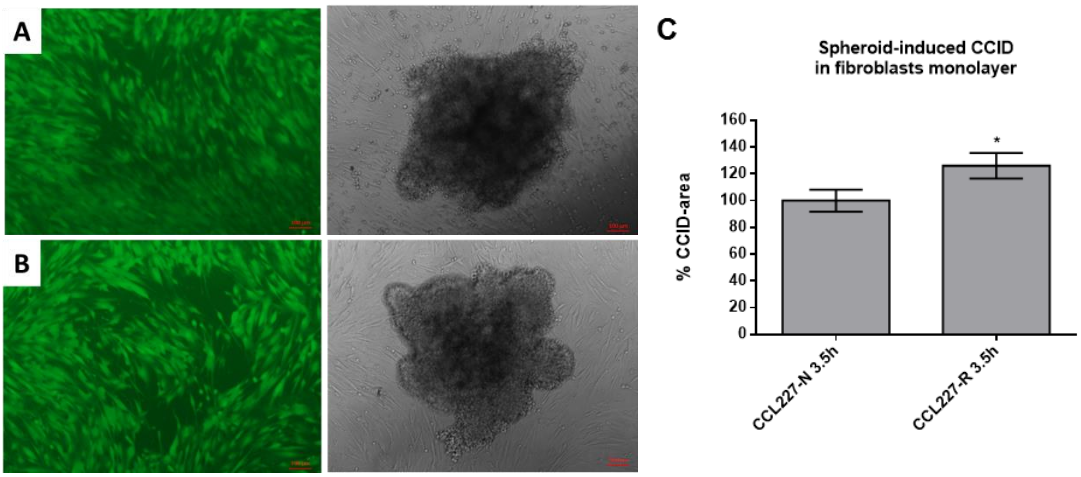

Figure 28: Statement of colon cancer entry into adjacent stroma. Phase contrast images of (A) CCL227-N, (B) CCL227-R spheroids and fluorescence images of the BEC monolayers underneath within the same optical frame to demonstrate the different CCID formation. Scale bar: 200 µm. (C) Colon Cancer spheroids induce the retraction of underneath growing CAFs generating CCIDs through which tumour cells can invade adjacent stroma (t-test; $P < 0.05$); error bars indicate mean ± S.E.M.

Colon tumour cells were grown as multicellular spheroids and subsequently placed onto colon cancer associated fibroblasts (CAFs) monolayers. After 3.5 h of co-cultultivation potential cell free areas directly underneath the CCL227 spheroids were investigated and, in fact, CRC spheroids induced the retraction of underneath growing fibroblasts generating CCIDs through which tumour cells may invade the nearby stroma. Therefore, the fibroblast-based CCID assay can be utilized to study mechanisms also of invasive processes (and not only of intravasative processes) in the course of tumour metastasis. A significant difference was observed between CCL227-N and CCL227-R spheroid-induced CCID formation of CAFs (Fig.28A-C). Therefore the acquisition of resistance to 5-FU also enforces CCID formation of the adjacent stroma.

Pharmacological inhibition of *in vitro* tumour breaching through the blood endothelial barrier

Currently it is impossible to perform successful therapeutic interventions based on molecular tools such as application of miRs. Therefore, pharmacological strategies using drugs that can pass biological membranes (these drugs are usually small) still have to be developed and investigated to combat the progress of cancer.

Principle mechanisms involved in CCID formation

The metabolite 12(S)-HETE that is a product of lipoxygenase 12 and 15 appeared to have a significant role in tumour metastasis (Uchide et al., 2007). 12(S)-HETE was previously shown to increase malignant behavior of some tumours and to increase endothelial cell motility thereby circularly repelling endothelial cells. Therefore, 12(S)-HETE is called "endothelial retraction factor" (Honn et al., 1994) and the effect on endothelial cells "circular chemorepellent induced defect" (Kerjaschki et al., 2011). From previous studies, it was known that breast cancer cell spheroids secret 12(S)-HETE and causes the retraction of lymphendothelial cells (Kretschy et al., 2013). CYP activity in breast cancer spheroids might also contribute to CCID formation of LECs by disturbing arachidonic acid metabolism (Kerjaschki et al., 2011; Vonach et al., 2011). Cytochrome p450 (CYP) and ALOX12/15 use arachidonic acid as a substrate. Also NF-κB activity plays a role for CCID formation and metastasis (N D Perkins & Gilmore, 2006; Neil D. Perkins, 2012; Vonach et al., 2011). Baicalein, bay-11 and proadifen (specific inhibitors of ALOX12/15, NF-κB and CYPs, respectively) significantly inhibit CCID formation in LEC monolayers induced by MCF-7 breast cancer cells (Kerjaschki et al., 2011; Kretschy et al., 2013; Viola et al., 2013). To investigate, whether similar mechanisms are also active in CRC cells, CCL227-N or CCL227-R spheroids were pre-treated with specific inhibitors for 20 min and then they were placed on BEC monolayers to perform CCID assays.

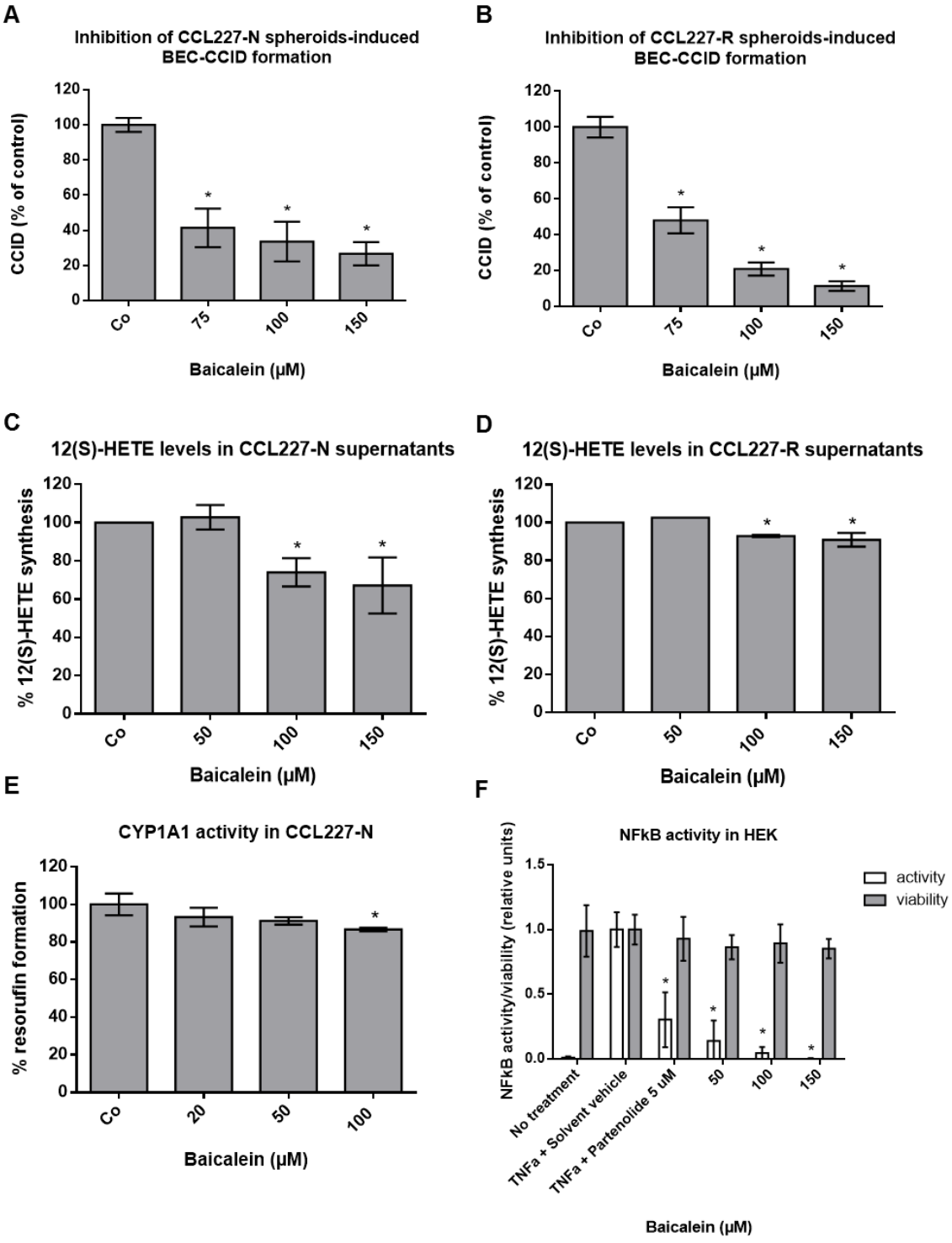

Figure 29: Inhibition of CCIDs by baicalein. CCL227 spheroids (A, B) were placed on BEC monolayers and co-cultivated for 3 h either with medium alone and solvent (DMSO; Co) or with increasing concentrations of baicalein, then the areas of CCIDs were measured. Areas underneath of at least 12 spheroids were analysed. Effect of baicalein on 12(S)-HETE levels. (C) CCL227-N and (D) CCL227-R cells were seeded in 3.5-cm dishes, grown to 80% confluence without selection pressure, and treated with 10 mM arachidonic acid together with the indicated concentrations of baicalein for 4 h. DMSO was used as control (Co). Then, 12(S)-HETE in the cell culture supernatants was measured. Experiments were performed in triplicate. (E) Drug effect on CYP1A1 activity in CCL227-N cells. CCL227-N cells were kept under steroid-free conditions and treated with the indicated concentrations of baicalein, or solvent

(DMSO; Co). 5 μM ethoxyresorufin was added, and after 30 min and 210 min, the formation of resorufin was analysed, which is specific for CYP1A1 activity. (F) Drug effect on NF-κB activation. HEK293-NFκB-Luc cells were transfected with an expression plasmid for green fluorescence protein. After incubation for 6 h, 4×10^4 cells per well were seeded in serum- and phenol red-free DMEM in a 96-transparent-well plate. On the next day, cells were treated with indicated drug concentrations of baicalein or parthenolide as a specific inhibitor of NF-κB, or solvent (DMSO; Co). One hour after treatment, cells were stimulated with 2 ng/ml human recombinant TNFα for additional 4 h. The luciferase signal derived from the NF-κB reporter was normalised by the GFP-derived fluorescence to account for differences in cell number. Asterisks indicate significance (one-way ANOVA compared with untreated control; $P < 0.05$); error bars indicate mean ± S.E.M.

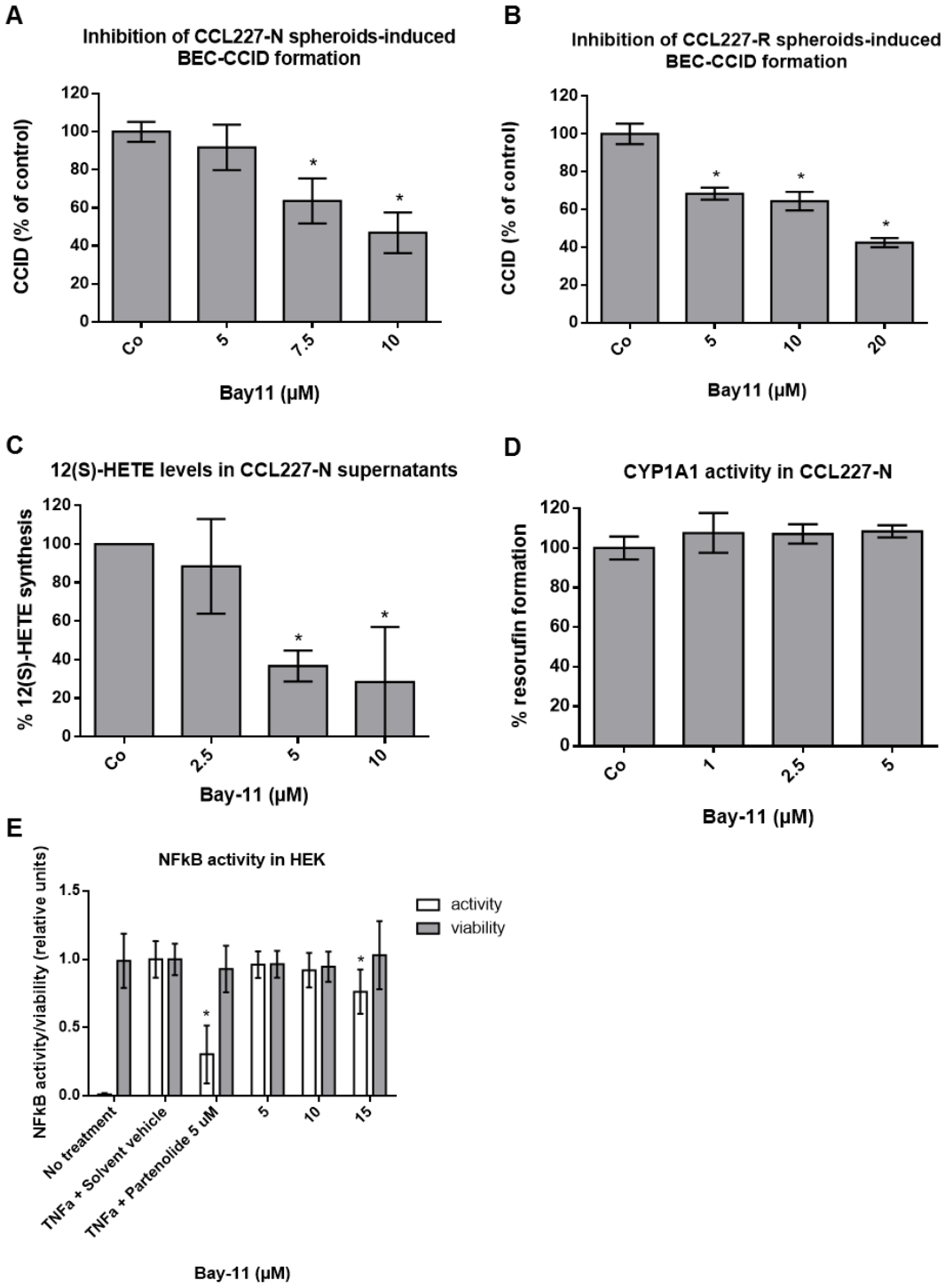

Figure 30: Inhibition of CCIDs by bay-11. CCL227 spheroids (A, B) were placed on BEC monolayers and co-cultivated for 3 h either with medium alone and solvent (DMSO; Co) or with increasing concentrations of bay-11, then the areas of CCIDs were measured. Areas underneath of at least 12 spheroids were analysed. (C) Effect of bay-11 on 12(S)-HETE levels. CCL227-N cells were seeded in 3.5-cm dishes, grown to 80% confluence without selection pressure, and treated with 10 mM arachidonic acid together with the indicated concentrations of bay-11 for 4 h. DMSO was used as control (Co). Then, 12(S)-HETE in the cell culture supernatants was measured. Experiments were performed in triplicate. (D) Drug effect on CYP1A1 activity in CCL227-N cells. CCL227-N cells were kept under steroid-free conditions and treated with the indicated concentrations of bay-11, or solvent (DMSO; Co). 5 µM ethoxyresorufin was added,

and after 30 min and 210 min, the formation of resorufin was analysed, which is specific for CYP1A1 activity. (E) Drug effect on NF-κB activation. HEK293-NFκB-Luc cells were transfected with an expression plasmid for green fluorescence protein. After incubation for 6 h, 4×10^4 cells per well were seeded in serum- and phenol red-free DMEM in a 96-transparent-well plate. On the next day, cells were treated with indicated drug concentrations of bay-11 or parthenolide as a specific inhibitor of NF-κB, or solvent (DMSO; Co). One hour after treatment, cells were stimulated with 2 ng/ml human recombinant TNFα for additional 4 h. The luciferase signal derived from the NF-κB reporter was normalised by the GFP-derived fluorescence to account for differences in cell number. Asterisks indicate significance (one-way ANOVA compared with untreated control; $P < 0.05$); error bars indicate mean ± S.E.M.

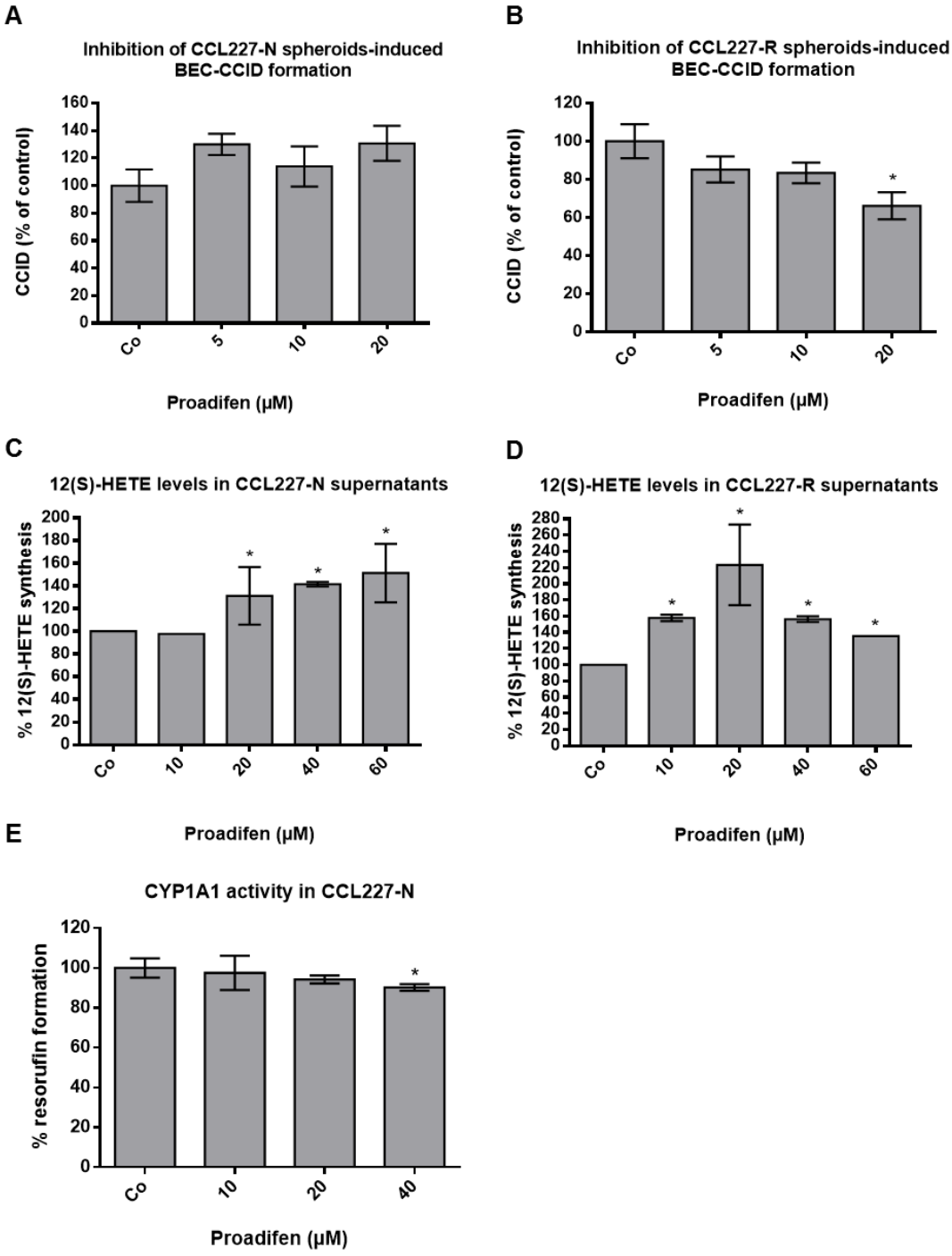

Figure 31: Inhibition of CCIDs by proadifen. CCL227 spheroids (A, B) were placed on BEC monolayers and co-cultivated for 3 h either with medium alone and solvent (DMSO; Co) or with increasing concentrations of proadifen, then the areas of CCIDs were measured. Areas underneath of at least 12 spheroids were analysed. (C, D) Effect of proadifen on 12(S)-HETE levels. CCL227 cells were seeded in 3.5-cm dishes, grown to 80% confluence without selection pressure, and treated with 10 mM arachidonic acid together with the indicated concentrations of proadifen for 4 h. DMSO was used as control (Co). Then, 12(S)-HETE in the cell culture supernatants was measured. Experiments were performed in triplicate. (E) Drug effect on CYP1A1 activity in CCL227-N cells. CCL227-N cells were kept under steroid-free conditions and treated with the indicated concentrations of proadifen, or solvent (DMSO; Co). 5 µM ethoxyresorufin was added, and after 30 min and 210 min, the formation of resorufin was

analysed, which is specific for CYP1A1 activity. Asterisks indicate significance (one-way ANOVA compared with untreated control; $P < 0.05$); error bars indicate mean ± S.E.M.

When CCL227-N colon cancer cells were placed on BECs the treatment with baicalein or bay11 inhibited CCID formation, whereas proadifen did not (Fig.29-31A). The strong inhibition of CCID formation by baicalein implicated that 12(S)-HETE was the major parameter generating CCIDs, however 12(S)-HETE synthesis was inhibited by only 25% upon treatment of CCL227-N cells with 100 µM baicalein, whereas NF-κB activity (in HEK) was inhibited almost completely (Fig.29C and F). This was unexpected, because baicalein was proposed as a *bona fide* inhibitor of ALOX12/15 but not of NF-κB.

Therefore, a cross-check experiment was performed to investigate the effect of the specific NF-κB inhibitor Bay11-7082 on 12(S)-HETE synthesis and NF-κB activity. Interestingly, bay11 inhibited 12(S)-HETE production even stronger than baicalein, but inhibited NF-κB synthesis much less efficiently than baicalein (Fig.30C and E). The data – in contrast to the above assumption- show that the inhibition of NF-κB better correlates with inhibition of CCID formation than inhibition of 12(S)-HETE synthesis. It has to be noted however, that NF-κB activity was measured in HEK cells (and not in CCL227).

The fact that proadifen did not exhibit an inhibitory effect on CCID formation is probably due to weak constitutive CYP activity (Fig.31A). Hence, this mechanism was not responsible for CCID formation induced by CCL227-N spheroids (Fig.31E). Nevertheless, proadifen was taken up by CCL227 cells (and not pumped out by respective proteins that are often overexpressed in cancer cells), because 12(S)-HETE synthesis was induced (Fig.31C). The increase of 12(S)-HETE levels by proadifen was already observed in MCF-7 breast cancer cells (Kretschy et al., 2013).

Since 5-FU-resistant CCL227-R cells were shown to be more aggressive and possess a stronger potential to induce CCID formation CCL227-R cells were also treated with baicalein, bay11 and proadifen (Fig.29-31B). Baicalein and bay11 inhibited CCL227-R-induced CCID formation equal effectively as CCL227-N-induced CCID formation. Hence, neither ALOX12/15 activity nor NF-κB activity are contributing to increased aggressiveness during acquisition of 5-FU-resistance. In contrast, proadifen, a *bona fide* inhibitor of CYPs (but also an inhibitor of NF-κB activity in HEK cells; (Kretschy et al., 2013), inhibited CCL227-R-induced CCID formation, which suggests that during

resistance development, additional mechanisms that are proadifen sensitive and responsible for CCID-formation become activated. This again links the development of chemoresistance mechanisms to a pro-metastatic phenotype. Whether proadifen modulates miR-200 family synthesis/excretion, or whether CYPs pose an own mechanisms to acquisited aggressiveness, needs to be investigated in the future.

Inhibition of mobility and adhesion markers

The formation of the entry gates directly underneath the colon cancer spheroids implicated the induction of BEC migration. Therefore the expression of mobility and adhesion markers were analyzed by western blotting.

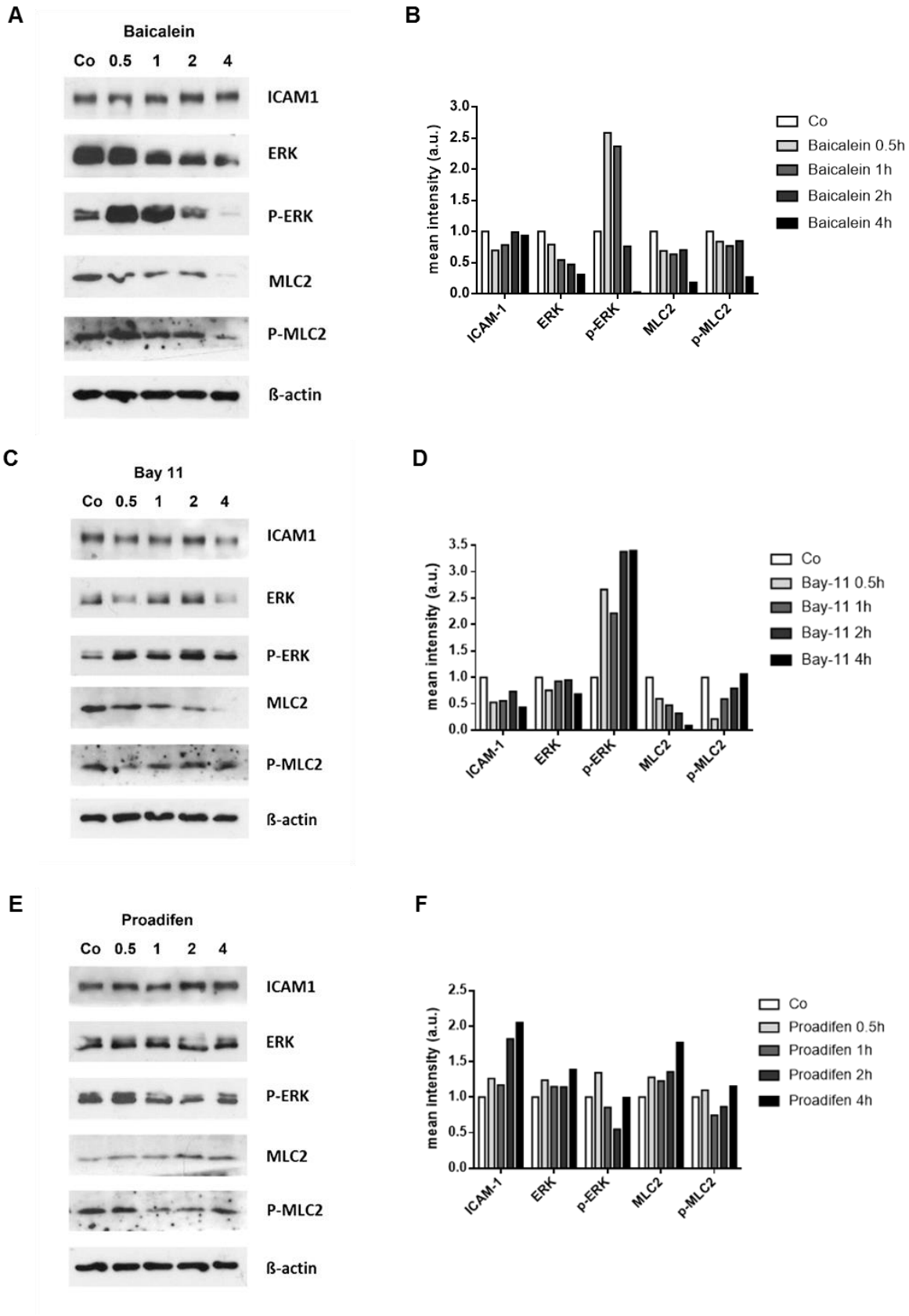

Figure 32: Analysis of protein expression. BECs were treated with (A) 100 µM baicalein, (C) 10 µM bay11 and (E) 20 µM proadifen for 0.5, 2 and 4 h. Then cells were lysed, proteins separated by SDS gel electrophoresis, and subjected to western blotting using the indicated antibodies. Staining with Ponceau S and immunoblotting with anti-β-actin antibody controlled

equal sample loading. (B, D, F) Densitometry analysis of the different mobility and adhesion markers normalized by ß-actin expression, represented by mean intensity (arbitrary units).

Baicalein inhibited the expression of ICAM-1 only transiently, whereas bay11 inhibited ICAM-1 expression for at least 4 h such as observed in LECs (Viola et al., 2013). Interestingly, baicalein activated (phosphorylated) Erk, a process required for a directionally migrating cell, which was strongly increased within 1 h, but then became dephosphorylated and was consequently inactive. In addition, the expression of the protein Erk was also decreased (Fig.32A and B). It was formerly shown that the expression and the phosphorylation patterns of Erk remained unchanged in presence of baicalein in LECs (Viola et al., 2013). Bay11 also strongly induced the phosphorylation of Erk (Fig.32C and D). Proadifen had no inhibitory effect on CCID formation of BECs but even induced ICAM-1 and MLC2 expression in BECs (Fig.32E and F), which implicates that the intravasative potential might have been even pushed by proadifen. This supports the hypothesis that proadifen targeted mechanisms just in resistant CCL227 cells (but not in naïve CCL227 cells or BECs) that are responsible for CCID-formation. This hypothesis was not pursued, however, because the focus of this investigation was on mechanism of the stroma facilitating CCID formation rather than mechanisms that were immanent to the tumour cells.

FDA-drugs: Nifedipin/Isoxsuprine/Acetohexamide/Carbamazepine

Neither baicalein, bay11, nor proadifen are available on prescription or in clinical use. However, recent studies showed that drugs approved by the FDA such as nifedipin, isoxsuprine, acetohexamide, and carbamazepine inhibited CCID formation dose dependently in the 3D model using MCF-7 spheroids and LEC monolayers, and also the putatively underlying mechanisms were analysed (Kretschy et al., 2013; Teichmann et al., 2014). Therefore, these clinical drugs were tested in the CCL227/ BEC model aiming to inhibit CCID formation in the naïve and resistant CRC clones.

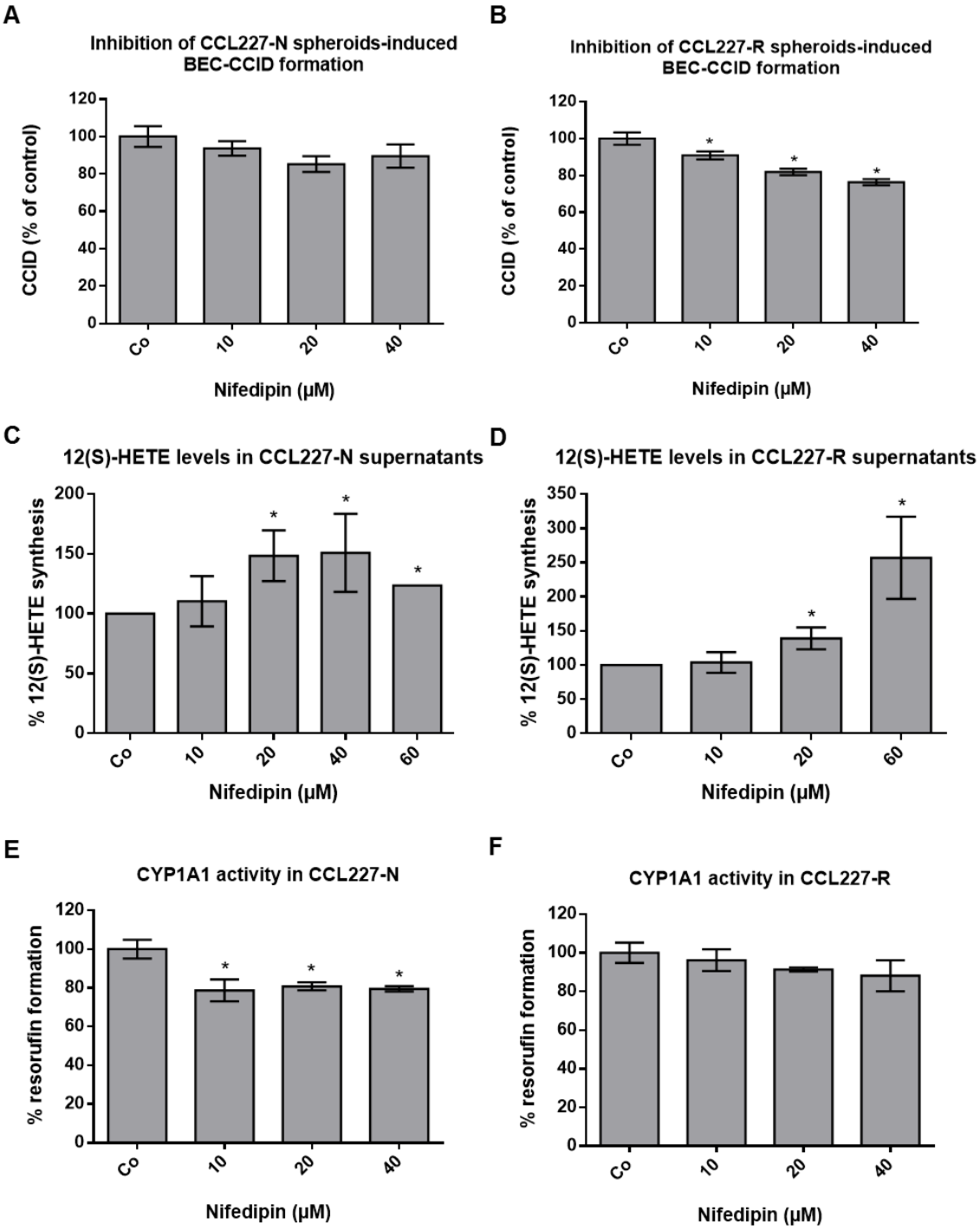

Figure 33: Inhibition of CCIDs by nifedipin. CCL227 spheroids (A, B) were placed on BEC monolayers and co-cultivated for 3 h either with medium alone and solvent (DMSO; Co) or with increasing concentrations of nifedipin, then the areas of CCIDs were measured. Areas underneath of at least 12 spheroids were analysed. (C, D) Effect of nifedipin on 12(S)-HETE levels. CCL227 cells were seeded in 3.5-cm dishes, grown to 80% confluence without selection pressure, and treated with 10 mM arachidonic acid together with the indicated concentrations of nifedipin for 4 h. DMSO was used as control (Co). Then, 12(S)-HETE in the cell culture supernatants was measured. Experiments were performed in triplicate. (E, F) Drug effect on CYP1A1 activity in CCL227-N and CCL227-R cells. CCL227 cells were kept under steroid-free conditions and treated with the indicated concentrations of nifedipin, or solvent (DMSO; Co). 5 µM ethoxyresorufin was added, and after 30 min and 210 min, the formation of resorufin

was analysed, which is specific for CYP1A1 activity. Asterisks indicate significance (one-way ANOVA compared with untreated control; $P < 0.05$); error bars indicate mean ± S.E.M.

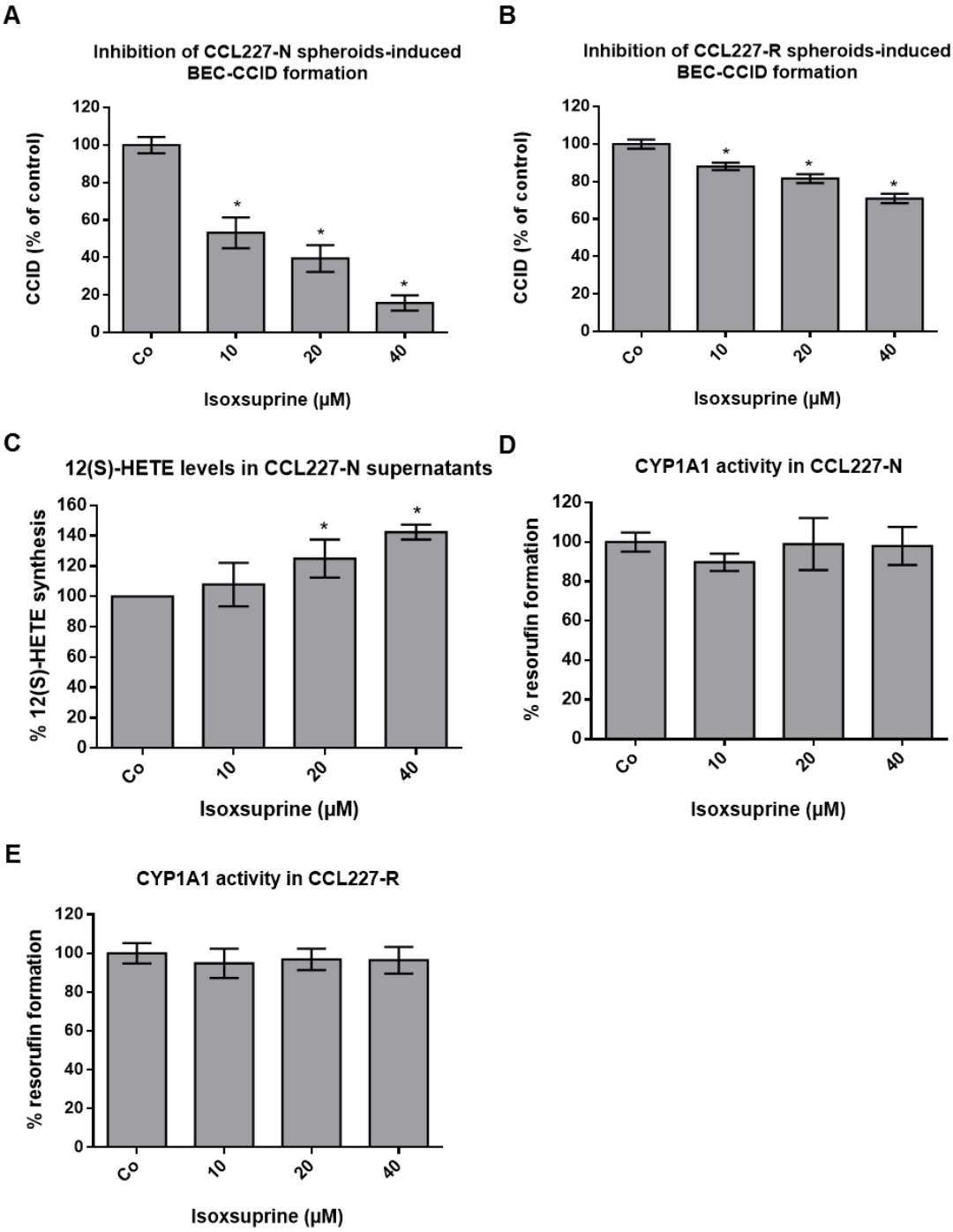

Figure 34: Inhibition of CCIDs by isoxsuprine. CCL227 spheroids (A, B) were placed on BEC monolayers and co-cultivated for 3 h either with medium alone and solvent (DMSO; Co) or with increasing concentrations of isoxsuprine, then the areas of CCIDs were measured. Areas underneath of at least 12 spheroids were analysed. (C) Effect of isoxsuprine on 12(S)-HETE levels. CCL227-N cells were seeded in 3.5-cm dishes, grown to 80% confluence without selection pressure, and treated with 10 mM arachidonic acid together with the indicated

concentrations of isoxsuprine for 4 h. DMSO was used as control (Co). Then, 12(S)-HETE in the cell culture supernatants was measured. Experiments were performed in triplicate. (D, E) Drug effect on CYP1A1 activity in CCL227-N and CCL227-R cells. CCL227 cells were kept under steroid-free conditions and treated with the indicated concentrations of isoxsuprine, or solvent (DMSO; Co). 5 μM ethoxyresorufin was added, and after 30 min and 210 min, the formation of resorufin was analysed, which is specific for CYP1A1 activity. Asterisks indicate significance (one-way ANOVA compared with untreated control; $P < 0.05$); error bars indicate mean ± S.E.M.

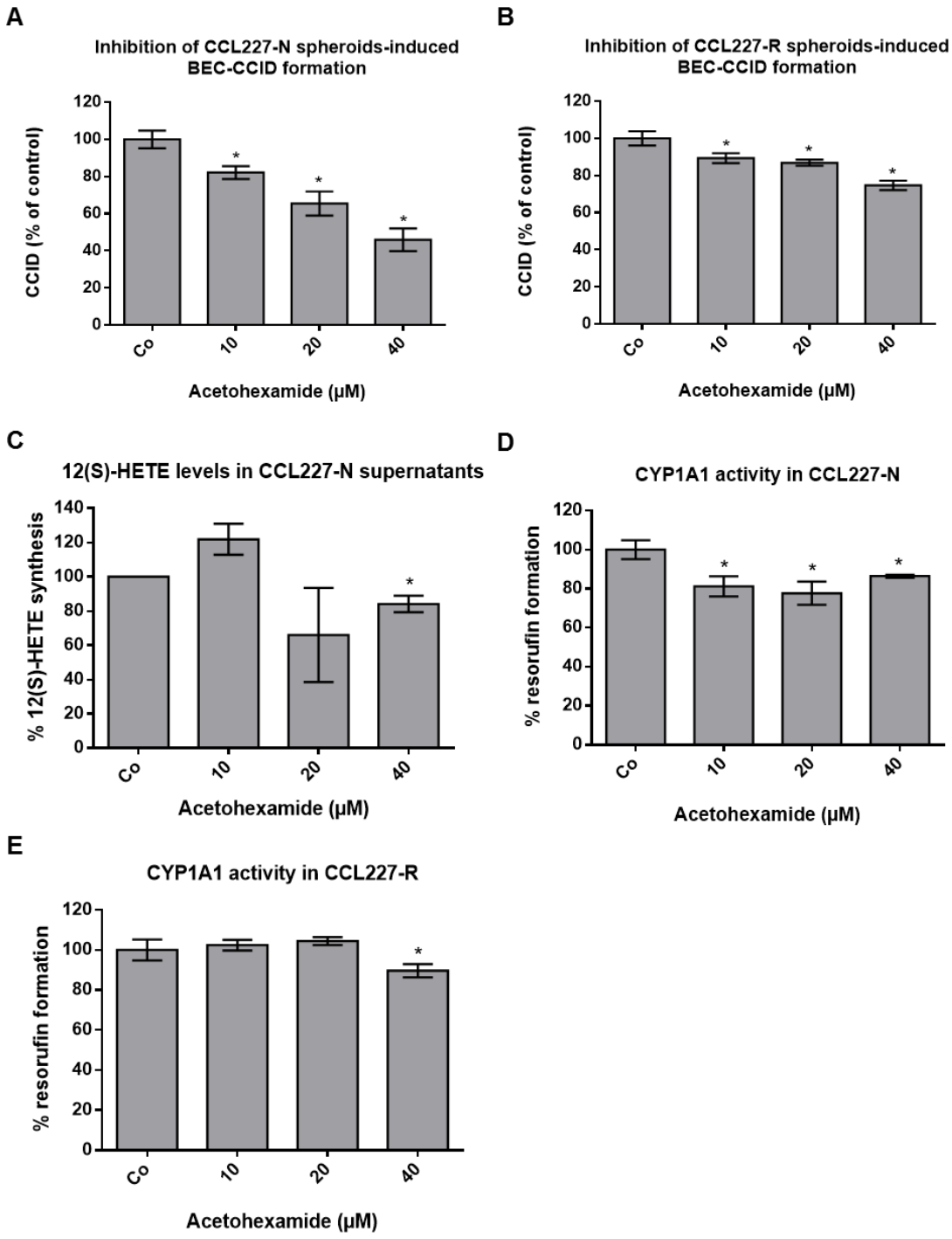

Figure 35: Inhibition of CCIDs by acetohexamide. CCL227 spheroids (A, B) were placed on BEC monolayers and co-cultivated for 3 h either with medium alone and solvent (DMSO; Co) or with increasing concentrations of acetohexamide, then the areas of CCIDs were measured. Areas underneath of at least 12 spheroids were analysed. (C) Effect of acetohexamide on 12(S)-HETE levels. CCL227-N cells were seeded in 3.5-cm dishes, grown to 80% confluence without selection pressure, and treated with 10 mM arachidonic acid together with the indicated concentrations of acetohexamide for 4 h. DMSO was used as control (Co). Then, 12(S)-HETE in the cell culture supernatants was measured. Experiments were performed in triplicate. (D, E) Drug effect on CYP1A1 activity in CCL227-N and CCL227-R cells. CCL227 cells were kept under steroid-free conditions and treated with the indicated concentrations of acetohexamide, or solvent (DMSO; Co). 5 µM ethoxyresorufin was added, and after 30 min and 210 min, the

formation of resorufin was analysed, which is specific for CYP1A1 activity. Asterisks indicate significance (one-way ANOVA compared with untreated control; $P < 0.05$); error bars indicate mean ± S.E.M.

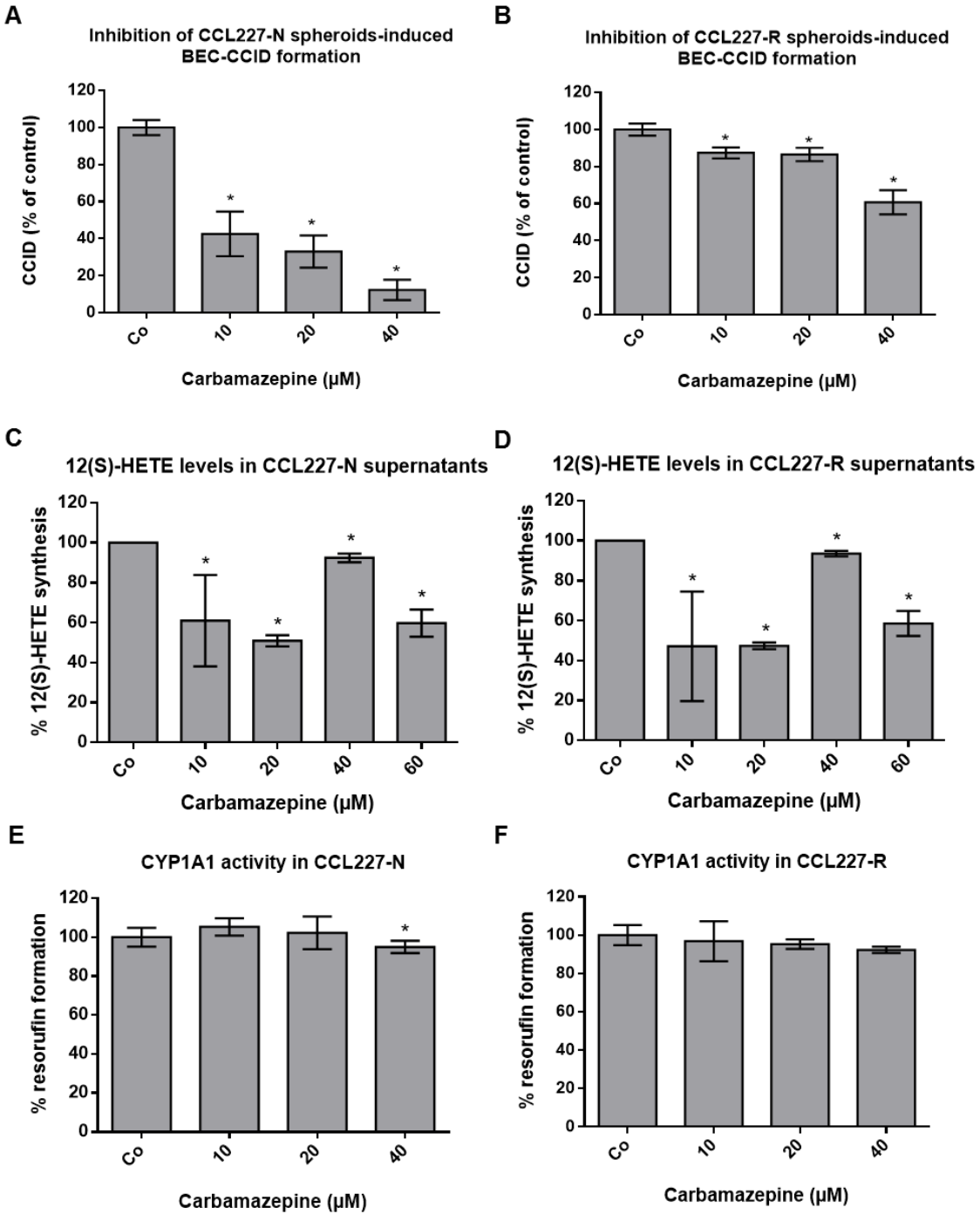

Figure 36: Inhibition of CCIDs by carbamazepine. CCL227 spheroids (A, B) were placed on BEC monolayers and co-cultivated for 3 h either with medium alone and solvent (DMSO; Co) or with increasing concentrations of carbamazepine, then the areas of CCIDs were measured. Areas underneath of at least 12 spheroids were analysed. (C, D) Effect of carbamazepine on 12(S)-HETE levels. CCL227 cells were seeded in 3.5-cm dishes, grown to 80% confluence

without selection pressure, and treated with 10 mM arachidonic acid together with the indicated concentrations of carbamazepine for 4 h. DMSO was used as control (Co). Then, 12(S)-HETE in the cell culture supernatants was measured. Experiments were performed in triplicate. (E, F) Drug effect on CYP1A1 activity in CCL227-N and CCL227-R cells. CCL227 cells were kept under steroid-free conditions and treated with the indicated concentrations of carbamazepine, or solvent (DMSO; Co). 5 µM ethoxyresorufin was added, and after 30 min and 210 min, the formation of resorufin was analysed, which is specific for CYP1A1 activity. Asterisks indicate significance (one-way ANOVA compared with untreated control; $P < 0.05$); error bars indicate mean ± S.E.M.

Whereas nifedipin had no significant effect in naïve CCL227 cells, isoxsuprine, acetohexamide and carbamazepine were strong inhibitors of CCID formation (Fig.33-36A). Recently, it was demonstrated that acetohexamide and isoxsuprine reduce the 12(S)-HETE level, whereas nifedipin and carbamazepine did not alter 12(S)-HETE synthesis in the MCF-7 model (Kretschy et al., 2013; Teichmann et al., 2014). Therefore, we analysed the 12(S)-HETE synthesis in CCL227 supernatants. Nifedipin and isoxsuprine induced 12(S)-HETE production whereas acetohexamide and carbamazepine supressed the 12(S)-HETE levels (Fig.33-36C). Hence, we conclude that 12(S)-HETE inhibition/activation was no reliable predictor and also other mechanisms must exist. Therefore, also CYP activity was analysed, but also this putative mechanism did not correlated with the inhibition of CCID formation (Fig.33E, 34-35D), particularly because carbamacepine, which inhibits CYP1A1 activity in MCF-7 cells (Teichmann et al., 2014), did not inhibit CYP1A1 activity in CCL227-N cells (Fig.36E).

Isoxsuprine, acetohexamide and carbamazepine reduced the migration of BECs that was induced also by CCL227-R spheroids. This inhibition was less efficiently inhibited than that induced by CCL227-N spheroids (Fig.34-36B). In contrast, nifedipin inhibited CCL227-R-induced CCID formation (Fig.33B) more efficiently than that induced by CCL227-N spheroids. This implicated that a mechanism became activated during acquisition of 5-FU resistance, which was contributing to the intravasative phenotype. The CYP1A1 activity in CCL227-R cells was only weakly inhibited by acetohexamide with 40 µM (Fig.35E), whereas nifedipin, isoxsuprine, and carbamazepine did not alter CYP1A1 activity (Fig.33F, 34E and 36F). Importantly, although this mechanism remains undiscovered, it can be targeted by pharmacological drugs. Therefore, additional FDA-approved drugs were screened in the CCL227/BEC model that were found to be inhibitory in other 3D models (Nguyen Huu et al., in preparation).

Effect of selected clinical drugs on CCID formation in BEC barriers

In previous investigations we identified a few clinical drugs as inhibitors of CCID formation in lymphendothelial monolayers that are induced by MCF-7 and MDA-MB231 breast cancer spheroids. Therefore, it was studied whether these drugs also inhibited CCID formation in blood endothelial monolayers that was induced by CCL227 colon cancer spheroids. Although no direct correlation between inhibition of CCID formation in BECs and 12(S)-HETE levels, or NF-κB activity could be observed, these factors doubtlessly do play a role for the formation of CCIDs at least in LECs (Kerjaschki et al., 2011; Kretschy et al., 2013; Vonach et al., 2011). Due to the similarity of CCL227-induced CCID formation in BECs and LECs we, nevertheless, continued to analyse the levels of 12(S)-HETE, NF-κB and CYP activity upon treatment with the here tested drugs.

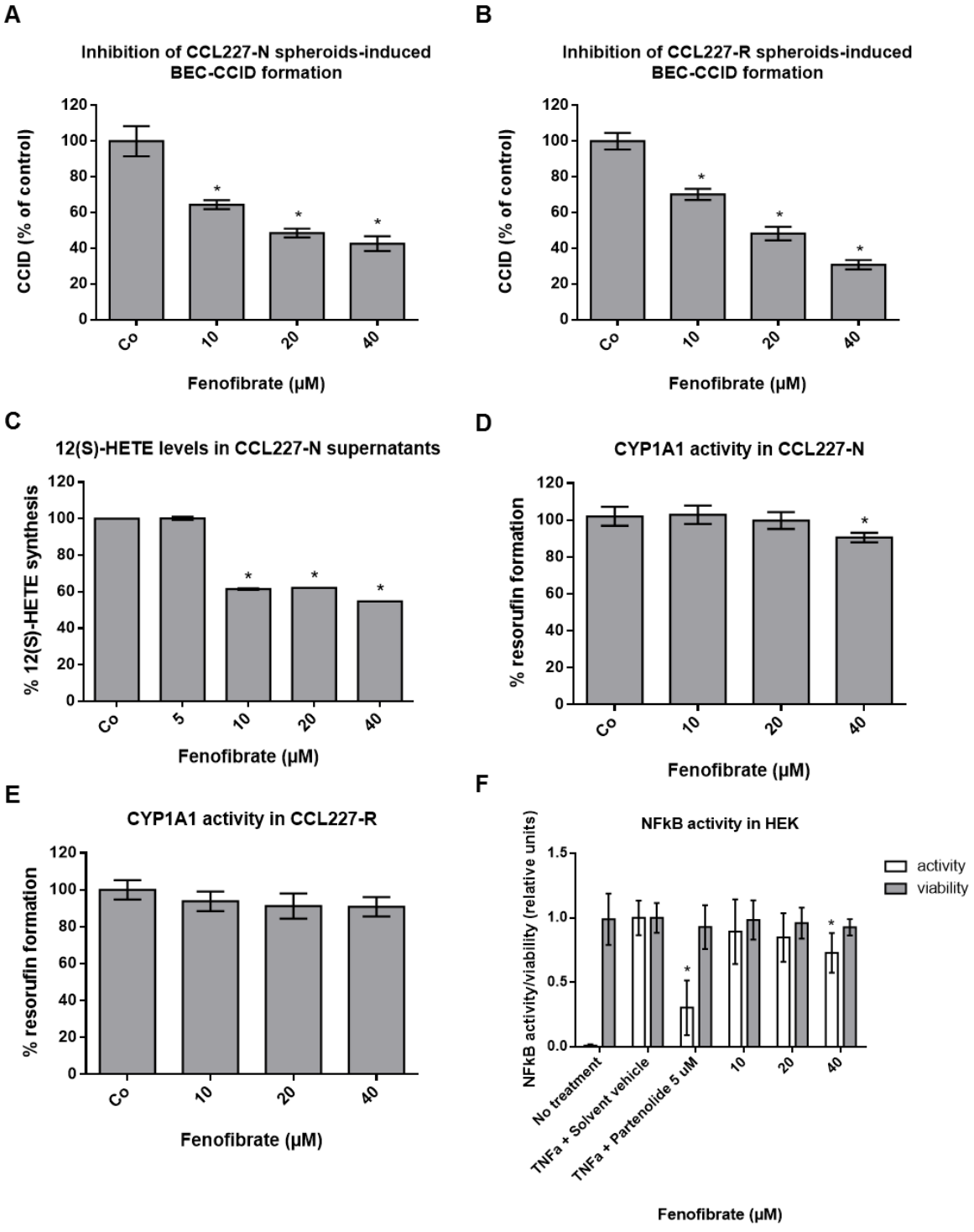

Figure 37: Inhibition of CCIDs by fenofibrate. CCL227 spheroids (A, B) were placed on BEC monolayers and co-cultivated for 3 h either with medium alone and solvent (DMSO; Co) or with increasing concentrations of fenofibrate, then the areas of CCIDs were measured. Areas underneath of at least 12 spheroids were analysed. (C) Effect of fenofibrate on 12(S)-HETE levels. CCL227-N cells were seeded in 3.5-cm dishes, grown to 80% confluence without selection pressure, and treated with 10 mM arachidonic acid together with the indicated concentrations of fenofibrate for 4 h. DMSO was used as control (Co). Then, 12(S)-HETE in the cell culture supernatants was measured. Experiments were performed in triplicate. (D, E) Drug effect on CYP1A1 activity in CCL227-N and CCL227-R cells. CCL227 cells were kept under steroid-free conditions and treated with the indicated concentrations of fenofibrate, or

solvent (DMSO; Co). 5 μM ethoxyresorufin was added, and after 30 min and 210 min, the formation of resorufin was analysed, which is specific for CYP1A1 activity. (F) Drug effect on NF-κB activation. HEK293-NFκB-Luc cells were transfected with an expression plasmid for green fluorescence protein. After incubation for 6 h, 4×10^4 cells per well were seeded in serum- and phenol red-free DMEM in a 96-transparent-well plate. The next day, cells were treated with indicated drug concentrations of fenofibrate or parthenolide as a specific inhibitor of NF-κB, or solvent (DMSO; Co). One hour after treatment, cells were stimulated with 2 ng/ml human recombinant TNFα for additional 4 h. The luciferase signal derived from the NF-κB reporter was normalised by the GFP-derived fluorescence to account for differences in cell number. Asterisks indicate significance (one-way ANOVA compared with untreated control; $P < 0.05$); error bars indicate mean ± S.E.M.

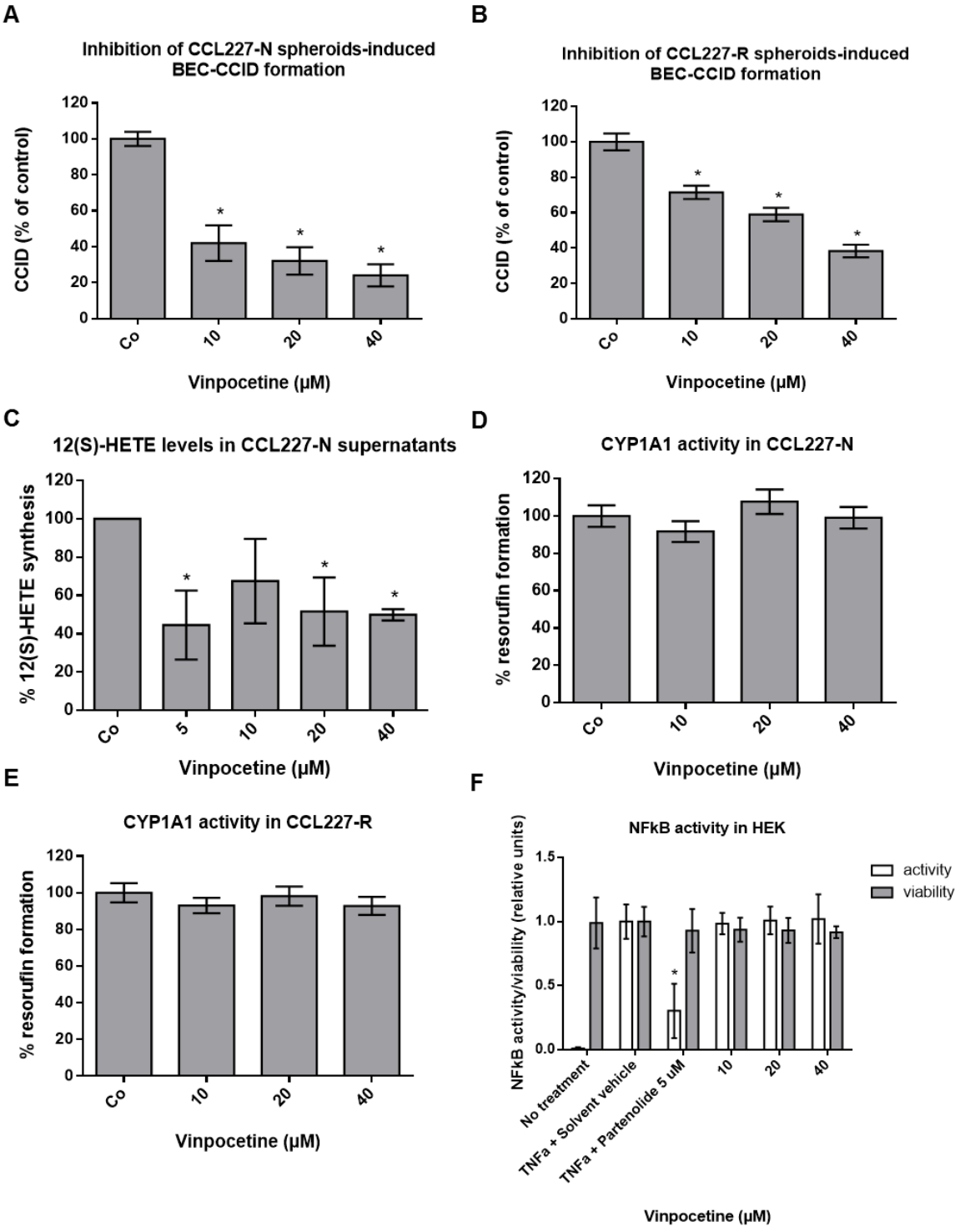

Figure 38: Inhibition of CCIDs by vinpocetine. CCL227 spheroids (A, B) were placed on BEC monolayers and co-cultivated for 3 h either with medium alone and solvent (DMSO; Co) or with increasing concentrations of vinpocetine, then the areas of CCIDs were measured. Areas underneath of at least 12 spheroids were analysed. (C) Effect of vinpocetine on 12(S)-HETE levels. CCL227-N cells were seeded in 3.5-cm dishes, grown to 80% confluence without selection pressure, and treated with 10 mM arachidonic acid together with the indicated concentrations of vinpocetine for 4 h. DMSO was used as control (Co). Then, 12(S)-HETE in the cell culture supernatants was measured. Experiments were performed in triplicate. (D, E) Drug effect on CYP1A1 activity in CCL227-N and CCL227-R cells. CCL227 cells were kept under steroid-free conditions and treated with the indicated concentrations of vinpocetine, or

solvent (DMSO; Co). 5 μM ethoxyresorufin was added, and after 30 min and 210 min, the formation of resorufin was analysed, which is specific for CYP1A1 activity. (F) Drug effect on NF-κB activation. HEK293-NFκB-Luc cells were transfected with an expression plasmid for green fluorescence protein. After incubation for 6 h, 4×10^4 cells per well were seeded in serum- and phenol red-free DMEM in a 96-transparent-well plate. The next day, cells were treated with indicated drug concentrations of vinpocetine or parthenolide as a specific inhibitor of NF-κB, or solvent (DMSO; Co). One hour after treatment, cells were stimulated with 2 ng/ml human recombinant TNFα for additional 4 h. The luciferase signal derived from the NF-κB reporter was normalised by the GFP-derived fluorescence to account for differences in cell number. Asterisks indicate significance (one-way ANOVA compared with untreated control; $P < 0.05$); error bars indicate mean ± S.E.M.

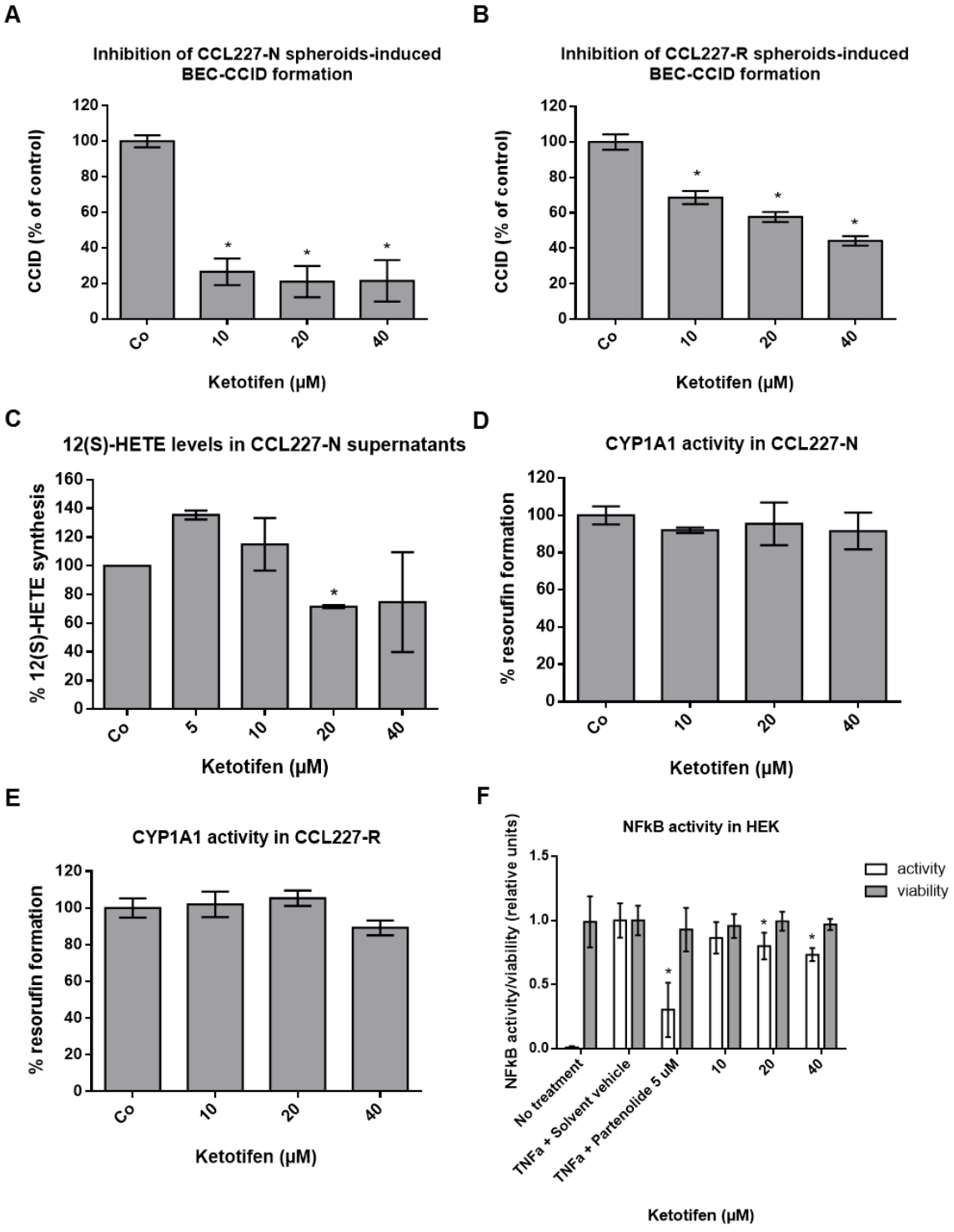

Figure 39: Inhibition of CCIDs by ketotifen. CCL227 spheroids (A, B) were placed on BEC monolayers and co-cultivated for 3 h either with medium alone and solvent (DMSO; Co) or with increasing concentrations of ketotifen, then the areas of CCIDs were measured. Areas underneath of at least 12 spheroids were analysed. (C) Effect of ketotifen on 12(S)-HETE levels. CCL227-N cells were seeded in 3.5-cm dishes, grown to 80% confluence without selection pressure, and treated with 10 mM arachidonic acid together with the indicated concentrations of ketotifen for 4 h. DMSO was used as control (Co). Then, 12(S)-HETE in the cell culture supernatants was measured. Experiments were performed in triplicate. (D, E) Drug effect on CYP1A1 activity in CCL227-N and CCL227-R cells. CCL227 cells were kept under steroid-free conditions and treated with the indicated concentrations of ketotifen, or solvent (DMSO;

Co). 5 μM ethoxyresorufin was added, and after 30 min and 210 min, the formation of resorufin was analysed, which is specific for CYP1A1 activity. (F) Drug effect on NF-κB activation. HEK293-NFκB-Luc cells were transfected with an expression plasmid for green fluorescence protein. After incubation for 6 h, 4×10^4 cells per well were seeded in serum- and phenol red-free DMEM in a 96-transparent-well plate. The next day, cells were treated with indicated drug concentrations of ketotifen or parthenolide as a specific inhibitor of NF-κB, or solvent (DMSO; Co). One hour after treatment, cells were stimulated with 2 ng/ml human recombinant TNFα for additional 4 h. The luciferase signal derived from the NF-κB reporter was normalised by the GFP-derived fluorescence to account for differences in cell number. Asterisks indicate significance (one-way ANOVA compared with untreated control; $P < 0.05$); error bars indicate mean ± S.E.M.

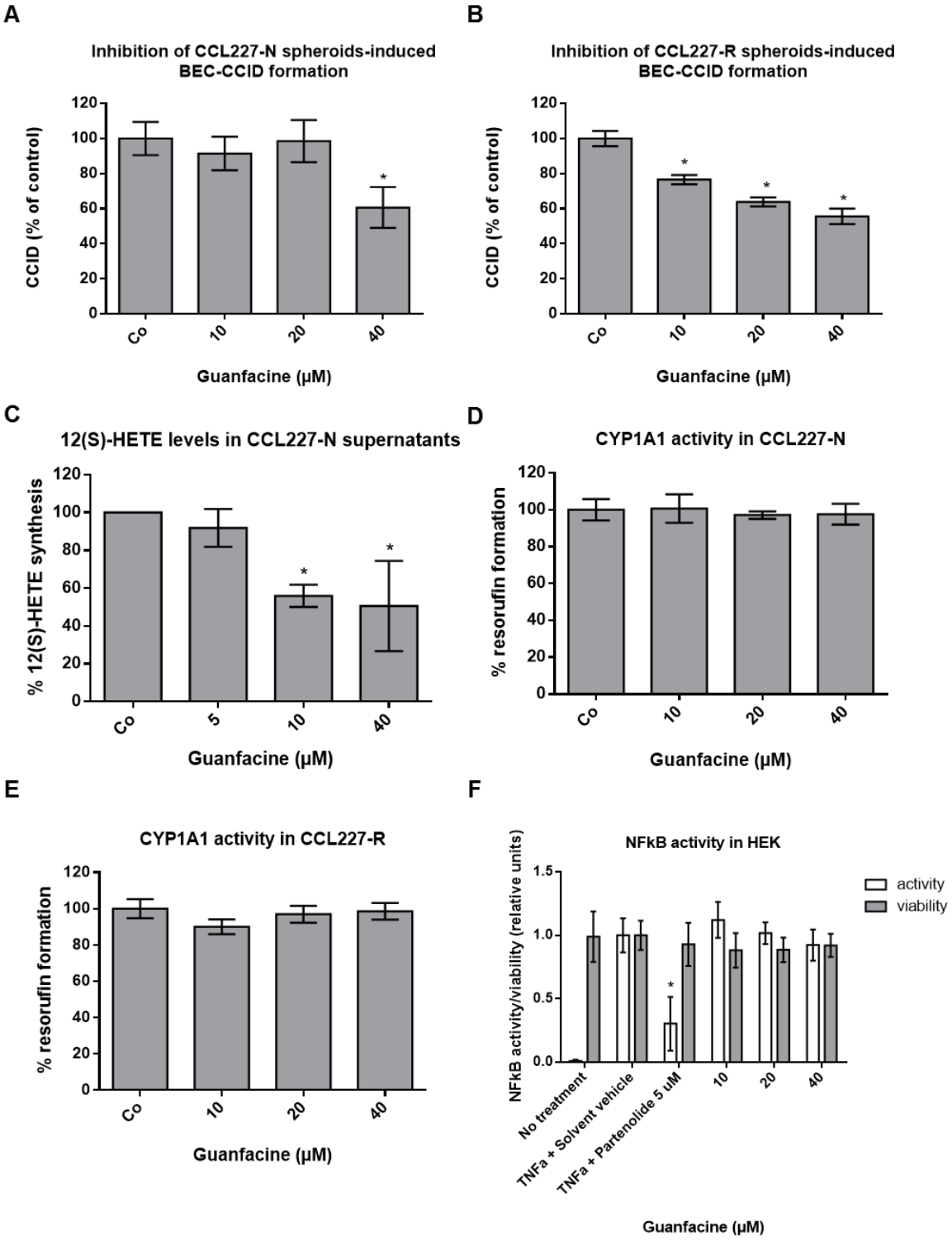

Figure 40: Inhibition of CCIDs by guanfacine. CCL227 spheroids (A, B) were placed on BEC monolayers and co-cultivated for 3 h either with medium alone and solvent (DMSO; Co) or with increasing concentrations of guanfacine, then the areas of CCIDs were measured. Areas underneath of at least 12 spheroids were analysed. (C) Effect of guanfacine on 12(S)-HETE levels. CCL227-N cells were seeded in 3.5-cm dishes, grown to 80% confluence without selection pressure, and treated with 10 mM arachidonic acid together with the indicated concentrations of guanfacine for 4 h. DMSO was used as control (Co). Then, 12(S)-HETE in the cell culture supernatants was measured. Experiments were performed in triplicate. (D, E) Drug effect on CYP1A1 activity in CCL227-N and CCL227-R cells. CCL227 cells were kept

under steroid-free conditions and treated with the indicated concentrations of guanfacine, or solvent (DMSO; Co). 5 µM ethoxyresorufin was added, and after 30 min and 210 min, the formation of resorufin was analysed, which is specific for CYP1A1 activity. (F) Drug effect on NF-κB activation. HEK293-NFκB-Luc cells were transfected with an expression plasmid for green fluorescence protein. After incubation for 6 h, 4×10^4 cells per well were seeded in serum- and phenol red-free DMEM in a 96-transparent-well plate. The next day, cells were treated with indicated drug concentrations of guanfacine or parthenolide as a specific inhibitor of NF-κB, or solvent (DMSO; Co). One hour after treatment, cells were stimulated with 2 ng/ml human recombinant TNFα for additional 4 h. The luciferase signal derived from the NF-κB reporter was normalised by the GFP-derived fluorescence to account for differences in cell number. Asterisks indicate significance (one-way ANOVA compared with untreated control; $P < 0.05$); error bars indicate mean ± S.E.M.

Fenofibrate, vinpocetine and ketotifen strongly inhibited CCID formation at low concentrations, whereas guanfacine had almost no effect (Fig.37-40A). Fenofibrate, vinpocetine and guanfacine reduced 12(S)-HETE synthesis at low concentrations (Fig.37C, 38C and 40C), whereas Fenofibrate only inhibited NF-κB activity weakly at a concentration of 40 µM (Fig.37D). Ketotifen inhibited activation of NF-κB (Fig.39E), but inhibited 12(S)-HETE production much less efficiently than the other compounds (Fig.39D). Vinpocetine, ketotifen, and guanfacine had no inhibitory effect on CYP activity in CCL227-N cells (Fig.37D), whereas fenofibrate only inhibited CYP activity weakly at a concentration of 40 µM (38-40D).

In 5-FU-resistant CCL227-R cells the effect of fenofibrate, vinpocetine and ketotifen on CCID was reduced (Fig.37-39B). In contrast and most interestingly, guanfacine inhibited CCL227-R spheroid-induced CCID formation significantly stronger than that induced by CCL227-N spheroids (Fig.40B). Also CYP activity was not inhibited in CCL227-R cells by fenofibrate, vinpocetine, ketotifen, and guanfacine (Fig.37-40E). This suggests that guanfacine targeted a similar mechanism(s) as proadifen or nifedipin, which became up-regulated in CCL227 cells during the acquisition of chemoresistance. Importantly, guanfacine represents an additional drug that may specifically target the highly malignant phenotype of acquisited 5-FU resistance.

Natural products as leads to develop novel drugs to attenuate breaching

Such as the flavonoid baicalein, also apigenin and hispidulin have similar chemical structures (Fig.41A, B and C). An extract of the traditional healing plant *Scrophularia lucida* was shown to inhibit CCID formation in the MCF-7/LEC model (Giessrigl et al., 2012), and the active principle was identified as hispidulin. Hence, hispidulin was tested regarding CCID inhibition in the CCL227/BEC model and compared to apigenin.

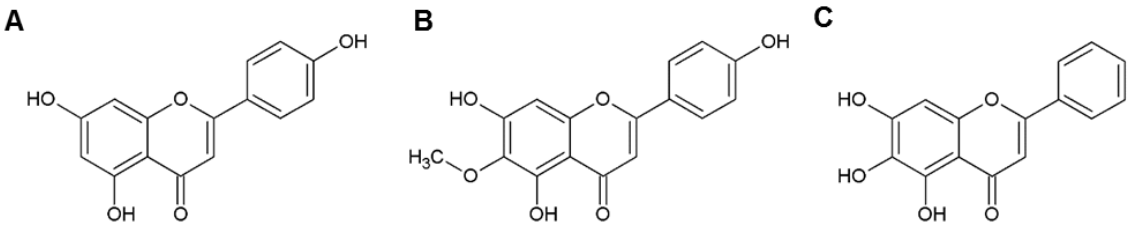

Figure 41: Chemical structures of (A) apigenin, (B) hispidulin and (C) baicalein.

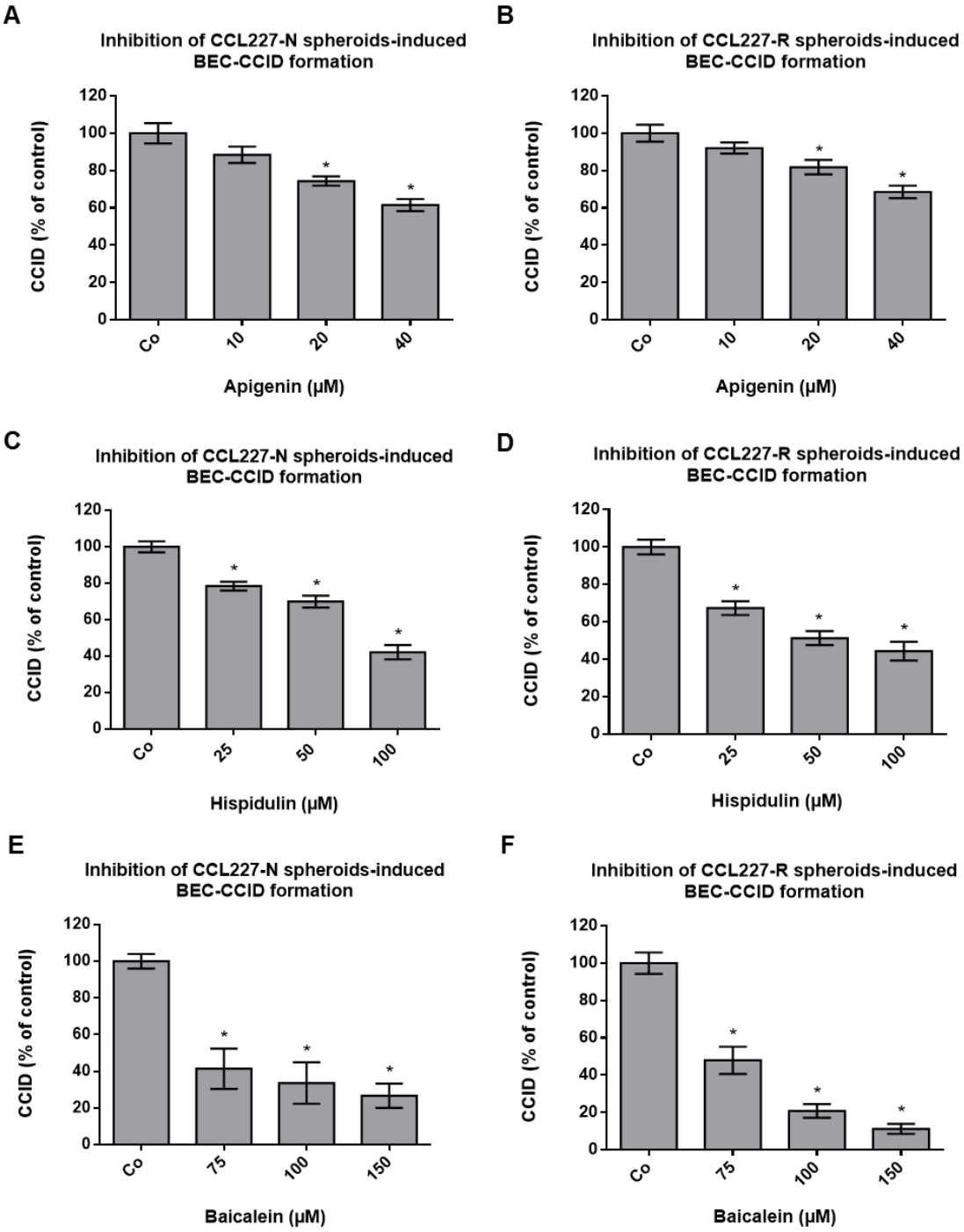

Figure 42: Inhibitory effect of apigenin, hispidulin and baicalein on CCID formation. CCL227 spheroids were placed on BEC monolayers and co-cultivated for 3 h either with medium alone and solvent (DMSO; Co) or with increasing concentrations of apigenin, hispidulin and baicalein, and then the areas of CCIDs were measured. Areas underneath of at least 12 spheroids were analysed. Asterisks indicate significance (one-way ANOVA compared with untreated control; $P < 0.05$); error bars indicate mean ± S.E.M.

The data evidence that baicalein inhibits CCID formation, which was induced by CCL227-N and CCL227-R spheroids more efficiently than hispidulin and apigenin (Fig.42A-F). This implicated that either the hydroxyl group at position C4´ reduced the inhibitory capacity or the hydroxyl group at position C4 was required for a stronger effect. Baicalein is the main component in the traditional Chinese medicine (TCM) formulation Huang-Lian-Jie-Du-Tang (HLJDT), which is used in the traditional treatment of cancer (Ma et al., 2005). Hence, the development of novel drugs from natural products against early steps of metastasis stand a good chance.

4. Discussion

The aim of this investigation was firstly, to test whether CRC spheroids show similar or distinct preference in breaching LEC or BEC barriers and whether the 5-FU resistant CCL227-R clone was more effective than the naïve CCL227-N cell line.

Secondly, to test whether members of the miR-200 family, which were recently reported to become packed into exosomes and released by CCL227 cells (Mader et al., 2011; Senfter et al., 2015), modulate the expression of the ZIB family of transcription factors when transfected into BECs. Thirdly, to study whether the formation of CCIDs in neighboring BEC monolayers was modulated when miR-200 members were re-expressed in CCL227-R spheroids that have lost miR-200 expression during resistance development (Mader et al., 2011; Senfter et al., 2015). Furthermore the capacity of selected compounds such as clinical drugs, which coincidentally inhibit also major CCID-forming pathways, or natural compounds that exist in ethnopharmaceutical herbs and fruits, as well as a bona fide HDAC inhibitor which was and is currently studied in 17 clinical trials (https://clinicaltrials.gov/ct2/results?term=mocetinostat&Search=Search), were tested.

Establishment of a novel CRC/BEC extravasation model

To extend the models of breast cancer MCF-7/LEC intravasation (Kerjaschki et al., 2011; Kretschy et al., 2013; Viola et al., 2013; Vonach et al., 2011), MDA-MB231/LEC extravasation (Nguyen et al., in preparation), hepatocellular carcinoma CCl-13, HCC3, HepG2, HCC-1.2/LEC,BEC barrier breaching (Gauglhofer et al., 2014), CRC CCL227/fibroblast CT5.3 invasion (Stadler et al., in preparation), and CCL227/LEC intravasation (Senfter et al., 2015), these well established 3D cell co-culture models were modified to study breaching (technically extravasation) of CRC through the blood microvascular wall using CCL227 clones and BECs, which were isolated from foreskin and then immortalized by TERT (Schoppmann et al., 2004). The reason for this attempt was the fact that CRC spreads through the lymphatic route generating lymph node metastases as well as through the blood stream, which leads to liver metastases (Gout & Huot, 2008). The CRC/LEC model, which was recently investigated (Senfter et al., 2015), can be now compared to the novel CRC/BEC model.

The present data demonstrate that CCL227 spheroids have no preference regarding the disintegration of LEC or BEC monolayers because they trigger CCID formation in the respective cell barriers with similar kinetics. These observation is in sharp contrast to the findings by Kerjaschki *et al.* (2011) demonstrating that LEC barriers were ~ 5 times more sensitive to MCF-7 spheroid-induced CCID formation than BEC barriers.

Unfortunately, resistance to 5-FU develops in the course of clinical CRC treatment with this standard therapeutic drug. Therefore, it was investigated whether a 5-FU resistant CCL227 subclone (CCL227-R) enforced its malignant activity towards BECs. In fact, the speed of breaching BEC- and LEC monolayers was faster underneath CCL227-R spheroids than under CCL227-N spheroids. This indicated that the plasticity of the endothelial cells was increased in the neighbourhood of 5-FU-resistant CRC spheroids. Consequently, resistant CCL227-R cells possess a higher malignant potential compared to naïve CCL227-N cells, which was recently demonstrated in the CRC/LEC model (Senfter et al., 2015).

MicroRNA-200 family and function in the colon cancer model

The assumption that exosomes act as potential modulators of CCID formation was supported by the fact that naïve CCL227-N spheroids, which were incubated with exosomes derived from the resistant CCL227-R, triggered the formation of significantly larger CCID areas within BEC monolayers than respective controls. Reciprocal experiments inhibited CCID formation. These effects were most likely due to dilution/concentration effects of either miR2-00-depleted or miR-200-enriched exosomes sticking to the spheroid surfaces. Senfter *et al.* (2015) demonstrated an increased metastatic property of resistant colon cancer cells through LEC barriers due to reduced miR-200 levels in their released exosomes. The miR-200 family is composed of five members, which are encoded in two genes on chromosomes 1 (miR-200b, 200a, 429) and 12 (miR-200c, 141) (Paterson et al., 2013).

Because of this miR-200 loss, we examined which of these members impose the strongest effect on EMT marker expression in BECs. All five members inhibited the expression of EMT transcription factors, i.e. ZEB1, ZEB2, SNAI and TWIST. EMT is a key process associated with the progression of CRC and its molecular and cellular implications were widely studied (Gregory, Bracken, et al., 2008; Lamouille et al., 2013; Thiery, 2002). To this end, it was shown that SNAI and ZEB2 contribute to EMT of

CRC and to its invasivity (Beltran et al., 2008; Larriba et al., 2009). In particular, miR-132 was shown to inhibit ZEB2, EMT and invasion of CRC (Zheng et al., 2014). Upon Snail1-induced EMT the synthesis of ZEB2 is up-regulated (Beltran et al., 2008). In human colon cancer, SNAI also shows a repressing effect on VDR, which itself mediates antitumoural action and is lost during colon cancer progression (Larriba et al., 2009).

Here we have shown that miR-200c, miR-141 and miR-429 of the miR-200 family were the strongest suppressors of ZEB2 and SNAI and hence, we focussed on the stromal (BEC) effects of CRC-derived EMT modulators and how this influenced malignant development. For this, precursors of miR-200c, miR-141 and miR-429 were transfected into CCL227-R spheroids, because the expression of the miR-200 family was reduced in the 5-FU-resistant clone (Mader et al., 2011; Senfter et al., 2015). Each of the transfected miR-200 inhibited CCL227-R spheroid-induced CCID formation in BEC monolayers significantly. This indicated that the miR-200 family was not only able to reduce ZIB family expression in adjacent stroma cells, but also to attenuate malignant progression through horizontal transfer of miR-200 to an alien cell type as it was demonstrated for LECs using miR-200c (Senfter et al., 2015). Importantly, cells in the invasive front of colorectal tumours, which have lost the miR-200 family members are more likely to intravasate into the blood or lymphatic system (Paterson et al., 2013).

The downregulation of ZEBs upon transfection of miR-200 into BECs was almost similar compared to LECs (Senfter et al., 2015) despite the fact that miR-200a and miR-200b did not influence ZEB2 expression and miR-200c inhibited SNAI expression only weakly in LECs, whereas both ZEBs were inhibited by these miRs in BECs.

Hence, the mechanisms that have taken over the behaviour of BECs to allow extravasation of CCL227 spheroids seemed to be similar to forcing LECs to open a gate for CCL227 cells to intravasate. The effect on ZEB expression in LECs and BECs seemed to vary slightly with respect to individual miR-200 but was in sum very likely equal, since exosomes from these CRC spheroids contained the entire set of miR-200 family members and not only just one individual miR-200 type.

The expression of VE-cadherin was also down regulated upon miR-200 transfection into BECs. Hence, unlike reciprocal expression of E-cadherin by ZEBs in epithelial cells, VE-cadherin in endothelial cells did not seem to be regulated by ZEBs. In previous experiments it was shown that VE-cadherin was not directly regulated by ZEB1 in LECs (Senfter et al., 2015) and also a knock down of ZEB1 in LECs did not influence the

expression of VE-cadherin (Vonach et al., 2011). Therefore, other mechanisms must have been involved in the regulation of VE-cadherin in BECs, which needs to be established.

HDAC inhibitors mocetinostat and sulforaphane

It was reported that loss of histone acetylation during colon tumour development correlates with advanced tumour stage and tumour invasion, because a reduction in global acetylation of histone H4 was observed in 80% of colon carcinomas and 39% of adenomas (Myzak et al., 2006). Hence, HDAC inhibitors are receiving increasing interest as chemopreventive and chemotherapeutic agents against various cancers. The class I HDAC inhibitor mocetinostat was shown to lead to a re-expression of miR-200 family members which re-establishes sensitivity to gemcitabine-induced apoptosis of otherwise treatment-resistant pancreatic cancer cells (Meidhof et al., 2015). Acetylation/deacetylation events go hand in hand also with DNA methylations/demethylations, which was recently observed for the miR141 and miR-200c loci *in vitro* and *in vivo* (Díaz-Martín et al., 2014). With the goal to re-express miR-200 family members and to reduce malignancy 5-FU-resistant CCL227-R spheroids were treated with mocetinostat, which actually reduced their CCID-forming property to that of naïve CCL227-N spheroids. Whether mocetinostat treatment restored sensitivity of CCL227-R cells to 5-FU (Meidhof et al., 2015) needs to be addressed. Furthermore, it has to be investigated whether mocetinostat treatment re-established miR-200 expression and this will be soon investigated in a separate cooperation. The short treatment time with mocetinostat (4-5 h) seemed to exclude an epigenetic re-arrangement of the chromatin as the causal event for miR-200 re-expression and for reduced aggressiveness. Treatment with the naturally occurring HDAC inhibitor sulforaphane also inhibited CCID formation significantly within 4 h of treatment. A treatment time of 6 h was sufficient to re-arrange the chromatin because within this period HDAC activity was inhibited in mouse colon and caused an increase in acetylated histones after a single oral dose of sulforaphane (Myzak et al., 2006). Švehlíková *et al.* (2004) demonstrated an induction of UGT1A1 and GSTA1 (detoxification enzymes) transcription after 4-6 h and reached the maximum value at 12 and 24 h in CaCo-2 cells upon sulforaphane (20 µM) treatment. Hence, also short treatment time may allow the re-expression of silenced genes. The activation of the promoter regions of *P21* and *bax*

genes as seen in mouse colon after sulforaphane treatment implicates epigenetic alterations in that short treatment period.

Pharmacological inhibition of in vitro tumour extravasation by clinical drugs

A better understanding as to how the tumour cells breach the blood- or lymphatic vasculature slowly emerges and this enables to interfere with mechanisms involved in the metastatic process i.e. by the use of FDA approved drugs. In previous studies, we identified few clinical drugs, which had inhibitory effects on CCID formation in LEC monolayers that are induced by MCF-7 and MDA-MB231 breast cancer spheroids (Nguyen et al., in preparation). We tested these selected drugs in the CRC/BEC model, because of their immediate clinical applicability. Isoxsuprine, acetohexamide, carbamazepine, fenofibrate, vinpocetine and ketotifen were also inhibitors of CCID formation in the here established CCL227-N/BEC model, whereas guanfacine and nifedipin had almost no inhibitory effect.

12(S)-HETE is known to cause retraction of blood microvascular endothelial cells (Honn et al., 1994; Uchide et al., 2007; Viola et al., 2013) as well as retraction of LECs (Kerjaschki et al., 2011) and CCL227 clones and MCF-7 cells were shown to secrete substantial amounts of this metabolite (Kerjaschki et al., 2011; Senfter et al., 2015). Under physiological conditions, 12(S)-HETE is produced by leucocytes, platelets, smooth muscle cells, neurons, epithelium and fibroblast cells (Honn et al., 1994; Viola et al., 2013). The reduced 12(S)-HETE secretion of CCL227-N cells upon treatment with fenofibrate, vinpocetine, guanfacine, acetohexamide and carbamazepine was most likely responsible for their in CCID inhibitory effect whereas nifedipin and isoxsuprine, in contrast, induced 12(S)-HETE production. This indicated that 12(S)-HETE was only one of more factors triggering CCID formation and hence, also other mechanisms must exist. The analysis of CYP activity, which is also involved in the processing of arachidonic acid into 12-S-HETE (yet independent of lipoxygenases activity), did not elucidate why these drugs inhibited CCID formation, because carbamazepine, an inhibitor of CYP1A1 activity in MCF-7 cells (Teichmann et al., 2014) had no effect in CCL227-N cells. CCL227-R induced-CCID formation was less efficiently inhibited by isoxsuprine, acetohexamide and carbamazepine compared to CCL227-N induced CCIDs. Interestingly, nifedipin had an inhibitory effect on CCID formation that was

induced by CCL227-R. This implicated that a metastatic mechanism became activated during acquisition of 5-FU resistance, which was targeted by nifedipin and also guanfacine inhibited the CCL227-R spheroids induced CCID formation more efficiently compared to CCL227-N spheroids.

Besides 12(S)-HETE also the activity NF-κB is involved in the formation of CCIDs in LECs (Kerjaschki et al., 2011; Kretschy et al., 2013; Viola et al., 2013). Due to the similarity of CCL227-induced CCID formation in BECs and LECs, we analysed also NF-κB activity which was inhibited by ketotifen.

Pharmacological inhibition of specific pathways involve in CCID formation

Typical pathway inhibitors such as baicalein (inhibitor of lipoxygenase ALOX12/15), Bay11-7082 (NF-κB inhibitor) and proadifen (inhibitor of CYPs) were tested as a proof of principle to address whether the CRC/BEC model entertains similar pathways of CCID formation as in breast cancer/LEC models (Kerjaschki et al., 2011; Kretschy et al., 2013; Viola et al., 2013). Baicalein and Bay11-7082 inhibited CCID formation that was triggered by naïve CCL227-N spheroids whereas proadifen had no inhibitory effect. Interestingly, the *bona fide* ALOX12/15 inhibitor baicalein inhibited NF-κB activity more effectively than Bay11-7082, and the *bona fide* NF-κB inhibitor Bay11-7082 inhibited 12(S)-HETE secretion more efficiently than baicalein. This fact indicated that inhibition of NF-κB activity, rather than ALOX12/15 activity, correlated with inhibition of CCID. NF-κB is involved in inflammatory processes and therefore, it was concluded that inflamed tumour-stroma poses an additional threat to cancer progression. Proadifen, a *bona fide* inhibitor of CYP activity had no effect on CCID formation probably because of weak constitutive CYP activity in CCL227-N cells. Hence, CYP was not responsible for CCID formation induced by CCL227-N spheroids. Since proadifen induced 12(S)-HETE synthesis in CCL227 cells it can be excluded that proadifen was pumped out by respective proteins that are often overexpressed in cancer cells. This increase of 12(S)-HETE levels by proadifen was also seen in MCF-7 breast cancer cells (Kretschy et al., 2013). We assume that during resistance development, additional CCID-forming mechanisms become activated that are targeted by the drugs nifedipin, guanfacine and proadifen because they inhibited CCIDs that were triggered by the resistant CCL227-R spheroids. Importantly, although these mechanisms remained undiscovered, they could be targeted by pharmacological drugs.

The CCL227-induced CCID formation requires BEC mobility and the adhesion to the tumour spheroids through activation/expression of MLC2, Erk1/2 and ICAM-1, respectively. These mobility markers may provide a mechanistic explanation for the inhibitory effects of the candidate drugs in the CCID-forming process, because baicalein transiently inhibited the expression of ICAM-1 in BECs and decreased the phosphorylation level of MLC2 and transiently increased that of Erk1/2. This was in contrast to the unchanged phosphorylation levels of MLC2 and Erk1/2 upon treatment of LECs with baicalein (Viola et al., 2013). The reason for the distinct response of LECs and BECs awaits elucidation.

The specific NF-κB inhibitor Bay11-7082 decreased ICAM-1 in LECs (Viola et al., 2013) and in BECs, in which also MLC2 expression was affected, and interfered therefore, with adhesion and mobility.

Proadifen induced ICAM-1 and MLC2 expression in BECs and this could explain why proadifen did not inhibit CCL227-N-triggered CCID formation in BECs. This supports the hypothesis that proadifen targeted mechanisms exclusively activated in resistant CCL227-R cells (but neither in naïve CCL227-N cells nor in BECs) that are responsible for CCID-formation. This hypothesis was not pursued, however, because the focus of this investigation was on mechanism of the stroma facilitating CCID formation rather than mechanisms that were immanent to the tumour cells. The data suggest that blocking interactions between tumour and stromal cells could provide new potential targets for therapeutic interventions.

The question arises whether the inhibition of mechanisms of *in vitro* extravasation of tumours through blood vessels can apply to human patients? It is conceivable to short-term-cultivate and test individual samples from tumour metastases of human patients and treat them with the here listed FDA-approved drugs to rapidly enable an improved therapy from bench to bedside.

Natural compounds and traditional medicine

Baicalein is isolated from the roots of *Scuttelaria baicalensis* (Ma et al., 2005) and Traditional Chinese Medicine uses baicalein, which is the main constituent of the well-established herbal mixture Huang-Lian-Jie-Du-Tang (HLJDT), for the treatment of various diseases such as gastritis, dermatitis and cancer. Therefore, natural products are

of particular interest, because of their availability, tolerability and multi-target properties (Viola et al., 2013).

In search of new natural compounds, we identified apigenin and hispidulin to achieve the CCID inhibitory effects as well. Due to the strong structural similarity to baicalein, apigenin and hispidulin may target the same CCID forming mechanisms. The strongest effect was observed for baicalein, which indicated that either the hydroxyl group at position C4´ reduced the inhibitory capacity or the hydroxyl group at position C4 was required for a stronger effect. These CCID inhibitory findings correlate with the induction of cell-cycle arrest by five of seven tested apigenin analogs in human colon carcinoma cell lines (Patel, Shukla, & Gupta, 2007). Hispidulin is reported to have antioxidative, antifungal, anti-inflammatory and antimutagenic activities (Kavvadias et al., 2004).

Conclusion

Summing up, a new 3D *in vitro* model was established recapitulating CRC extravasation through the blood endothelial barrier.

Furthermore, we demonstrate that the miR-200 family acts epigenetically across cell type boundaries as anti-metastatic mechanism.

Chemoresistant colon cancer cells acquire an increased metastatic property, because miR-200 are repressed and transfection of miR-200c, miR-141 and miR-429 reduced CCID formation of BECs and therefore, *in vitro* malignancy of resistant colon cancer spheroids.

MicroRNAs are not established as therapeutic strategy and therefore, a few FDA-approved drugs that inhibited CCID formation can be used instead.

5. References

Al-Hajj, M., & Clarke, M. F. (2004). Self-renewal and solid tumor stem cells. *Oncogene*, *23*(43), 7274–7282. http://doi.org/10.1038/sj.onc.1207947

Aslam, M. I., Patel, M., Singh, B., Jameson, J. S., & Pringle, J. H. (2012). MicroRNA manipulation in colorectal cancer cells: from laboratory to clinical application. *Journal of Translational Medicine*, *10*(1), 128. http://doi.org/10.1186/1479-5876-10-128

Baldwin, a. S. (2001). Control of oncogenesis and cancer therapy resistance by the transcription factor NF-κB. *Journal of Clinical Investigation*, *107*(3), 241–246. http://doi.org/10.1016/S0304-419X(00)00002-0

Beltran, M., Puig, I., Peña, C., García, J. M., Álvarez, A. B., Peña, R., … Herreros, A. G. De. (2008). A natural antisense transcript regulates Zeb2 / Sip1 gene expression during Snail1-induced epithelial – mesenchymal transition, 756–769. http://doi.org/10.1101/gad.455708.in

Botteri, E., Iodice, S., Bagnardi, V., Raimondi, S., Lowenfels, a. B., & Maisonneuve, P. (2008). Smoking and Colorectal Cancer: A Meta-analysis. *JAMA: The Journal of the American Medical Association*, *300*(23), 2765–2778. http://doi.org/10.1001/jama.2008.839

Camacho, L., Guerrero, P., & Marchetti, D. (2013). MicroRNA and Protein Profiling of Brain Metastasis Competent Cell-Derived Exosomes. *PLoS ONE*, *8*(9). http://doi.org/10.1371/journal.pone.0073790

Chao, J.-I., Su, W.-C., & Liu, H.-F. (2007). Baicalein induces cancer cell death and proliferation retardation by the inhibition of CDC2 kinase and survivin associated with opposite role of p38 mitogen-activated protein kinase and AKT. *Molecular Cancer Therapeutics*, *6*(11), 3039–3048. http://doi.org/10.1158/1535-7163.MCT-07-0281

Cheng, H., Zhang, L., Cogdell, D. E., Zheng, H., Schetter, A. J., Nykter, M., … Zhang, W. (2011). Circulating plasma MiR-141 is a novel biomarker for metastatic colon cancer and predicts poor prognosis. *PLoS ONE*, *6*(3), 1–8. http://doi.org/10.1371/journal.pone.0017745

Dashwood, R. H., & Ho. (2007). Dietary histone deacetylase inhibitors: From cells to mice to man. *Semin Cancer Biol.*, *17*(5), 363–369. http://doi.org/10.1016/j.biotechadv.2011.08.021.Secreted

De Angelis, P. M., Svendsrud, D. H., Kravik, K. L., & Stokke, T. (2006). Cellular response to 5-fluorouracil (5-FU) in 5-FU-resistant colon cancer cell lines during treatment and recovery. *Molecular Cancer*, *5*, 20. http://doi.org/10.1186/1476-4598-5-20

De Krijger, I., Mekenkamp, L. J. M., Punt, C. J. a, & Nagtegaal, I. D. (2011). MicroRNAs in colorectal cancer metastasis. *The Journal of Pathology*, *224*(4), 438–447. http://doi.org/10.1002/path.2922

Deryugina, E. I., & Quigley, J. P. (2006). Matrix metalloproteinases and tumor metastasis. *Cancer and Metastasis Reviews*, *25*(1), 9–34. http://doi.org/10.1007/s10555-006-7886-9

Díaz-Martín, J., Díaz-Lõpez, A., Moreno-Bueno, G., Castilla, M. Á., Rosa-Rosa, J. M., Cano, A., & Palacios, J. (2014). A core microRNA signature associated with inducers of the epithelial-to-mesenchymal transition. *Journal of Pathology*, *232*(3), 319–329. http://doi.org/10.1002/path.4289

Dolznig, H., Rupp, C., Puri, C., Haslinger, C., Schweifer, N., Wieser, E., … Garin-Chesa, P. (2011). Modeling colon adenocarcinomas in vitro: A 3D co-culture system induces cancer-relevant pathways upon tumor cell and stromal fibroblast interaction. *American Journal of Pathology*, *179*(1), 487–501. http://doi.org/10.1016/j.ajpath.2011.03.015

Duda, D. G., Ancukiewicz, M., Isakoff, S. J., Krop, I. E., & Jain, R. K. (2014). Seeds and Soil: Unraveling the Role of Local Tumor Stroma in Distant Metastasis. *JNCI Journal of the National Cancer Institute*, *106*(8), dju187–dju187. http://doi.org/10.1093/jnci/dju187

Edwards, B. K., Noone, A. M., Mariotto, A. B., Simard, E. P., Boscoe, F. P., Henley, S. J., … Ward, E. M. (2014). Annual Report to the Nation on the status of cancer, 1975-2010, featuring prevalence of comorbidity and impact on survival among persons with lung, colorectal, breast, or prostate cancer. *Cancer*, *120*(9), 1290–1314. http://doi.org/10.1002/cncr.28509

Farquharson, S., Gift, A., Shende, C., Inscore, F., Ordway, B., Farquharson, C., & Murren, J. (2008). Surface-enhanced Raman spectral measurements of 5-fluorouracil in saliva. *Molecules*, *13*(10), 2608–2627. http://doi.org/10.3390/molecules13102608

Fennema, E., Rivron, N., Rouwkema, J., van Blitterswijk, C., & De Boer, J. (2013). Spheroid culture as a tool for creating 3D complex tissues. *Trends in Biotechnology*, *31*(2), 108–115. http://doi.org/10.1016/j.tibtech.2012.12.003

Ferlay, J., Soerjomataram, I., Dikshit, R., Eser, S., Mathers, C., Rebelo, M., … Bray, F. (2015). Cancer incidence and mortality worldwide : Sources , methods and major patterns in GLOBOCAN 2012, *386*. http://doi.org/10.1002/ijc.29210

Ferrari, P., Jenab, M., Norat, T., Moskal, A., Slimani, N., Olsen, A., … Riboli, E. (2007). Lifetime and baseline alcohol intake and risk of colon and rectal cancers in the European Prospective Investigation into Cancer and Nutrition (EPIC). *International Journal of Cancer*, *121*(9), 2065–2072. http://doi.org/10.1002/ijc.22966

Freeman, Z. T., Rice, K. a, Soto, P. L., Pate, K. a M., Weed, M. R., Ator, N. a, … Hutchinson, E. K. (2015). Neurocognitive dysfunction and pharmacological intervention using guanfacine in a rhesus macaque model of self-injurious behavior. *Translational Psychiatry*, *5*(5), e567. http://doi.org/10.1038/tp.2015.61

Garcia-Ramírez, M., Hernández, C., Palomer, X., Vázquez-Carrera, M., & Simó, R. (2015). Fenofibrate prevents the disruption of the outer blood retinal barrier through downregulation of NF-κB activity. *Acta Diabetologica*. http://doi.org/10.1007/s00592-015-0759-3

Gauglhofer, C., Paur, J., Schrottmaier, W. C., Wingelhofer, B., Huber, D., Naegelen, I., … Grasl-Kraupp, B. (2014). Fibroblast growth factor receptor 4: a putative key driver for the aggressive phenotype of hepatocellular carcinoma. *Carcinogenesis*, *35*(10), 2331–2338. http://doi.org/10.1093/carcin/bgu151

Giessrigl, B., Yazici, G., Teichmann, M., Kopf, S., Ghassemi, S., Atanasov, A. G., … Krupitza, G. (2012). Effects of Scrophularia extracts on tumor cell proliferation, death and intravasation through lymphoendothelial cell barriers. *International Journal of Oncology*, *40*(6), 2063–2074. http://doi.org/10.3892/ijo.2012.1388

Gout, S., & Huot, J. (2008). Role of cancer microenvironment in metastasis: Focus on colon cancer. *Cancer Microenvironment*, *1*(1), 69–83. http://doi.org/10.1007/s12307-008-0007-2

Gregory, P. a, Bert, A. G., Paterson, E. L., Barry, S. C., Tsykin, A., Farshid, G., … Goodall, G. J. (2008). The miR-200 family and miR-205 regulate epithelial to mesenchymal transition by targeting ZEB1 and SIP1. *Nature Cell Biology*, *10*(5), 593–601. http://doi.org/10.1038/ncb1722

Gregory, P. a., Bracken, C. P., Bert, A. G., & Goodall, G. J. (2008). MicroRNAs as regulators of epithelial-mesenchymal transition. *Cell Cycle*, *7*(20), 3112–3117. http://doi.org/10.4161/cc.7.20.6851

Holzapfel, B., & Wickert, L. (2007). Die quantitative Real-Time-PCR (qRT-PCR). Methoden und Anwendungsgebiete. *Biologie in Unserer Zeit*, *37*(2), 120–126. http://doi.org/10.1002/biuz.200610332

Honn, K. V., Tang, D. G., Grossi, I., Duniec, Z. M., Timar, J., Renaud, C., … Marnett, L. J. (1994). Tumor cell-derived 12(S)-hydroxyeicosatetraenoic acid induces microvascular endothelial cell retraction. *Cancer Research*, *54*(2), 565–574.

Humphries, A., & Wright, N. a. (2008). Colonic crypt organization and tumorigenesis. *Nature Reviews. Cancer*, *8*(6), 415–424. http://doi.org/10.1038/nrc2392

Hur, K., Toiyama, Y., Takahashi, M., Balaguer, F., Nagasaka, T., Koike, J., … Goel, a. (2012). MicroRNA-200c modulates epithelial-to-mesenchymal transition (EMT) in human colorectal cancer metastasis. *Gut*, 1315–1326. http://doi.org/10.1136/gutjnl-2011-301846

Ivascu, A., & Kubbies, M. (2007). Diversity of cell-mediated adhesions in breast cancer spheroids. *International Journal of Oncology*, *31*(6), 1403–1413. http://doi.org/10.3892/ijo.31.6.1403

Ji, Q., Liu, X., Han, Z., Zhou, L., Sui, H., Yan, L., … Li, Q. (2015). Resveratrol suppresses epithelial-to-mesenchymal transition in colorectal cancer through TGF-

β1/Smads signaling pathway mediated Snail/E-cadherin expression. *BMC Cancer*, *15*(1), 1–12. http://doi.org/10.1186/s12885-015-1119-y

Juncker-Jensen, A., Deryugina, E. I., Rimann, I., Zajac, E., Kupriyanova, T. a., Engelholm, L. H., & Quigley, J. P. (2013). Tumor MMP-1 activates endothelial PAR1 to facilitate vascular intravasation and metastatic dissemination. *Cancer Research*, *73*(14), 4196–4211. http://doi.org/10.1158/0008-5472.CAN-12-4495

Kahlert, C. (2014). Exosomes in Tumor Microenvironment Influence Cancer Progression and Metastasis. *Journal of Molecular Medicine*, *91*(4), 431–437. http://doi.org/10.1007/s00109-013-1020-6.Exosomes

Katz, J. P., Perreault, N., Goldstein, B. G., Lee, C. S., Labosky, P. A., Yang, V. W., & Kaestner, K. H. (2002). The zinc-finger transcription factor Klf4 is required for terminal differentiation of goblet cells in the colon. *Development (Cambridge, England)*, *129*(11), 2619–2628. http://doi.org/10.1037/a0013262.Open

Kavvadias, D., Sand, P., Youdim, K. a, Qaiser, M. Z., Rice-Evans, C., Baur, R., … Schreier, P. (2004). The flavone hispidulin, a benzodiazepine receptor ligand with positive allosteric properties, traverses the blood-brain barrier and exhibits anticonvulsive effects. *British Journal of Pharmacology*, *142*(5), 811–820. http://doi.org/10.1038/sj.bjp.0705828

Kerjaschki, D., Bago-horvath, Z., Rudas, M., Sexl, V., Schneckenleithner, C., Wolbank, S., … Alitalo, K. (2011). Lipoxygenase mediates invasion of intrametastatic lymphatic vessels and propagates lymph node metastasis of human mammary carcinoma xenografts in mouse, *121*(5). http://doi.org/10.1172/JCI44751DS1

Kim, H. J., Park, M. K., Kim, S. Y., & Lee, C. H. (2014). Novel Suppressive Effects of Ketotifen on Migration and Invasion of MDA-MB-231 and HT-1080 Cancer Cells, *22*(6), 540–546.

Kohn, A. D., & Moon, R. T. (2005). Wnt and calcium signaling: ??-Catenin-independent pathways. *Cell Calcium*, *38*(3-4 SPEC. ISS.), 439–446. http://doi.org/10.1016/j.ceca.2005.06.022

Kretschy, N., Teichmann, M., Kopf, S., Atanasov, a G., Saiko, P., Vonach, C., … Krupitza, G. (2013). In vitro inhibition of breast cancer spheroid-induced lymphendothelial defects resembling intravasation into the lymphatic vasculature by acetohexamide, isoxsuprine, nifedipin and proadifen. *British Journal of Cancer*, *108*(3), 570–8. http://doi.org/10.1038/bjc.2012.580

Krishnan, N., Bencze, G., Cohen, P., & Tonks, N. K. (2013). The anti-inflammatory compound BAY 11-7082 is a potent inhibitor of Protein Tyrosine Phosphatases. *FEBS J.*, *280*(12), 2830–2841. http://doi.org/10.1016/j.biotechadv.2011.08.021.Secreted

Lamouille, S., Subramanyam, D., Blelloch, R., & Derynck, R. (2013). Regulation of epithelial-mesenchymal and mesenchymal-epithelial transitions by microRNAs. *Curr Opin Cell Biol.*, *25*(2), 200–207. http://doi.org/10.1016/j.biotechadv.2011.08.021.Secreted

Langheinrich, M. C., Schellerer, V., Perrakis, A., Lohmüller, C., Schildberg, C., Naschberger, E., … Croner, R. S. (2012). Molecular mechanisms of lymphatic metastasis in solid tumors of the gastrointestinal tract. *International Journal of Clinical and Experimental Pathology*, *5*(7), 614–623.

Larriba, M. J., Martín-Villar, E., García, J. M., Pereira, F., Peña, C., García de Herreros, A., … Muñoz, A. (2009). Snail2 cooperates with Snail1 in the repression of vitamin D receptor in colon cancer. *Carcinogenesis*, *30*(8), 1459–1468. http://doi.org/10.1093/carcin/bgp140

Lawes, D., & Boulos, P. B. (2002). Advances in the management of rectal cancer. *Journal of the Royal Society of Medicine*, *95*(12), 587–590. http://doi.org/10.1258/jrsm.95.12.587

Liu, R. T., Wang, A., To, E., Gao, J., Cao, S., Cui, J. Z., & Matsubara, J. a. (2014). Vinpocetine inhibits amyloid-beta induced activation of NF-κB, NLRP3 inflammasome and cytokine production in retinal pigment epithelial cells. *Experimental Eye Research*, *127*, 49–58. http://doi.org/10.1016/j.exer.2014.07.003

Ma, Z., Otsuyama, K. I., Liu, S., Abroun, S., Ishikawa, H., Tsuyama, N., … Kawano, M. M. (2005). Baicalein, a component of Scutellaria radix from Huang-Lian-Jie-Du-Tang (HLJDT), leads to suppression of proliferation and induction of apoptosis in human myeloma cells. *Blood*, *105*(8), 3312–3318. http://doi.org/10.1182/blood-2004-10-3915

Mader, R. M., Sieder, A. E., Braun, J., Rizovski, B., Kalipciyan, M., Mueller, M. W., … Steger, G. G. (1997). Transcription and activity of 5-fluorouracil converting enzymes in fluoropyrimidine resistance in colon cancer in vitro. *Biochemical Pharmacology*, *54*(11), 1233–1242. http://doi.org/10.1016/S0006-2952(97)00330-4

Mader, R. M., Wieser, M., Berger, W., Kalipciyan, M., Hackl, M., Steger, G. G., & Grillari, J. (2011). Relevance of microRNA modulation in chemoresistant colon cancer in vitro. *International Journal of Clinical Pharmacology and Therapeutics*, *49*(1), 67–68. http://doi.org/10.5414/CPP49067

McDonald, S. a C., Preston, S. L., Lovell, M. J., Wright, N. a, & Jankowski, J. a Z. (2006). Mechanisms of disease: from stem cells to colorectal cancer. *Nature Clinical Practice. Gastroenterology & Hepatology*, *3*(5), 267–274. http://doi.org/10.1038/ncpgasthep0473

McKeown, E., Nelson, D. W., Johnson, E. K., Maykel, J. a., Stojadinovic, A., Nissan, A., … Steele, S. R. (2014). Current approaches and challenges for monitoring treatment response in colon and rectal cancer. *Journal of Cancer*, *5*(1), 31–43. http://doi.org/10.7150/jca.7987

McLeod, H. L., Sargent, D. J., Marsh, S., Green, E. M., King, C. R., Fuchs, C. S., … Goldberg, R. M. (2010). Pharmacogenetic predictors of adverse events and response to chemotherapy in metastatic colorectal cancer: Results from North American Gastrointestinal Intergroup Trial N9741. *Journal of Clinical Oncology*, *28*(20), 3227–3233. http://doi.org/10.1200/JCO.2009.21.7943

Meidhof, S., Brabletz, S., Lehmann, W., Preca, B., Lübbert, M., Puhr, M., … Bronsert, P. (n.d.). ZEB1-associated drug resistance in cancer cells is reversed by the class I HDAC-inhibitor mocetinostat.

Miyazaki, K., Shibahara, T., Sato, D., Uchida, K., Suzuki, H., Matsui, H., … Matsuzaki, Y. (2006). Influence of chemotherapeutic agents and cytokines on the expression of 5-fluorouracil-associated enzymes in human colon cancer cell lines. *Journal of Gastroenterology*, *41*(2), 140–150. http://doi.org/10.1007/s00535-005-1733-6

Mohan, M., Kavita, M. S., & Karuna, M. S. (2015). Lifestyle, Eating Pattern and Comorbidities among Colorectal Cancer Patients Undergoing Cancer Therapies. *IOSR Journal of Dental and Medical Sciences*, *14*(6), 2279–861. http://doi.org/10.9790/0853-14664955

Myzak, M. C., Dashwood, W. M., Orner, G. a, Ho, E., & Dashwood, R. H. (2006). Sulforaphane inhibits histone deacetylase in vivo and suppresses tumorigenesis in Apc-minus mice. *The FASEB Journal : Official Publication of the Federation of American Societies for Experimental Biology*, *20*(3), 506–508. http://doi.org/10.1096/fj.05-4785fje

Myzak, M. C., Tong, P., Dashwood, W.-M., Dashwood, R. H., & Ho, E. (2007). Sulforaphane retards the growth of human PC-3 xenografts and inhibits HDAC activity in human subjects. *Experimental Biology and Medicine (Maywood, N.J.)*, *232*(2), 227–234. http://doi.org/232/2/227 [pii]

Pantel, K., & Brakenhoff, R. H. (2004). Dissecting the metastatic cascade. *Nature Reviews. Cancer*, *4*(6), 448–456. http://doi.org/10.1038/nrc1370

Patel, D., Shukla, S., & Gupta, S. (2007). Apigenin and cancer chemoprevention: Progress, potential and promise (Review). *International Journal of Oncology*, *30*(1), 233–245.

Paterson, E. L., Kazenwadel, J., Bert, A. G., Khew-Goodall, Y., Ruszkiewicz, A., & Goodall, G. J. (2013). Down-regulation of the miRNA-200 family at the invasive front of colorectal cancers with degraded basement membrane indicates EMT is involved in cancer progression. *Neoplasia (New York, N.Y.)*, *15*(2), 180–91. http://doi.org/10.1593/neo.121828

Perkins, N. D. (2012). The diverse and complex roles of NF-κB subunits in cancer. *Nature Reviews Cancer*, (January). http://doi.org/10.1038/nrc3204

Perkins, N. D., & Gilmore, T. D. (2006). Good cop, bad cop: the different faces of NF-kappaB. *Cell Death and Differentiation*, *13*(5), 759–772. http://doi.org/10.1038/sj.cdd.4401838

Pischon, T., Lahmann, P. H., Boeing, H., Friedenreich, C., Norat, T., Tjønneland, A., … Riboli, E. (2006). Body size and risk of colon and rectal cancer in the European Prospective Investigation into Cancer and Nutrition (EPIC). *Journal of the National Cancer Institute*, *98*(13), 920–931. http://doi.org/10.1093/jnci/djj246

Preston, S. L., Wong, W. M., Chan, A. O. O., Poulsom, R., Jeffery, R., Goodlad, R. a., … Wright, N. a. (2003). Bottom-up histogenesis of colorectal adenomas: Origin in the monocryptal adenoma and initial expansion by crypt fission. *Cancer Research*, *63*(13), 3819–3825. http://doi.org/63:3819-3825

Radtke, F., & Clevers, H. (2005). Self-renewal and cancer of the gut: two sides of a coin. *Science (New York, N.Y.)*, *307*(5717), 1904–1909. http://doi.org/10.1126/science.1104815

Rauert-Wunderlich, H., Siegmund, D., Maier, E., Giner, T., Bargou, R. C., Wajant, H., & Stühmer, T. (2013). The IKK Inhibitor Bay 11-7082 Induces Cell Death Independent from Inhibition of Activation of NFκB Transcription Factors. *PLoS ONE*, *8*(3), 1–10. http://doi.org/10.1371/journal.pone.0059292

Ruggiero, S., Clavenna, A., Reale, L., Capuano, A., Rossi, F., & Bonati, M. (2014). Guanfacine for attention deficit and hyperactivity disorder in pediatrics: A systematic review and meta-analysis. *European Neuropsychopharmacology : The Journal of the European College of Neuropsychopharmacology*, *376*, 1578–1590. http://doi.org/10.1016/j.euroneuro.2014.08.001

Rupp, C., Scherzer, M., Rudisch, a, Unger, C., Haslinger, C., Schweifer, N., … Garin-Chesa, P. (2014). IGFBP7, a novel tumor stroma marker, with growth-promoting effects in colon cancer through a paracrine tumor-stroma interaction. *Oncogene*, (April 2013), 1–11. http://doi.org/10.1038/onc.2014.18

Sanoff, H. K., Sargent, D. J., Campbell, M. E., Morton, R. F., Fuchs, C. S., Ramanathan, R. K., … Goldberg, R. M. (2008). Five-year data and prognostic factor analysis of oxaliplatin and irinotecan combinations for advanced colorectal cancer: N9741. *Journal of Clinical Oncology*, *26*(35), 5721–5727. http://doi.org/10.1200/JCO.2008.17.7147

Schoppmann, S. F., Soleiman, A., Kalt, R., Okubo, Y., Benisch, C., Nagavarapu, U., … Geleff, S. (2004). Telomerase-immortalized lymphatic and blood vessel endothelial cells are functionally stable and retain their lineage specificity. *Microcirculation (New York, N.Y. : 1994)*, *11*(3), 261–269. http://doi.org/10.1080/10739680490425967

Schwenk, W. (2002). Randomized clinical trial of the effect of open versus laproscopically assisted colectomy on systemic immunity in patients with colorectal cancer. *The British Journal of Surgery*, *89*(4), 497. http://doi.org/10.1046/j.1365-2168.2002.208821.x

Senfter, D., Holzner, S., Kalipciyan, M., Staribacher, a., Walzl, a., Huttary, N., … Mader, R. M. (2015). Loss of miR-200 family in 5-fluorouracil resistant colon cancer drives lymphendothelial invasiveness in vitro. *Human Molecular Genetics*, (April), 1–10. http://doi.org/10.1093/hmg/ddv113

Shih, I. M., Wang, T. L., Traverso, G., Romans, K., Hamilton, S. R., Ben-Sasson, S., … Vogelstein, B. (2001). Top-down morphogenesis of colorectal tumors. *Proceedings of the National Academy of Sciences of the United States of America*, *98*(5), 2640–2645. http://doi.org/10.1073/pnas.051629398

Strickson, S., Campbell, D. G., Emmerich, C. H., Knebel, A., Plater, L., Ritorto, M. S., … Cohen, P. (2013). The anti-inflammatory drug BAY 11-7082 suppresses the MyD88-dependent signalling network by targeting the ubiquitin system. *The Biochemical Journal*, *451*(3), 427–37. http://doi.org/10.1042/BJ20121651

Švehlíková, V., Wang, S., Jakubíkova, J., Williamson, G., Mithen, R., & Bao, Y. (2004). Interactions between sulforaphane and apigenin in the induction of UGT1A1 and GSTA1 in CaCo-2 cells. *Carcinogenesis*, *25*(9), 1629–1637. http://doi.org/10.1093/carcin/bgh169

Tamatani, T., Ferdous, T., Takamaru, N., Hara, K., Kinouchi, M., Kuribayashi, N., … Miyamoto, Y. (2012). Antitumor efficacy of sequential treatment with docetaxel and 5-fluorouracil against human oral cancer cells. *International Journal of Oncology*, *41*(3), 1148–1156. http://doi.org/10.3892/ijo.2012.1544

Tanaka, H., & Ogishima, S. (2015). Network biology approach to epithelial – mesenchymal transition in cancer metastasis : three stage theory, *7*, 253–266.

Teichmann, M., Kretschy, N., Kopf, S., Jarukamjorn, K., Atanasov, A. G., Viola, K., … Krupitza, G. (2014). Inhibition of tumour spheroid-induced prometastatic intravasation gates in the lymph endothelial cell barrier by carbamazepine: Drug testing in a 3D model. *Archives of Toxicology*, *88*(3), 691–699. http://doi.org/10.1007/s00204-013-1183-5

Thiery, J. P. (2002). Epithelial-mesenchymal transitions in tumour progression. *Nature Reviews. Cancer*, *2*(6), 442–454. http://doi.org/10.1038/nrc822

Uchide, K., Sakon, M., Ariyoshi, H., Nakamori, S., Tokunaga, M., & Monden, M. (2007). Cancer cells cause vascular endothelial cell (vEC) retraction via 12(S)HETE secretion; the possible role of cancer cell derived microparticle. *Annals of Surgical Oncology*, *14*(2), 862–868. http://doi.org/10.1245/s10434-006-9225-3

Van den Boorn, J. G., Daßler, J., Coch, C., Schlee, M., & Hartmann, G. (2013). Exosomes as nucleic acid nanocarriers. *Advanced Drug Delivery Reviews*, *65*(3), 331–335. http://doi.org/10.1016/j.addr.2012.06.011

Vinci, M., Gowan, S., Boxall, F., Patterson, L., Zimmermann, M., Court, W., … Eccles, S. a. (2012). Advances in establishment and analysis of three-dimensional tumor spheroid-based functional assays for target validation and drug evaluation. *BMC Biology*, *10*(1), 29. http://doi.org/10.1186/1741-7007-10-29

Viola, K., Kopf, S., Huttary, N., Vonach, C., Kretschy, N., Teichmann, M., … Grusch, M. (2013). Bay11-7082 inhibits the disintegration of the lymphendothelial barrier triggered by MCF-7 breast cancer spheroids; the role of ICAM-1 and adhesion. *British Journal of Cancer*, *108*(3), 564–9. http://doi.org/10.1038/bjc.2012.485

Vonach, C., Viola, K., Giessrigl, B., Huttary, N., Raab, I., Kalt, R., … Krupitza, G. (2011). NF-κB mediates the 12(S)-HETE-induced endothelial to mesenchymal transition of lymphendothelial cells during the intravasation of breast carcinoma cells. *British Journal of Cancer*, *105*(2), 263–271. http://doi.org/10.1038/bjc.2011.194

Weitz, J., Koch, M., Debus, J., Höhler, T., Galle, P. R., & Büchler, M. W. (2005). Colorectal cancer. *The Lancet*, *365*(9454), 153–65. http://doi.org/10.1016/S0140-6736(05)17706-X

Wellner, U., Brabletz, T., & Keck, T. (2010). ZEB1 in pancreatic Cancer. *Cancers*, *2*(3), 1617–1628. http://doi.org/10.3390/cancers2031617

Yang, M., Chen, J., Su, F., Yu, B., Su, F., Lin, L., … Song, E. (2011). Microvesicles secreted by macrophages shuttle invasion-potentiating microRNAs into breast cancer cells. *Molecular Cancer*, *10*(1), 117. http://doi.org/10.1186/1476-4598-10-117

Young-Fadok, T. M., & Pemberton, J. H. (1998). Laparoscopic versus open resection for colorectal cancer. *Journal of the American College of Surgeons*, *187*(1), 55–57.

Zheng, Y. Bin, Luo, H. P., Shi, Q., Hao, Z. N., Ding, Y., Wang, Q. S., … Tong, S. L. (2014). miR-132 inhibits colorectal cancer invasion and metastasis via directly targeting ZEB2. *World Journal of Gastroenterology*, *20*(21), 6515–6522. http://doi.org/10.3748/wjg.v20.i21.6515

6. Acknowledgment

English

First of all, I would like to thank Dr. Georg Krupitza for providing me the opportunity to work on this project. His excellent network within and outside of the medical university has helped me to proceed in my scientific career.

Furthermore, I would like to thank our cooperating partners Dr. Robert Mader and Dr. Helmut Dolznig for their overwhelming support, which enabled us to reach our goals.

Also, a huge thank you to our very helpful technicians. Maria Kalipcijan, who always managed to put a smile on my face and Nicole Huttary, who helped me with whatever I needed and nonetheless never lost her patience. Whenever I had problems or questions, they were so kind as to support me with their expertise and knowledge.

Of course, I would also like to thank all of the other members of the laboratory, who not only were my colleagues but most notably became friends. Thus, I would like to thank Chi Nguyen, Daniel Senfter, Serena Stadler and Michael Blaschke for the entertaining lunch breaks as well as for the professional football analysis during our coffee breaks.

A, as we used to say, “bäääriges” thank you to my friend Philipp Klambauer, whom I will definitely coach to be a supermodel and / or actor someday; Anna Staribacher, as well as, Marlies Moshammer for the good time we spent together during and outside of work.

Moreover, I wish to thank Klaus and Markus for the myriad of shared hours in the library.

Last but not least, I want to thank my family. My parents, Josef and Helga, without whom I would not have had the opportunity to study and my brothers Mario and Marco, to whom I always feel connected, even if we are thousands of kilometres apart.

On that note, thank you very much!

Deutsch

Als Erstes will ich Dr. Georg Krupitza danken, dafür dass er es mir ermöglicht hat an diesem Projekt zu arbeiten. Sein exzellentes Network innerhalb und außerhalb der Medizinischen Universität, hat mir in meiner wissenschaftlichen Karriere sehr weitergeholfen.

Desweitern möchte ich mich bei unseren Kooperationspartner Dr. Robert Mader und Dr. Helmut Dolznig bedanken, für den exzellenten Einsatz (Input), damit wir unsere Ziele erreichen.

Ein großes Dankeschön an unseren zwei hilfreichen Technikerinnen Maria Kalipcijan, die mir immer ein Lächeln ins Gesicht zauberte und Nicole Huttary, die mir jegliche Bestellwünsche erfüllte und nie die Geduld verlor. Aber auch bei aufgekommenen Problemen standen sie mir mit hilfreichen Methoden und Verfahren stets zur Seite.

Natürlich will ich mich auch bei allen anderen Labor Mitgliedern bedanken, die nicht nur Kollegen, sondern auch Freunde waren und immer noch sind. Daher ein großes Dankeschön an Chi Nguyen, Daniel Senfter, Serena Stadler und Michael Blaschke für die lachenden Mittagspausen und für die professionellen Fußball Analysen während der Kaffeepausen. Ein „bäääriges“ Dankeschön auch an Philipp Klambauer, den ich noch groß als Model und Schauspieler rausbringe, Anna Staribacher und Marlies Moshammer für die schöne Zeit bei und außerhalb der Arbeit.

Für die unzähligen gemeinsamen Bibliotheksstunden möchte ich mich recht herzlich bei Klaus und Markus bedanken.

Der letzte und doch größte Dank gilt meinen Eltern, Josef und Helga, für die Unterstützung während meiner gesamten Studienzeit und dafür, dass sie mir das Studium ermöglicht haben, und meinen Brüdern Mario und Marco, trotz einiger Kilometer Distanz, habe ich mich stets verbunden gefühlt.

In diesem Sinne, herzlichen Dank!

7. Appendix

Abstract English

The benefit of two dimensional (2D) monolayer cell cultures to investigate e.g. colorectal cancer (CRC) models is limited because is lacks structural architecture. 3D aggregates, known as multicellular tumour spheroids, overcome these limitations and display drug sensitivity and radiation resistance patterns as seen regularly *in vivo* and therefore, tumour spheroids are considered as a valuable tool for drug screening. On top of that, the co-cultivation of cancer cell spheroids together with endothelial cells allows the analysis of tumour intra-/extravasation mechanisms and potential intervention strategies. A validated quantitative assay measuring the tumour spheroid-triggered retraction of beneath growing endothelial cells (circular chemorepellent induced defects -"CCID"- assay) was used to study the malignant potential of CRC spheroids formed by CCL227 (syn. SW620) cells, or by the 5-FU-resistant subclone CCL227-R, to analyze the breakthrough of the blood endothelial cell (BEC) barrier. Acquisition of drug resistance is a complex process that profoundly alters gene expression on the genetic and epigenetic level and impacts on cell behavior such as epithelial to mesenchymal transition (EMT) and enhanced cell migration. Members of the microRNA-200 (miR-200) family act as regulatory molecules suppressing EMT and migration. MiR-200a, miR-200b, miR-200c, miR-141 and miR-429 were shown to become encapsulated into exosomes of naïve CRC cells and are subsequently taken up by adjacent lymphendothelial cells (LECs). This investigation shows that miR-200 suppressed the migratory phenotype and inhibited the expression of members of the ZEB family of transcription factors (ZEB1, ZEB2, SNAI and TWIST; expression of SLUG was below the detection limit) in BECs. Hence, miR200 derived from naïve CRC spheroids, strengthened the BEC barrier and partly antagonized the effect of 12(S)-HETE (secreted by CCL227 cells), which forces endothelial retraction and CCID formation. The resistant CCL227-R clone reportedly quit miR-200 expression and thus increased the plasticity of BECs resulting in more severe CCID formation. Therefore, metastasis formation might be understood not only as an active process from the malignant cell, but also as an orchestrated and transient take-over of the endothelial barrier. CRC spheroids affected the integrity of BEC and LEC barriers alike, which is in agreement with the observation that CRC metastasises into the liver (via blood stream) or lymph nodes (via lymphatics) alike.

Treatment with specific inhibitors demonstrates that breaching of the BEC barrier involves the activities of lipoxygenases 12/15, NF-κB, and cytochromes P450. The inhibition of these mechanisms is crucial to attenuate tumour progression. Currently, there are no therapies that specifically target tumour intravasation. Pharmaceuticals often exhibit activities against diseases they have not been developed for. To discover compounds, which inhibit CCID formation, drugs approved by the US Food and Drug Administration (FDA) which also inhibit at least one of the above mentioned mechanisms, were tested, because they can be made readily available to patients. Ketotifen and carbamazepine were the most potent CCID inhibitors followed by isoxsuprine, vinpocetine and acetohexamide. The effect of these drugs was reduced in the CCL227-R model, whereas fenofibrate was similarly active in the naïve CCL227-N and resistant CCL227-R model. Notably, guanfacine and nifedipin exhibited activity only on the resistant CCL227-R model. The flavonoids apigenin and hispidulin, which are related to baicalein and constituents of pharmacological plants, were similarly effective in the naïve and resistant model, but were less potent than baicalein. The HDAC inhibitor mocetinostat, which was reported to induce the expression of specific miRs and which is tested in clinical trials, significantly inhibited CCID formation such as the HDAC inhibitor sulforaphane. Hence, pharmaceutical drugs that attenuate tumour-forced breaching of the blood endothelial barrier *in vitro* indeed exist and moreover, plant constituents may help to prevent tumour progression.

Abstract Deutsch

Die Nützlichkeit von zweidimensionalen (2D) Monolayer Zell-Kulturmodellen ist, aufgrund der fehlenden Strukturarchitektur, begrenzt. 3D-Aggregate, wie mehrzellige Tumorsphäroide, überwinden diese Einschränkungen und spiegeln Arzneimittelempfindlichkeit und Strahlungsbeständigkeit wie *in vivo* wieder und werden auch als ein wertvolles Instrument für Wirkstoff-Screening gehandhabt. Hinzu kommt, dass die Co-Kultivierung von Krebszellen Sphäroiden mit Endothelzellen die Untersuchung von Mechanismen der Tumor Intra- / Extravasation und mögliche Interventionsstrategien ermöglicht. Ein validierter quantitativer Assay wurde verwendet, um die, von Tumor Sphäroiden ausgelöste, Retraktion der Endothelzellen (circular chemorepellent induzierte Defekte - "CCID" - Test) zu messen und somit das maligne Potenzial der CRC Sphäroiden, gebildet von CCL227 (SW620) Zellen oder

durch den 5-FU resistenten Subklon CCL227-R, zu studieren. Der Erwerb von Medikamentenresistenz ist ein komplexer Prozess, der hochgradig die Genexpression auf genetischer und epigenetischer Ebene verändert und auf das Zellverhalten wirkt, wie zum Beispiel epitheliale zu mesenchymale Transition (EMT) und erhöhte Zellmigration. Mitglieder der microRNA-200 (miR-200) Familie wirken als regulatorische Moleküle zur Unterdrückung von EMT und Migration. Bei miR-200a, miR-200b, miR-200c, miR-141 und miR-429 wurde gezeigt, dass diese in Exosomen von naiven CRC-Zellen eingekapselt werden und anschließend von angrenzenden lymphendothelial Zellen (LECs) aufgenommen werden. Diese Untersuchung zeigt, dass miR-200 den Migrationsphänotyp unterdrückt und die Expression von Mitgliedern der ZEB Transkriptionsfaktoren Familie (ZEB1, ZEB2, SNAI und TWIST; Expression von SLUG war unterhalb der Nachweisgrenze) in BECs inhibiert. Daher verstärkt die miR-200 Familie von naiven CRC Sphäroide die BEC-Barriere und wirkt teilweise als Antagonist von 12(S)-HETE (sekretiert von CCL227 Zellen), welches endothelial Retraktion und CCID Formation verstärkt. Die resistenten CCL227-R Zellen verlieren, Berichten zufolge, die Expression von miR200, wodurch sich die Plastizität der BECs erhöht und zu starker CCID Bildung führt. Daher kann die Metastasenbildung nicht nur als ein aktiver Prozess der malignen Zelle, sondern auch als Manipulation und vorübergehende Übernahme der endothelialen Barriere verstanden werden. CRC Sphäroide beeinflussen die Integrität der BEC und LEC Barrieren gleich, was mit der Beobachtung übereinstimmt, dass CRC in die Leber (via Blutbahn) oder Lymphknoten (via Lymphbahnen) gleicherweise metastasiert.

Die Behandlung mit spezifischen Inhibitoren zeigt, dass das Durchbrechen der BEC Barriere die Aktivitäten der Lipoxygenasen 12/15, NF-κB und Cytochrom P450 beinhaltet. Die Hemmung dieser Mechanismen ist entscheidend, um die Tumorprogression zu schwächen. Derzeit gibt es keine Therapien, die spezifisch Tumor-Intravasation angreifen. Medikamente zeigen oft Aktivitäten gegen Krankheiten, für die sie nicht entwickelt worden sind. Um Präparate zu finden, welche die CCID Bildung hemmen wurden Arzneimittel getestet welche von der US „Food and Drug Administration“ (FDA) zugelassen wurden, da diese leicht zugänglich für die Patienten sind, und gezeigt, dass zumindest einer der oben genannten Mechanismen gehemmt wurde. Ketotifen und Carbamazepin waren die stärksten CCID-Hemmer, gefolgt von Isoxsuprin, Vinpocetin und Acetohexamid. Die Wirkung dieser Medikamente war im CCL227-R Modell reduziert, während Fenofibrat im naiven

CCL227-N und resistenten CCL227-R Modell ähnlich aktiv war. Bemerkenswert ist, dass Guanfacin und Nifedipin nur im resistenten CCL227-R Modell Aktivitäten zeigten. Die Flavonoide Apigenin und Hispidulin, die ähnlich sind wie Baicalein und wesentliche Bestandteile pharmakologischer Pflanzen sind, waren im naiven und resistenten Modell gleich effektiv, aber weniger wirksam als Baicalein. Der HDAC-Inhibitor Mocetinostat, von dem berichtet wurde, die Expression spezifischer miRs zu induzieren und welcher in klinischen Versuchen getestet wird, hemmt deutlich die CCID Bildung, wie auch der HDAC-Inhibitor Sulforaphan. Daher gibt es in der Tat Medikamente, die das, durch Tumor erzwungene, Durchbrechen der Blut Endothelbarriere *in vitro* schwächen und auch Pflanzenbestandteile die dazu beitragen können, Tumorprogression zu verhindern.

Curriculum Vitae

Name:	Silvio Holzner BSc
Place of Birth:	Wörgl, Austria
Date of Birth:	05.11.1988
Nationality:	Austria
E-Mail address:	silvio_holzner@hotmail.com

Curriculum Vitae

Education

10.2012 – 09.2015	**University of Vienna / Austria** Master's degree course: Molecular Biology Focus: Molecular Medicine Master's thesis: "The microRNA-200 family and FDA approved drugs as inhibitors of tumour intravasation through the blood vessel endothelium"
02.2009 – 09.2012	**Leopold- Franzens University of Innsbruck / Austria** Bachelor's degree course: Biology Focus: Molecular Biology, Microbiology Bachelor's thesis: „Culture-technical characterization of microorganisms isolated from Moonmilk"
10.2008 – 01.2009	**Leopold- Franzens University of Innsbruck / Austria** Bachelor's degree course: Chemistry
1999 – 2007	**Bundesrealgymnasium Wörgl / Austria** Degree: General qualification for university entrance in German, mathematics, English, descriptive geometry and biology

---

Professional Experience

11.2013 – 12.2014	**Institute of Clinical Pathology** / Position: Master Student Supervision: Prof. Dr. Georg Krupitza Terms of reference: Tumour-stroma interaction in human cancer
04.2013 – 07.2013	**Institute of Medical Genetics** – Position: Student Apprentice Supervision: Prof. Dr. Helmut Dolznig Terms of reference: Tumour-stroma interaction in human cancer

06.2011 – 08.2011	**Headquarter Spar AG Wörgl** – Position: Summer intern Department: Clean Away Terms of reference: Monitoring and implementation of entrepreneurial recycling targets; Food inspection
06.2010 – 08.2010	**Headquarter Spar AG Wörgl** – Position: Summer intern Department: Fresh assortment Terms of reference: Food inspection, logistical activities

---

Publication

*Daniel Senfter, **Silvio Holzner**, Maria Kalipciyan, Anna Staribacher, Angelika Walzl, Nicole Huttary, Sigurd Krieger, Stefan Brenner, Walter Jäger, Georg Krupitza, Helmut Dolznig, Robert M. Mader.* Loss of miR-200 family in 5-fluorouracil resistant colon cancer drives lymphendothelial invasiveness *in vitro*. Human Molecular Genetics 2015.

*Michael Blaschke, Ruxandra McKinnon, Chi Huu Nguyen, **Silvio Holzner**, Martin Zehla, Atanas Georgiev Atanasov, Karin Schelch, Sigurd Krieger, Rene Diaze,Richard Frisch, Björn Feistel, Walter Jäger, Gerhard F. Ecker, Verena M. Dirsch, Michael Grusch, Istvan Zupko, Ernst Urban, Brigitte Kopp, Georg Krupitza*. A eudesmane-type sesquiterpene isolated from Pluchea odorata (L.) Cass. combats three hallmarks of cancer cells: Unrestricted proliferation, escape from apoptosis and early metastatic outgrowth *in vitro.* Mutation Research 777 (2015) 79–90.

Social Competence

2008 – 2012	**Football** Captain of the first team (SV Wörgl-football); Youth coach; Support for various events on the football field and representation of the association at regional events

Additional Skills

Language

German	mother tongue
English	business fluent

Computer Literacy

Microsoft Word, Microsoft Excel, Microsoft PowerPoint, Adobe Photoshop, Statistika, GraphPad Prism 6

Hobbies

Language, traveling, cultures and sport